LA-11737-MS, Vol. I
BEAR-DT-7-1

BEAR
(BEAM EXPERIMENTS ABOARD A ROCKET)
PROJECT

FINAL REPORT
VOLUME I: PROJECT SUMMARY

K 5 3 8 1

Los Al

Accession Number: 5381

Publication Date: Jan 01, 1990

Title: Ream Experiments Aboard a Rocket (BEAR) Project Final Report Vol 1; Project Summary

Personal Author: Nunz, G.J.

Corporate Author Or Publisher: Bear Project Staff

Report Prepared for: Strategic Defense Initiative Organization Directed Energy Office Washington, DC

Abstract: The U.S. Department of Defense's Strategic Defense Initiative Organization is sponsoring the development of neutral particle beam (NPB) techonolgy for strategic defense applications. The first step in demonstrating the functioning of an NPB in space was the development and launch of the Beam Experiments Aboard a Rocket (BEAR) in New Mexico in July 1989. A government, laboratory, and industrial team, under the technical coordination of Los Alamos National Laboratory, designed, developed, and tested the BEAR payload. The primary objective of BEAR was the operation of an NPB accelerator in space. The payload was also designed to study (1) the efects on the space vehicle of emitting an NPB and associated charged beams into the space environment; (2) the propagation and attenuation characteristics of an NPB in space; (3) the dynamics of the charged particle components of the beam in the geomagnetic field; (4) the effects of neutral effuents from the vehicle; and (5) any anomalous or unanticipated phenomena associated with operating an NPB in the space environment. The BEAR experiment successfully demonstrated operation of an NPB accelerator and propagation of the neutral beam as predicted in space, obtained first-of-a-kind NPB space physics data, and demonstrated the ability of the BEAR accelerator to survive recovery and to continue operating normally. No unanticipated phenomena were encountered that would significantly delay further development of NPB technology for defensive, space-based weapon systems.

Descriptors, Keywords: BEAR, NPB, Rocket

Pages: 103

Cataloged Date: May 08, 1996

Document Type: HC

Number of Copies In Library: 000001

Record ID: 40704

BEAR payload launched at White Sands Missile Range, Launch Complex 36, 2:30 a.m. MDT, July 13, 1989.

ABSTRACT

The US Department of Defense's Strategic Defense Initiative Organization is sponsoring the development of neutral particle beam (NPB) technology for strategic defense applications. The first step in demonstrating the functioning of an NPB in space was the development and launch of the Beam Experiments Aboard a Rocket (BEAR) in New Mexico in July 1989. A government, laboratory, and industrial team, under the technical coordination of Los Alamos National Laboratory, designed, developed, and tested the BEAR payload. The primary objective of BEAR was the operation of an NPB accelerator in space. The payload was also designed to study (1) the effects on the space vehicle of emitting an NPB and associated charged beams into the space environment; (2) the propagation and attenuation characteristics of an NPB in space; (3) the dynamics of the charged particle components of the beam in the geomagnetic field; (4) the effects of neutral effluents from the vehicle; and (5) any anomalous or unanticipated phenomena associated with operating an NPB in the space environment. The BEAR experiment successfully demonstrated operation of an NPB accelerator and propagation of the neutral beam as predicted in space, obtained first-of-a-kind NPB space physics data, and demonstrated the ability of the BEAR accelerator to survive recovery and to continue operating normally. No unanticipated phenomena were encountered that would significantly delay further development of NPB technology for defensive, space-based weapon systems.

ACKNOWLEDGMENTS

LA-11737-MS, Vol. I

BEAR-DT-7-1
UC-000
Issued: January 1990

Beam Experiments Aboard a Rocket
(BEAR)
Project

FINAL REPORT
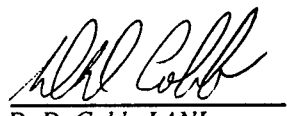
Volume I: Project Summary
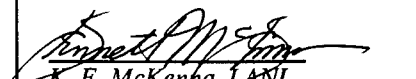
Prepared by

G. J. Nunz, LANL
BEAR Project Staff

Approved by

R. J. Barick, LANL
NPB Program Director

K. F. McKenna, LANL
BEAR Deputy Program Manager

D. D. Cobb, LANL
BEAR Program Manager

M. B. Pongratz, LANL
BEAR Chief Scientist

Submitted to

Strategic Defense Initiative Organization
Directed Energy Office
Washington, DC

LOS Alamos   Los Alamos National Laboratory
Los Alamos, New Mexico 87545

Preceding Page Blank

EXECUTIVE SUMMARY

The US Department of Defense, Strategic Defense Initiative Organization (SDIO), as part of its effort in Directed Energy Weapons is sponsoring the development of neutral particle beam (NPB) technology for strategic defense applications. On July 13, 1989, the BEAR (Beam Experiments Aboard a Rocket) was launched at White Sands Missile Range. BEAR was the first demonstration in space of an NPB system and represents a major milestone in the advancement of the SDI program. Indeed, BEAR was the first space demonstration of a candidate directed energy weapon technology.

The BEAR payload was launched on an ARIES booster at 2:30 a.m. Mountain Daylight Time. The payload followed closely the planned flight path, attaining an apogee of 195 km. The accelerator emitted 50-μs-long pulses of 1-MeV neutral hydrogen atoms and hydrogen ions throughout the 4.5 min of planned operational time, during which the payload was above an altitude of 90 km. All diagnostic instrumentation functioned normally, recording data throughout the flight.

The BEAR experiment successfully attained all its objectives and established a first-of-its-kind NPB space physics data base. The experiment demonstrated

- autonomous operation of an NPB accelerator in space,

- spacecraft charging to hundreds of volts with no detectable effect on the payload,

- beam propagation consistent with classical physics predictions,

- particle return to the payload with no significant effect, and

- no significant effects from neutral gas effluents.

No "unknowns" were observed. Because the BEAR space flight uncovered no NPB "show-stopping" phenomena, the NPB space technology development program can be vigorously pursued.

The primary objective of the BEAR Project was to design, build, and operate an NPB accelerator in space. Although conceptually based on the

ground-based NPB technology developed at Los Alamos National Laboratory, the BEAR accelerator was unique both in operation and hardware, and its development presented a major technological challenge. In meeting the primary BEAR objective, several technological advances were achieved, including the development of 1-gm/W solid-state power amplifiers, a highly stable monolithic radio frequency (rf) quadrupole (RFQ) accelerator structure, a highly compact, high-voltage H^- injector, and space-qualified vacuum pumps.

The second objective of the BEAR Project was the resolution of several space physics issues that were potential obstacles to successful continuation of the NPB program. Specifically, the BEAR payload was designed to study (1) the effects on the space vehicle (particularly spacecraft charging) of emitting a neutral beam and associated charged beams into the space environment; (2) the propagation and attenuation characteristics of an NPB in space; (3) the dynamics of the charged particle components of the beam in the geomagnetic field; (4) the effects of neutral effluents from the vehicle; and (5) any anomalous or unanticipated phenomena associated with operating an NPB in the space environment.

The design, development, testing, and successful flight of the BEAR accelerator system and the space physics diagnostics required the dedicated efforts and close cooperation of an integrated government, laboratory, and industrial team. The focus of this team was the BEAR Project Office (BPO) established at Los Alamos in January 1988 to "fast-track" the BEAR Project. The success of this small, dedicated team of technical experts is best illustrated by the fact that, starting from detailed designs, the required flight-qualified hardware was delivered in 13 months. The flight hardware was then integrated, tested, and launched in 5 additional months. Thus, 18 months after BPO had been formed, BEAR was launched successfully. The total cost was approximately $60 million spread over a 5-year program. In addition to Los Alamos, the other laboratories participating in BEAR were the Air Force Geophysics Laboratory (AFGL), which served as integrator of the ARIES rocket, and the Naval Research Laboratory, which carried out some of the space plasma physics experiments. AFGL also had responsibility for the payload support systems, including the attitude control, telemetry, and recovery systems. Industrial team members included Grumman Space Systems and McDonnell Douglas Missile Systems Co., who provided aerospace design, engineering, and fabrication support of NPB accelerator components and subsystems. Westinghouse Electric Corp. designed and built flight-qualified rf amplifiers, while SAIC, Inc., and EG&G provided diagnostic instruments, an electrostatic analyzer, and an intensified TV system.

Beam propagation was measured by on-board instruments (intensified TVs and solid-state detectors) out to the sensor limits, about 1.3 km from the payload. The results appear to be consistent with classical physics predictions; that is, there apparently were no unanticipated effects of space on the propagation of the beam. Future NPB space experiments with

deployable, cooperative targets will be required to validate the long-range propagation of NPBs in space.

Some charging of the spacecraft was observed but produced no detectable disruption of the accelerator or the beam. During normal operation with a neutralized beam, a net negative current of less than 1 mA was maintained. This caused the vehicle to charge to a low potential of several tens of volts in a background plasma of $\sim 10^3/\text{cm}^3$. During the flight, the gas neutralizer was turned off for two 10-sec intervals, producing beam pulses of approximately 10-mA negative current. The inferred vehicle potential during this period was less than 1 kV. When the beam was either neutralized or underneutralized, the vehicle charged rapidly only during the beam pulse and returned to near zero potential following the beam pulse, with no deleterious effects on accelerator operation or associated vehicle systems. It is important to emphasize that spacecraft charging effects must be carefully considered in future NPB space systems. The BEAR results indicate that charging effects can be controlled to acceptable levels through proper design.

Beam particles that exited the BEAR payload, which were already charged or which had become charged in collisions with the background atmosphere and then had been reflected back toward the spacecraft by the earth's magnetic field, produced no significant effects. In future flights, these potentially damaging beam particles can be avoided by controlling the attitude of the spacecraft relative to the earth's magnetic field during beam firings. Furthermore, predictions of single-particle models appear adequate to predict the dynamics of the charged beam particles.

Neutral effluents from attitude control thrusters, outgassing, etc., caused no significant effects on the payload or the beam. However, sensitive plasma instruments indicated a significant depletion of the local plasma density associated with thruster firings of the Attitude Control Subsystem. At times, under nominal neutralization, this plasma depletion appeared to amplify both the rate and level of vehicle charging.

The BEAR payload was returned to Los Alamos on July 21 and was erected vertically on its support stand. No damage to the accelerator was detected. On July 26, the accelerator was operated. All accelerator systems came on rapidly with no rf conditioning of the RFQ required, and nominal accelerator output beam current (>10 mA H^-) was obtained shortly after full operation was initiated.

Two important lessons learned for future NPBs in space may be summarized as follows. First, although the NPB accelerator operated successfully in space, loss of some beam pulses occurred, which has been traced to higher-than-expected shock loadings on the hydrogen gas valve that feeds the ion source. This unexpected shock loading occurred at the time the payload separated from the booster. This result emphasizes the importance of carefully specifying anticipated flight-induced shock and vibration

environments before designing flight hardware. This result has also stimulated new work on the parameters of stable ion source/injector operation, which could provide important design guidance for future NPB space systems. Second, spacecraft charging should be an important consideration in designing future NPB platforms for space. In particular, provisions must be made to protect against deleterious effects that might result from an unanticipated loss of beam neutralization.

The BEAR experiment successfully attained all of its objectives. Operation of an NPB in space was demonstrated for the first time, and first-of-a-kind NPB space physics data were obtained. The ability of the BEAR accelerator to survive recovery and to continue operating normally demonstrated the ruggedness of NPB systems, as postflight operation was not a design criterion. Perhaps most importantly, no phenomena were encountered that could significantly delay further development of NPB technology for space. Analysis of these data is continuing and will support the design of future NPB space experiments.

CONTENTS

FIGURES

TABLES

1. THE BEAR PROJECT

The Strategic Defense Initiative Office (SDIO), as part of its effort in Directed Energy Weapons, has been sponsoring the development of neutral particle beam (NPB) technology for use in space. As part of the initial development effort, a relatively low-cost precursory project was formulated to conduct an initial series of experiments using a small NPB accelerator launched along a suborbital trajectory by a ballistic rocket. This endeavor was called the Beam Experiments Aboard a Rocket (BEAR) Project. The intent was to adapt Los Alamos National Laboratory's (LANL's) ground-based NPB accelerator technology to spaceworthy hardware and test it in flight, thus obtaining an early data base on the engineering and phenomenological aspects of operating an accelerator in space. Such data will be invaluable in guiding the design of subsequent more sophisticated and expensive NPB space experiments.

The BEAR mission was successfully accomplished with the launch of the BEAR payload in July 1989 (frontispiece). This report documents the formulation and evolution of the project, the system flown, the results obtained, and the implications of those results for future space-based NPB systems. This volume provides a brief synopsis of the project and the flight hardware, together with an overview of the results. Its companion volume, Volume II, contains a detailed discussion and evaluation of the hardware and data produced by each major subsystem of the system flown.

The BEAR flight produced a plethora of valuable data, some not yet analyzed, correlated, or evaluated at this writing. Therefore, the results presented in this report, although reasonably definitive in most areas, are subject to change following further analysis. Topical reports will be forthcoming as a comprehensive data analysis is completed.

BEAR OBJECTIVES

The BEAR Project was formulated to provide at least preliminary answers to questions and issues concerning a space-based NPB system in two general categories: engineering and technology issues and space physics and phenomenology issues. These issues and questions were addressed under six specific mission objectives:

1. Operation in Space

The overriding objective of the mission was to demonstrate the successful operation of an NPB accelerator in space. Up to this point in its development, the NPB accelerator comprised a laboratory full of equipment: the beamline proper and all of the supporting vacuum equipment, radio frequency (rf) power supplies, controls, etc.—none of which was compact or rugged enough for flight and which required constant human surveillance and adjustment. The BEAR mission demanded miniaturization and weight reduction, ruggedization to survive flight environments, and the capability of autonomous operation.

2. Assessment of Beam Propagation

Because the NPB is unaffected by the earth's magnetic field, elementary considerations predict that the beam will propagate over large distances in space and that it will gradually be attenuated over its path by stripping interactions with gas molecules in the tenuous atmosphere. The concern was whether more subtle effects, such as anomalous stripping processes, would inhibit long-distance propagation. The BEAR experiment was designed to examine this issue. (Far-field beam magnetic optics distortion, caused by higher-order aberrations in the magnetic optics, is also of concern but could not be addressed by the BEAR configuration because the beam profile was not measured in the far field.)

3. Measurement of Spacecraft Charging

Since present technology does not permit creation of a beam consisting of 100% neutral species, the beam emitted by the accelerator contains a net charged component. Emission of some charged particles constitutes a loss of charge by the spacecraft, which will then undergo an increase in potential to a maximum voltage until this effect is nullified, on some time scale, by a return current from the ambient plasma. The concern was that differences in the voltage level attained by different parts of the spacecraft might result in effects deleterious to the accelerator or other spacecraft subsystems and/or might interfere with subsequent emission of the beam. The BEAR flight plan and instrumentation were therefore designed to address this important issue.

4. Studies of Neutral Effluent Effects

In addition to its primary "effluent"—the beam itself—the spacecraft inevitably produces effluents consisting of neutral gases. These effluents stem from normal, continuous, low-level outgassing from the exposed surfaces of spacecraft components; leaks from pressurized systems; and intermittent high-level bursts of gas from the neutralizer and the attitude control thrusters. The neutral gas effluents might affect NPB operation through high-voltage breakdown caused by trapped gases, beam stripping,

or enhanced spacecraft charging as a result of depletion of the ambient neutralizing plasma. Hence, these effects were investigated during the BEAR flight.

5. Investigation of Beam Avoidance

Since some charged particles are also generated in production of an NPB, the question arose of whether emitted ions gyrating around the geomagnetic field would return and strike the spacecraft and (at least in the case of a weapon-class system) cause significant damage, a potential shoot-yourself-in-the-foot syndrome. Two classes of potentially returning ions are generated: "prompt" ions emitted along with the neutral atoms in the beam and "delayed" ions produced when the neutral atoms are subsequently stripped by interaction with atmospheric particles. The BEAR payload was to be instrumented, and its trajectory and attitude relative to the geomagnetic field were planned, to collect and evaluate the returning particles. The data collected would be used to determine whether classical single-particle dynamics theory adequately predicts ion motion or whether beam "blowup" would occur as a result of collective plasma effects.

6. Observation of Unanticipated Phenomena

The final objective was of a catch-as-catch-can variety. It reflects the possibility that always exists in a first-of-a-kind set of experiments of this nature that some unanticipated space physics phenomenon might appear that would have deleterious effects (the unknown "unknowns"). A carefully planned set of relevant observations would be made within the limits of the capabilities of the on-board instruments and the variations in the space environment afforded by the flight profile.

Not every issue involving space operation of an NPB system could be answered, or even addressed, by the single, short-duration, suborbital BEAR mission. In particular, the phenomenology of beam/target interactions could not be investigated and had to be left to a subsequent space experiment.

ORGANIZATION AND HISTORY

The concept of an early suborbital flight of a small, treaty-compliant NPB accelerator on an instrumented sounding rocket was formulated in 1984. On June 3, 1985, after some preliminary planning and negotiations that had begun in April 1985, the BEAR Project received its initial funding. In this early phase of the project, SDIO placed the overall BEAR Project management under the Air Force's Space Technology Center through the Air Force Weapons Laboratory (AFWL) at Kirtland Air Force Base (AFB), New Mexico. Primary responsibility for development of the BEAR Project's scientific payload segment, subsequently named the Accelerator Payload Segment (APS), was assigned to LANL, although AFWL and the Naval Research Laboratory (NRL) were to provide some of the scientific instrumentation. Provision of the remainder of the vehicle system,

as well as integration and launch of the system, was the responsibility of the Air Force Geophysics Laboratory (AFGL), Hanscom AFB, Massachusetts. This management configuration, which is described in the Project Plan[1] and diagrammed in Figure 1, persisted through 1987. Early in this period, the conceptual design of the BEAR payload and a preliminary draft of the Experimentation Plan[2] were completed.

In FY 1986, the project effort was primarily directed at design— preliminary subsystem design and detailed component design—with the addition of supporting laboratory experiments. The preliminary design review (PDR)[3] occurred at AFWL in December 1985. In the course of the design and laboratory tests, the combined impact of both hardware requirements (minimal weight and packaging, thermal control, isolation of components, electromagnetic compatibility, and resistance to launch shock and vibration) and the need to maintain performance led to significant unanticipated basic design and development in several areas previously considered to be routine engineering tasks. Most important of these were the flight injector electronics, the rf amplifiers, the rf quadrupole (RFQ) cavity structure, and the Flight Vacuum Subsystem. LANL awarded a development subcontract to the Westinghouse Electric Corp. for the rf amplifiers and two major task order subcontracts for engineering support to Grumman Space Systems and McDonnell Douglas Missile Systems Co. (Section 3). The critical design review (CDR)[4] of the APS took place at AFWL in June 1986.

Detailed design and development continued through FY 1987. The unexpectedly large development effort resulted in a shortage of program funds in FY 1987 and delay of fabrication work. In addition, the then-current APS design was reviewed for the purposes of reducing weight and costs and shortening the schedule, and a revised configuration was established, which was essentially the design flown (Section 3).

In January 1988, SDIO redirected the project to pursue a very tight schedule. SDIO assumed direct management of the project and assigned to LANL overall technical responsibility for, and centralized technical management of, the project, including coordination of payload integration and provision of the plasma physics instruments. Interagency agreements were therefore established between the Department of Energy (DOE)/LANL and AFGL, between DOE/LANL and NRL, and between DOE/LANL and the National Aeronautics and Space Administration (NASA). LANL awarded an additional subcontract to SAIC, Inc., to meet this expanded responsibility. A BEAR Project team was formed at LANL, which included assignees from Grumman and McDonnell Douglas and was located in the immediate vicinity of the primary hardware development, test, and integration areas. This organization (Figure 2) remained in place through completion of design, fabrication, assembly, integration, test, launch, and postflight evaluation of the BEAR payload.
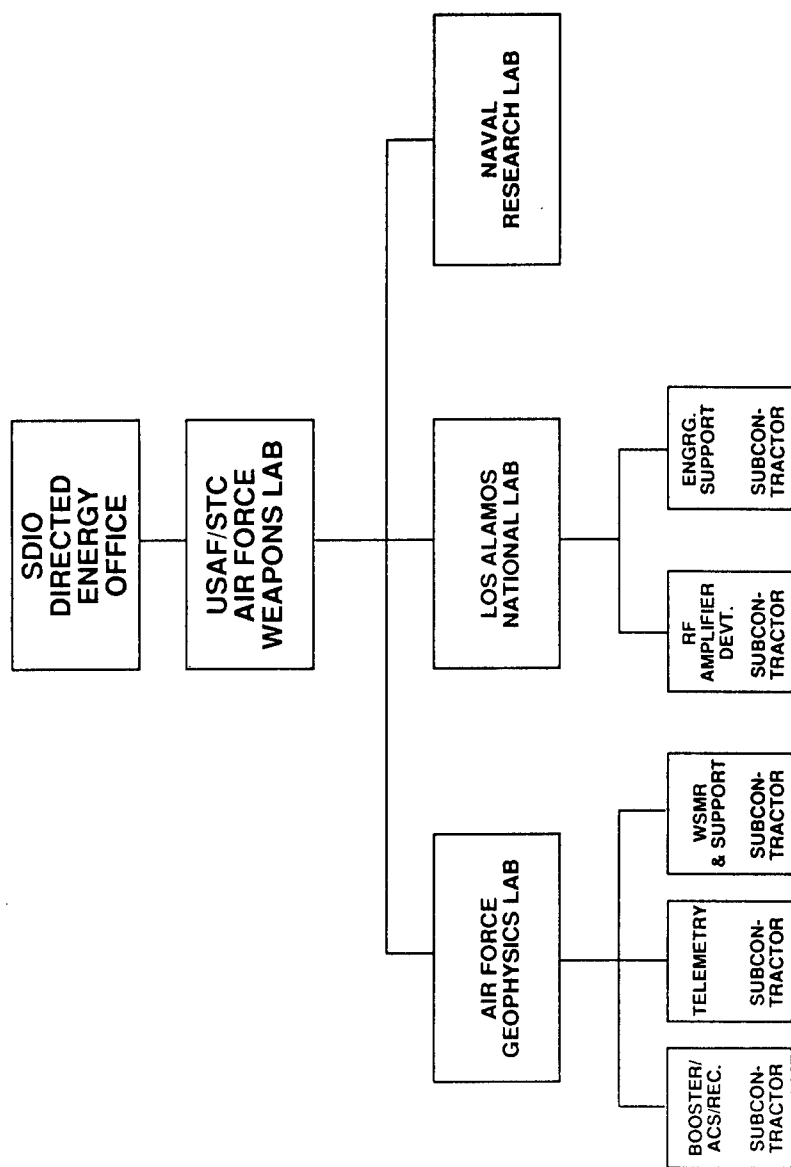
Figure 1. Original BEAR Project organization.
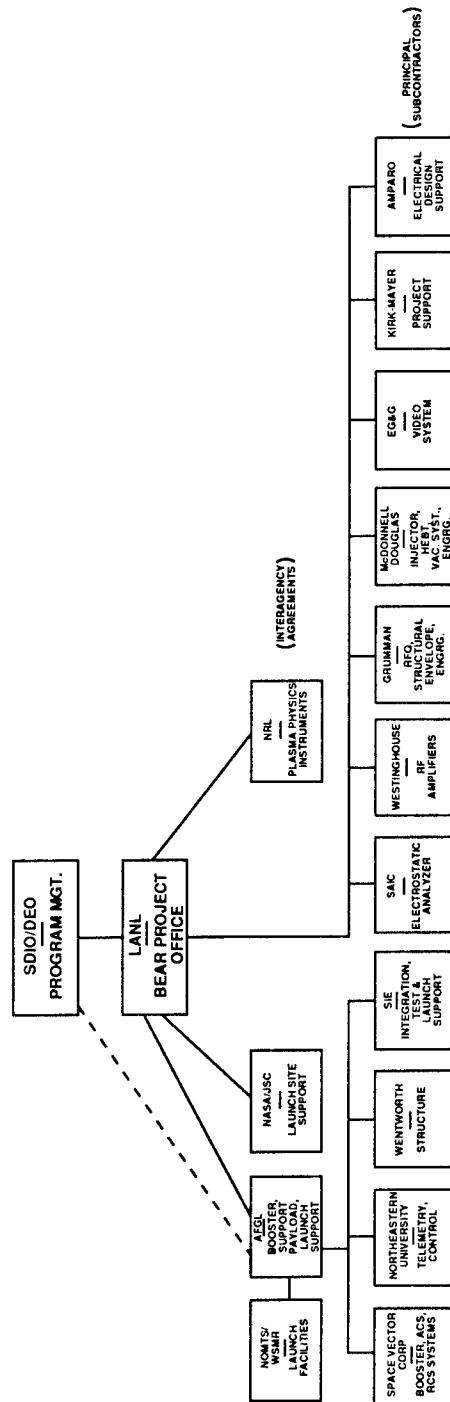
Figure 2. Organization of the redirected BEAR Project.

Integration and checkout of the payload system assembly were completed at LANL, and the system was shipped to White Sands Missile Range (WSMR) in April 1989. There the system was subjected to functional and environmental tests and, after one launch attempt in June that was aborted by a malfunction in the Booster Ignition Subsystem, the BEAR vehicle was launched successfully at 2:30 a.m. Mountain Daylight Time (MDT) on July 13, 1989, just 18 months after the project had been redirected. The major activities in the BEAR Project are shown in Figure 3.
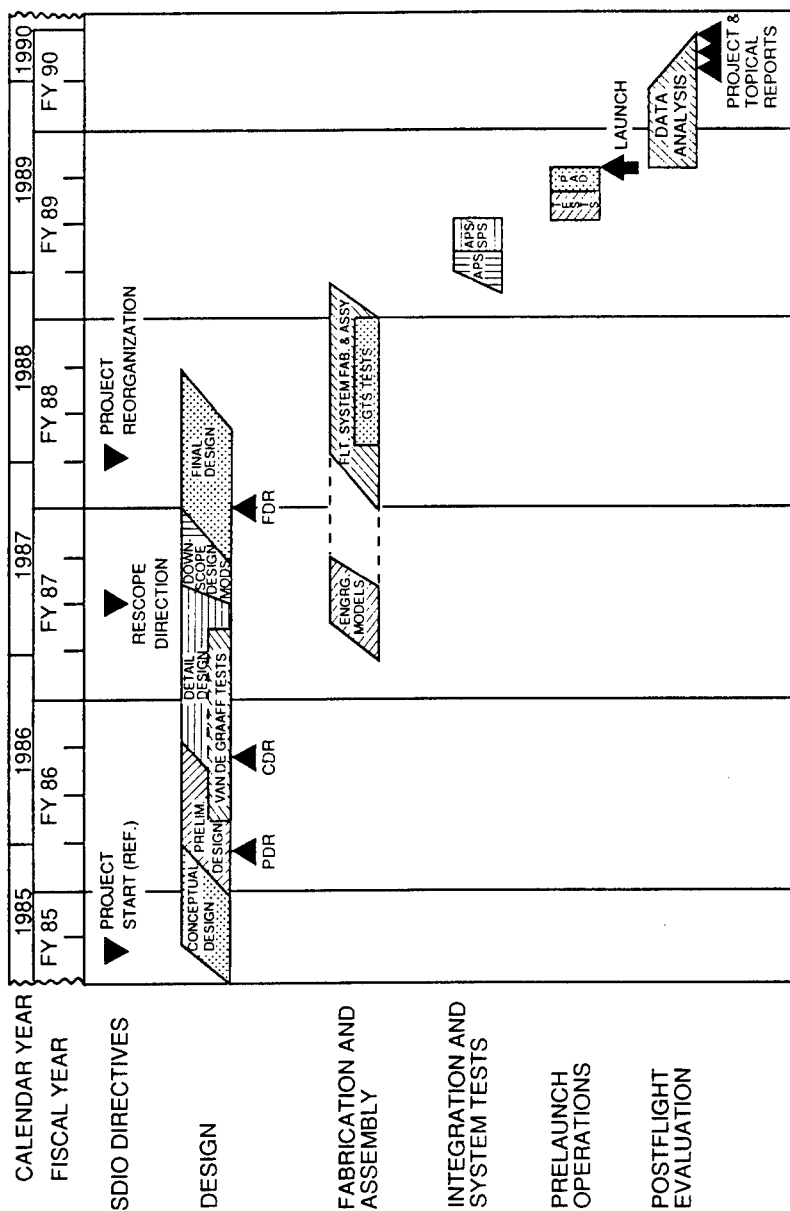
Figure 3. BEAR Project chronology.

2. THE BEAR EXPERIMENT

In addition to demonstrating the operation of an NPB system in space, the BEAR mission addressed several related space physics issues. The mission's objectives were to be satisfied by launching a scientific package comprising a small (1-MeV, 10-mA-equivalent neutral beam current) NPB accelerator and a complement of diagnostic instruments on a high-apogee ballistic trajectory. Appropriate data on the accelerator's performance, beam characteristics, and interactions of the vehicle with the environment were telemetered back to ground stations as the package executed preprogrammed maneuvers along the scientifically usable portion of its trajectory. Selected subsets of the data streams were also stored in an on-board recorder to provide redundancy of data acquisition; thus, the payload system contained a large parachute to permit a soft landing and recovery.

The design of the payload package reflected three major constraints:

- launch by a relatively small, single-stage booster (ARIES), which imposed severe weight limits, and, because the launch was suborbital, provided only a short time period above minimum useful altitude;

- limited funds and tight deadlines, which did not permit pursuit of an alternative design or provision of a spare unit (except in the case of the rf amplifier) for any major component; and

- design simplicity, because it is a one-of-a-kind unit and the first flight version of an NPB accelerator, and the system needed to have the highest possible reliability at the lowest possible cost.

These constraints mandated an accelerator whose operating conditions were fixed by prelaunch set points (Section 3). No uplink was provided to the vehicle (except Range Safety's command destruct capability), obviating any real-time in-flight adjustment of parameters. The only accelerator parameter somewhat under the experimenter's control was the degree of beam neutralization, which could be—and was—varied in a preprogrammed mode over a limited range.

The experimenters had limited control over the following external conditions:

- ambient pressure, by virtue of the change in altitude along the flight trajectory;

- condition of the local ionosphere, as a result of changes in altitude and the time of day selected for launch;

- payload attitude (beam direction vector) relative to the local geomagnetic field through programming of the Attitude Control Subsystem (ACS); and

- rate (or lack) of payload spin about its longitudinal axis, also through ACS programming.

All of these controllable factors were used in formulating an experimentation plan to meet BEAR mission objectives.

EXPERIMENTATION PLAN

The BEAR Experimentation Plan[2] describes the predicted trajectory and attitude maneuvers of the payload, the changing ambient neutral particle and plasma environment, and the programmed operation of the xenon gas injection neutralizer to nominally neutralize, underneutralize (not neutralize at all), or overneutralize the accelerated beam of H^- ions. The payload trajectory provides the variation in the ambient neutral atmospheric density to measure beam propagation and attenuation over a wide range of the parameter $n\sigma_x$. This parameter represents the product of the classical stripping cross section, σ_x, and neutral column density, n (over the distance propagation can be measured). The trajectory is also designed to include variations in the density and temperature of the background plasma so that spacecraft charging theories could be tested. The neutral atmospheric density varies from about $1 \times 10^{14}/cm^3$ at 90 km to $1 \times 10^{10}/cm^3$ at apogee. Therefore, before stripping, H^o would propagate about 1 meter at 90 km and about 9 km at apogee. Variation in ambient plasma density over the flight was from order $10^3/cm^3$ to order $10^4/cm^3$.

The BEAR flight had to be conducted at nighttime (i.e., after sunset at predicted apogee altitude) over White Sands Missile Range (WSMR). The ambient neutral atmosphere and ionosphere over WSMR are strongly influenced by two factors: time of day and solar activity. The time of day for launch could be selected arbitrarily. Since June 1976 was about the time of minimum activity for the solar cycle, a still relatively modest solar activity was expected in mid-1989, assuming that the 11-yr solar cycle held. To ensure optical observation, especially from the ground stations, it was also imperative that the moon not be within or near the field of view. These diurnal requirements were major factors in setting the launch window during each potential launch day.

BASELINE FLIGHT PROFILE

Figure 4 illustrates the baseline mission flight profile showing the nominal trajectory and planned attitude maneuvers. The predicted trajectory[5] is based upon an ARIES booster of nominal performance, together with the most recent prelaunch geometry and mass property estimates for the payload.

The vehicle is launched on an approximately due north azimuth and on a nearly vertical trajectory to maximize the apogee and to minimize downrange distance to impact. Booster burnout occurs after about 1 min at 44 km altitude, and separation of the payload is programmed at T + 85 sec (~80 km). During the next 10 sec, the sensor-covering doors are jettisoned and the boom-mounted sensors are deployed. The first programmed pitch maneuver is executed concurrently, rotating the payload through an angle of about 30° in the pitch plane to align the beam axis with the local geomagnetic field (**B**) vector, with the beam aimed downward along the field. The beam itself is emitted into the atmosphere beginning at about T + 128 sec, near the minimum useful experimental altitude of 135 km. For about the next 48 sec, over an altitude increment of some 43 km, the accelerator is operated in this attitude, followed by a quick pitch maneuver of about 90° inaugurated to orient the beamline approximately orthogonal to the local **B** vector and pointing 155° SSE azimuth. Roll rates of 4 rpm, followed by 12 rpm and finally 20 rpm, are then introduced. Next, the 20-rpm roll, coupled with programmed pitch-and-yaw impulse bits, causes the direction of the beam axis to nutate conically over a small angle, approximately ±4°, about the normal to the **B** vector. The accelerator continues to operate in this orientation and "coning" mode through apogee (at about T + 249 sec and 204 km) and back down to below the 135-km experimental altitude limit. At T + 390 sec and approximately 114 km, the beam is shut down and the vehicle is reoriented for reentry. Thus, the scientifically usable part of the trajectory nominally spans an altitude range of 114 to 205 km and lasts about 4-1/2 min. The parachute is deployed at low altitude (4 to 6 km) and retards the impact velocity to 6 to 9 meters/sec (20 to 30 ft/sec), permitting recovery some 80 km downrange of the launch point.

The first attitude maneuver is designed to provide maximum airglow signal for the TV cameras as the beam is aligned with the geomagnetic field. The injections perpendicular to **B** are used to measure NPB propagation and to test for plasma instabilities in the concomitant ion beams. Varying the spacecraft's orientation also changes the electron current collection area perpendicular to the **B** vector. Spinning the payload provides a small modulation of the injection pitch angle (via the induced coning), varies the direction of the $\mathbf{v} \times \mathbf{B}$ force on the H^- ions in the accelerator, causes a small artificial gravity for nonaxially mounted components, and varies the orientation of sensors with respect to the geomagnetic field. The Experimentation Plan also used ACS subsystem firings to provide mild shocks to the payload and to generate neutral effluents.

11

BEAR MISSION FLIGHT PROFILE
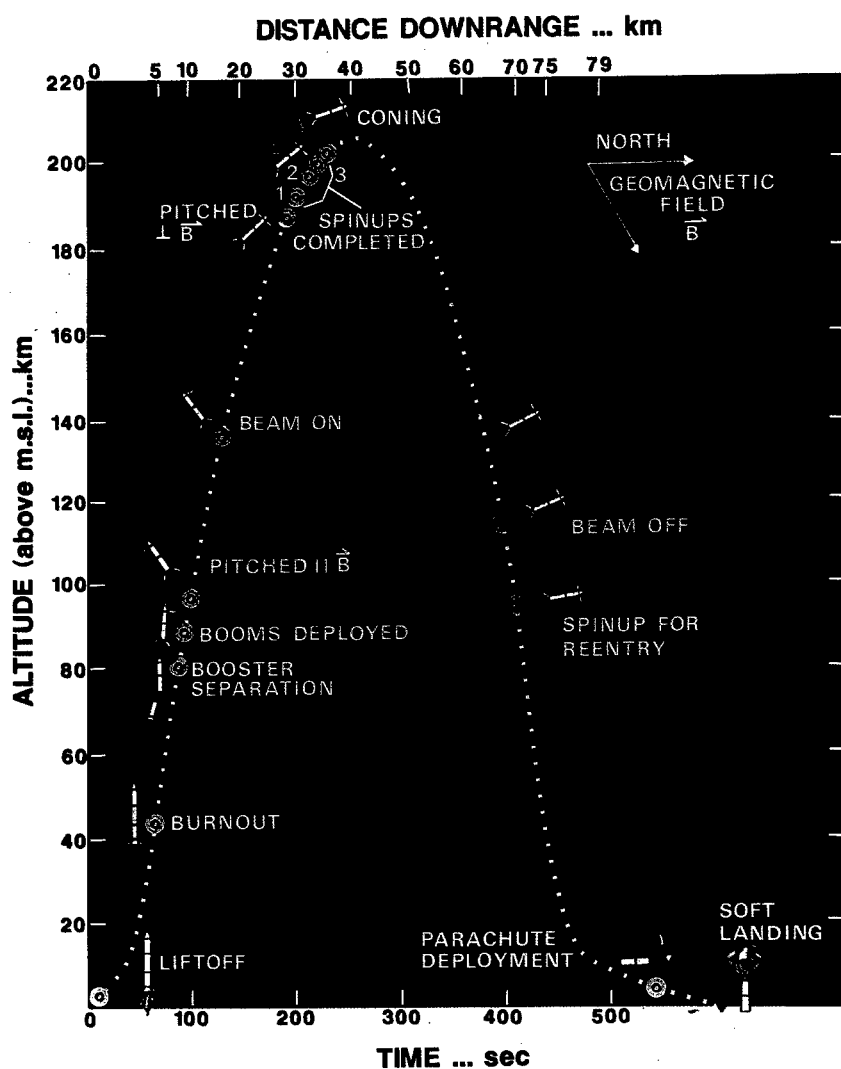
Figure 4. BEAR mission flight profile (baseline).

The xenon neutralizer is turned on at T + 127 sec, off at T + 260 sec, on at T + 270 sec, off at T + 322 sec, and back on at T + 332 sec. At T + 360 sec, the overneutralize command is given, and extra xenon is added to each subsequent neutralizer pulse. Modifying the neutralizer operation provides the test of spacecraft charging theories. When the neutralizer is operating nominally, only about 0.8 mA net negative current is emitted during each pulse. When the neutralizer is turned off, the net negative current leaving the spacecraft is much larger, about minus 10 mA. Overneutralizing changes the net current emitted to approximately 1 mA positive.

INSTRUMENT COMPLEMENT

The payload contained four classes of instrumentation:

- accelerator internal diagnostic (AID) instrumentation,

- beam diagnostics (BD) instrumentation,

- plasma physics diagnostics (PPD) instrumentation, and

- dynamics instrumentation.

The AID instrumentation comprises a set of distributed measurements internal to the beamline components and some of their supporting electronics. These measurements, summarized in Table I, are principally voltages and currents, together with a few pressure, temperature, flow, position, and frequency measurements. Together, they continually monitor the state of health and performance of each of the accelerator's subsystems and serve as diagnostics in the event of anomalous performance.

The BD instrumentation, comprising the Shadow Wire Scanner (SWS), Beam Current Monitor (BCM), and video cameras, is located in the BD Section of the payload, just aft of the Accelerator Payload Segment (APS), and the beam traverses this section in exiting the vehicle. The objective of this set of instruments is to observe the composition, flux, pointing, divergence, and energy characteristics of the pulsed beam in both spatial and temporal dimensions. A summary of the instruments used and the characteristics measured by the BD set is presented in Table II. Although the geomagnetic field and airglow are not strictly "instruments" in the sense of discrete on-board packages, the spacecraft trajectory and attitude maneuvers are configured to quantitatively exploit these phenomena in assessing the beam's behavior. This minimal set of selected instruments still provides a considerable degree of redundancy.

The purpose of the PPD instrument set, which is located partially in the BD Section and partially in the Telemetry/Physics (TP) Section of the payload, was to study the interactions of the accelerator and its effluent particles with the vehicle itself and with the ambient rarefied atmosphere in various orientations relative to the local geomagnetic field. Specifically,

13

TABLE I

ACCELERATOR INTERNAL DIAGNOSTIC MEASUREMENTS

	VOLTAGE	CURRENT	FREQ.	PRESSURE	TEMP.	FLOW	POSITION
ION SOURCE							
Arc Discharge	●	●					
Hydrogen Gas				(2)		●	
I&C Power	●	●					
250-V Power Supply	●	●					
Cathode Heater	●	●					
Anode Heater	●	●					
75-V Bus	●						
Filament		●					
High-Voltage Pow. Sup.	●	●					
Anode					●		
Cathode					●		
Arc Region Housing					●		
Extractor Pulser	●	●					
Extractor Heater	●	●					
Extractor		●			●		
LEBT							
Gate Valves							(2)
56-V Input	●	●					
Beam Current Monitor		(2)					
Faraday Cup Valve							●
Faraday Cup		●					
Seg. Aperture Assy. I		(4)					
Seg. Aperture Assy. II		(4)					
Seg. Aperture Assy. III		(4)					
Vacuum H_2	●			●			
Xenon Gas	●			(2)			
OTHER INJECTOR							
Freon Coolant						●	
Coolant Inlet					●		
Coolant Differential					●		
Cold Plates					(2)		
28-V Supply	●	●					
RF POWER							
40-V Reg. A and B	(2)						
Power A and B	(2)						
5-V DC 1 and 2	(2)						
±15-V DC 1 and 2	(2)						
15-V DC Linear 1 and 2	(2)						
RF Control Voltage	●						
Onboard 5-V DC	●						
VCO			●				
Amplifier B Cur. Mon.		●					
Forward RF Waveform	(2)						
Reflected RF Waveform	(2)						
RFQ Cavity Waveform	(2)						

TABLE I (continued)

ACCELERATOR INTERNAL DIAGNOSTIC MEASUREMENTS

	VOLTAGE	CURRENT	FREQ.	PRESSURE	TEMP.	FLOW	POSITION
HEBT							
Beam Current, Fwd.		●					
Beam Current, Aft		●					
Shadow Wire		●					
Pin Probe Assy.		(4)					
Seg. Aperture Assy.		(4)					
Vacuum				●			
Gate Valve							●
BEAMLINE CRYOTRAP							
APS Ambient at BLC				●			
300-K-Range Temps.					(3)		
30-K-Range Temps.					(3)		
NEUTRALIZER							
Vacuum				(2)			
Xenon Gas Supply				●			
Pulse Valve					●		
Body					●		
Skin					(2)		
N$_2$ Bottle Press Switch							●
Beamline Valve							●
DC POWER SUBSYST.							
Battery #1	●				●		
Battery #2	●				●		
Battery #3	●				●		
Battery #4	●				●		
Accel. Relay Box				●	●		
CONTROL SUBSYST. SETPOINTS							
250-V PS Voltage	●						
Arc Current	●						
Anode Heater Temp.	●						
Cathode Heater Temp.	●						
High-Voltage Power Supply	●						
H$_2$ Valve	●						
Xe Valve	●						
Extractor Heater Temp.	●						
Extractor High Voltage	●						
RF Amplifier	●						
Gas Pulse Width	●						
Arc Pulse Width	●						

15

TABLE II

BEAM DIAGNOSTICS

Instrument / Parameter	Geomagnetic Field	Beam Current Monitor	Shadow Wire Sensor	uv TV + Airglow
Charge Composition	●	●		●
Beam Current		●	●	●
Beam Pointing			●	●
Beam Divergence			●	●
Pulse-to-Pulse and Intrapulse Jitter			●	
Emittance			●	
Pulse Temporal Profile		●	●	

these instruments monitored beam propagation, changes in vehicle potential, return flux of charged particles, the neutral density path, the density and temperature of proximate plasma, and radiated emissions in the form of airglow and plasma waves. Table III shows a similar matrix of PPD instruments used versus parameters observed. Several of these instruments are mounted on extensible booms, which were deployed after booster separation.

The fourth class, dynamics instruments, consists of the booster and attitude control gyro subsystems, which are used to monitor the dynamics of the vehicle as a whole, as well as a set of strategically mounted low-range and high-range accelerometers to meter the relative motions of portions of the payload structure caused by flight shocks and vibration. Also included in this category is the intensified, visible-light TV camera, which observes vehicle motion from its perspective inside the BD Section, as well as beam efflux and other local events inside that section.

The AID and dynamics instruments were functional throughout the flight until powerdown at reentry. The remaining instruments were turned on after booster separation, operated through the experimental portion of the flight, and were turned off at powerdown. Dual redundant data streams were produced and transmitted at a 64-kbit/sec data rate with backup onboard recording. Optical isolation was provided in critical signal lines in the Accelerator Section to preclude induced electromagnetic interference.

OVERVIEW OF THE VEHICLE

The BEAR vehicle is essentially a large, single-stage, solid-propellant rocket. The cutaway perspective (Figure 5) indicates the division of the vehicle assembly into three principal segments.

- Launch Vehicle Segment (LVS),

- APS, and

- Support Payload Segment (SPS).

The LVS is the separable booster, while the other two segments—the APS plus SPS—constitute the experimental payload system. Figure 6 describes schematically, and Figure 7 shows pictorially, the stackup on the launch pad.

Each segment is functionally divided into two sections. The LVS is made up of the Booster or Rocket Motor (RM) Section and a Motor Adaptor (MA) Section. The RM Section is a refurbished Minuteman I second-stage, solid-propellant motor fitted with a new hydraulic control system for the nozzles' thrust vector control actuators and a "tailcan" with fins that provide aerodynamic stability. In this configuration, the motor is called an ARIES booster. The MA Section, as its name suggests, provides the mechanism to mate the motor to the payload. Equally important, the MA

17

TABLE III

PLASMA PHYSICS DIAGNOSTICS

Instrument / Parameter	Solid-State Particle Detectors (SSD)	Narrow-Band uv TV	Cold-Cathode Ionization Gage (CCIG)	Electrostatic Analyzer (ESA)	Langmuir Probes	High-Voltage Detector (HIV)	Plasma Wave Receiver (PWR)
Beam Propagation	●	●					
Spacecraft Potential				●		●	
Return Particle Flux	●			●			
Neutral Density Path			●				
Local Plasma Electron Density and Temperature					●		
Plasma Waves							●
Airglow		●					

BEAR MISSION ROCKET ASSEMBLY

Figure 5. BEAR mission rocket assembly.

19
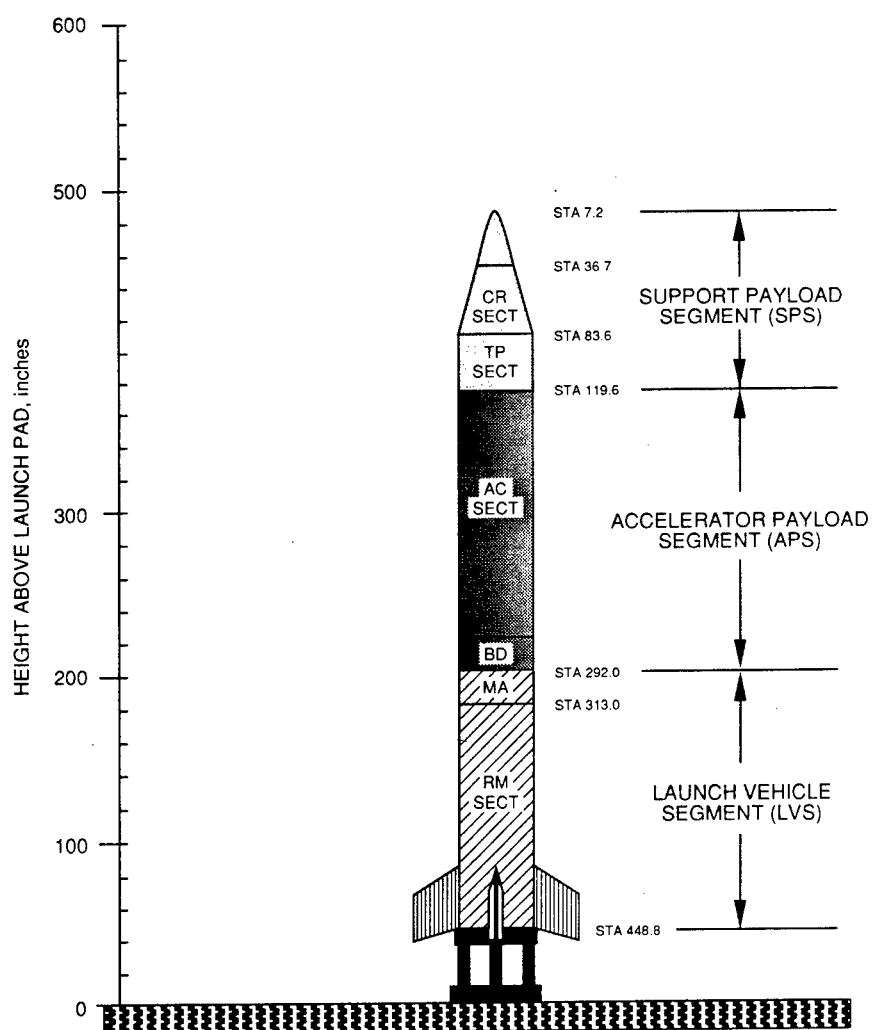
Figure 6. Stackup of the BEAR vehicle.
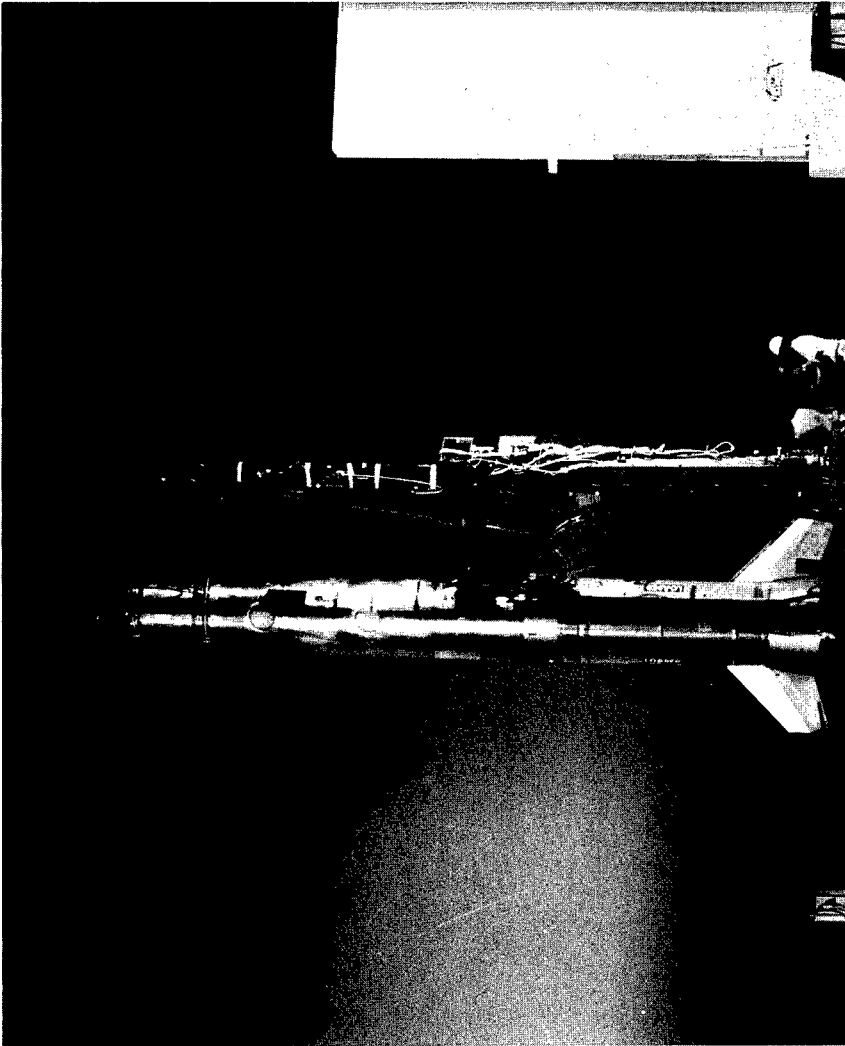
Figure 7. BEAR vehicle on launch pad.

Section contains the Booster Control Subsystem, the payload separation mechanism, Range Safety's Command Destruct Subsystem, and a small light source to calibrate the ultraviolet (uv) TV.

The SPS comprises the Control and Recovery (CR) Section and the TP Section. The CR Section houses the ACS—platform with gyros and electronics; gaseous nitrogen feed system; and pitch, yaw, and roll thrusters—and the 104-ft-diameter recovery parachute with its deployment mechanism. During launch, this section was capped by a subsequently jettisoned conical aerodynamic nose fairing. The TP Section is axially partitioned into two subsections. The forward section contains the PPD instruments (other than the Langmuir probes) with associated electronics and deployment mechanisms, and the aft subsection contains the redundant pulse-code-modulated (PCM) and video telemetry subsystem, the on-board recorder, and certain controls.

The geometry and mass properties of the BEAR vehicle are summarized in Table IV. A list of the responsible organizations and primary subcontractors (where applicable) for the major subsystems is given in Table V. Since this report deals primarily with the scientific payload and its performance, that portion of the vehicle is discussed further in Sections 3 and 4 and is addressed in detail in Volume II.

TABLE IV
BEAR VEHICLE GEOMETRY AND MASS PROPERTIES

SEGMENT	DIAMETER (in.)	(cm)	LENGTH (ft/in)	(m)	LIFTOFF WEIGHT (lb)	(kg)
SUPPORT PAYLOAD SEGMENT (*without nose fairing)	44.0 max. 18.4 min.*	111.8 46.8	9'4.4"	2.85	947.	429.5
ACCELERATOR PAYLOAD SEGMENT	44.0	111.8	14'4.4"	4.38	2461.	1116.3
SUBTOTALS, PAYLOAD SYSTEM			23'8.8"	7.23	3408.	1545.8
LAUNCH VEHICLE SEGMENT	44.0	111.8	13'1.0"	3.99	12,270.	5565.6
TOTALS, BEAR VEHICLE			36'9.8"	11.22	15,678.	7111.4

TABLE V

BEAR VEHICLE SUBSYSTEM RESPONSIBILITIES

SEGMENT	RESPONSIBLE AGENCY	SECTION	SUBSYSTEM	PRINCIPAL SUBCONTRACTOR(S)
LVS	AFGL	RM	M56A-1 Motor	—
			Tailcan and Actuators	Space Vector Corp.
		MA	Structure	Space Vector Corp.
			Booster Control	Space Vector Corp.
			Separation	Space Vector Corp.
			Command Destruct	WSMR Range Safety
APS	LANL	Accelerator	Structure	Grumman/LANL
			Beamline	LANL/Grumman/ McDonnell Douglas
			RF Power	Westinghouse/LANL
			Vacuum	LANL/McDonnell Douglas
			DC Power	LANL
			Control/Data Acq.	LANL
		BD	Structure	Grumman/LANL
			SWS/BCM	LANL
			Video	EG&G
			CCIGs	AFWL/LANL
			SSDs	LANL
			Langmuir Probes	Naval Res. Lab
SPS	AFGL	TP	Structure	Wentworth
			DC Power	Northeastern Univ.
			Telemetry/Recording	Northeastern Univ.
			Master Command	Northeastern Univ.
			ESA	SAIC, Inc.
			PWR	Naval Res. Lab
			HIV	Naval Res. Lab
		CR	Structure	Space Vector Corp.
			ACS	Space Vector Corp.
			Recovery	Space Vector Corp.

24

3. THE BEAR SCIENTIFIC PAYLOAD

The complete BEAR payload system (Figure 8) consists of the Accelerator Payload Segment (APS) and the Support Payload Segment (SPS). The scientific part of this system, i.e., those elements responsible for creation of the beam and for measuring its characteristics and observing its interactions, comprises most of the subsystems and the instruments housed in the APS, together with the instruments and some of the equipment located in the Telemetry/Physics (TP) and Control and Recovery (CR) sections of the SPS. The configuration and operation of these subsystems and instruments only are summarized in this section. They are discussed in greater detail—along with supporting subsystems, wiring, incidental structure, etc.—in Volume II and in References 5 and 6.

ACCELERATOR

The accelerator proper—the complex mechanism that produces the beam—is the heart of the scientific payload and occupies a major fraction of the APS. The accelerator is made up of a group of serially connected subsystems called the beamline, which form and contain the beam, and is coupled to the necessary power and gas supplies and the evacuation subsystem. The role of each of these subsystems in the operation of the NPB accelerator is illustrated conceptually in Figure 9.

Since only a beam of electrically *charged* particles can be accelerated electromagnetically to high energy levels, the NPB begins its life as a plasma of negatively charged particles, i.e., negative *ions*, in the *ion source*. Between the anode and cathode of the ion source, a strong electric current is passed through ordinary hydrogen gas containing a small amount of metallic cesium vapor (to facilitate production of H^- ions). In the intense arc that results, some of the hydrogen molecules are broken into individual atoms, and these, in turn, acquire an extra electron to become the H^- ions from which the beam is formed. The ion source is biased at a potential of -30 kV relative to the extractor electrode. The H^- ions are accelerated across the gap between the ion source aperture and the extractor. Electrons are separated from the H^- ions by a dipole magnetic field near the source.

Passing through the narrow slit in the extractor electrode, the H^- ions enter the next beamline subsystem, the Low-Energy Beam Transport (LEBT), as a thin diverging beam. Although essentially a passive component, the LEBT accomplishes three important functions: its externally

BEAR PAYLOAD SYSTEM

SUPPORT PAYLOAD SEGMENT (112 in.)

ACCELERATOR SECTION (172 in.)

RECOVERY PARACHUTE

ACS N₂ BOTTLE (1 of 4)

HIGH IMPEDANCE VOLTMETER BOOM

TELEMETRY EQUIPMENT

PLASMA WAVE RECEIVER BOOM (1 of 2)

GETTER PUMP (1 of 3)

INJECTOR

VACUUM ISOLATION GATE VALVE (1 of 3)

RADIO FREQUENCY QUADRUPOLE (RFQ)

RF AMPLIFIER (1 of 2)

HEBT

BEAMLINE CRYOTRAP

MASTER CONTROLLER

SPACE FRAME

N₂ RESERVOIR

ELECTRON SWEEP MAGNET

BEAM CURRENT MONITOR

VISIBLE VIDEO CAMERA

BATTERY BOX (1 of 6)

XENON RESERVOIRS

MIRROR (1 of 2)

SOLID-STATE DETECTOR

NEUTRALIZER ASSY

CCIG (1 of 2)

INTENSIFIED 'ULTRAVIOLET' VIDEO CAMERA

SHADOW WIRE SCANNER SENSOR ASSY.

LANGMUIR PROBES (1 of 4)

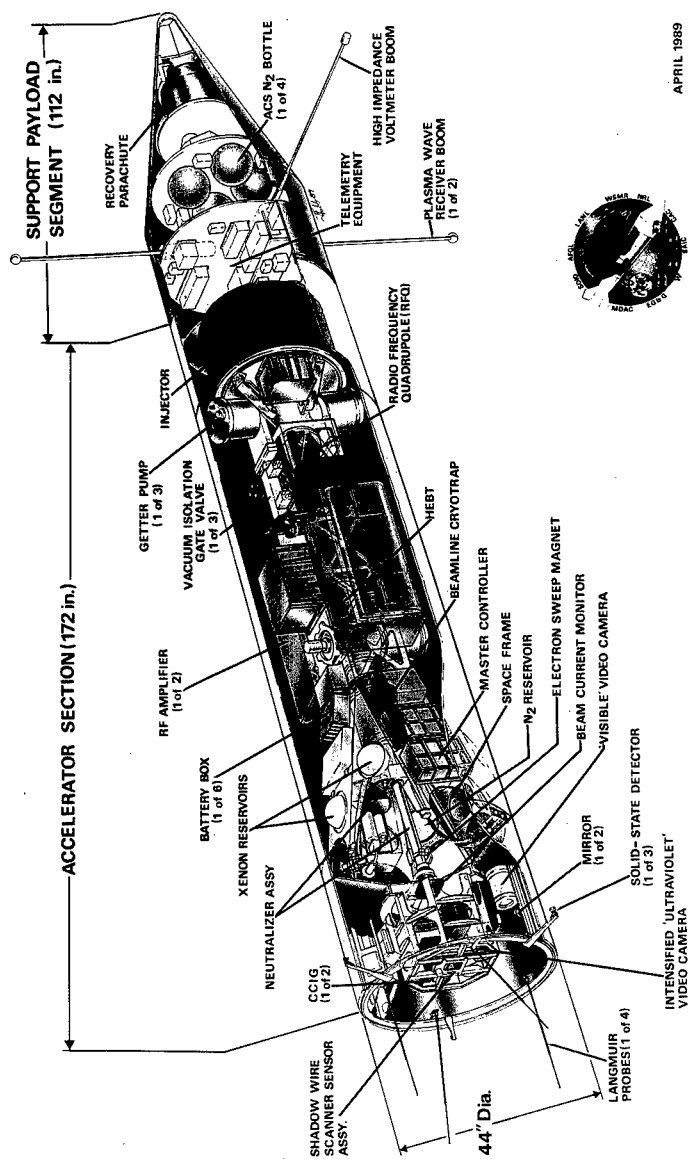44" Dia.

APRIL 1989

Figure 8. BEAR Payload System.

Figure 9. The NPB accelerator.

27

mounted vacuum ("getter") pumps remove the excess (nonionized) hydrogen that escapes from the ion source, preserving the vacuum; it adds a tiny amount of xenon gas needed to stabilize the beam; and, most importantly, its set of powerful permanent magnets focuses and "matches" the H^- beam so that the next assembly downstream, the rf quadrupole (RFQ) cavity, will accept that beam. Using the BEAR Project's terminology, the ion source and the LEBT assembly with its associated electronics and ancillary components will hereafter be referred to as the Injector Subsystem.

The RFQ is a uniquely configured resonant cavity in which the final and major part of the beam acceleration takes place. Leaving the injector and entering the RFQ, the H^- ions carry an energy of about 30 keV. Interaction with the high-frequency rf fields as they traverse the RFQ focuses and "bunches" the H^- ions and accelerates them to an essentially uniform energy of 1 MeV.

Following the RFQ is another passive subsystem of magnetic optics, similar to the LEBT in the injector assembly, which is called the High-Energy Beam Transport (HEBT). The HEBT reshapes the divergent beam of high-energy H^- ions leaving the RFQ into a collimated (parallel) beam of the desired diameter—in this instance 2.5 cm.

From the HEBT, the beam passes through a cryotrap—an annular cryocondensation pump cooled with liquid helium to about 4 K—which removes the other (nonhydrogen) trace gases from the beamline vacuum space. Finally, the H^- beam enters the neutralizer. The BEAR accelerator uses a gas-cell-type neutralizer in which the beam is passed through a precisely metered and spatially dispersed puff of xenon gas. Some of the H^- ions pass through unaffected. The others undergo stripping collisions with the xenon atoms. In some of these collisions, the extra electron added in the ion source is removed from the H^- ion, leaving it a neutral H° atom (the desired neutralization effect); in other cases, hydrogen's normal electron and the extra electron are stripped away, leaving an H^+ ion (i.e., a proton). Thus, the beam exiting the accelerator is not constituted of 100% neutral particles but is rather a mixture of neutrals with both positively and negatively charged species. Theory predicts, and measurements have confirmed, that a maximum of about 52% neutralization can be achieved in this process.

The principal components of the BEAR accelerator are shown in Figure 10. It is operated in a pulsing mode to conserve battery power and to minimize cooling problems. It produces beam pulses 50 μs in duration at a repetition rate of 5 pulses/sec. The fundamental design parameters for the BEAR accelerator's output beam are listed in Table VI, and its integrated configuration is shown in Figure 11.

Between February 1988 and January 1989, the primary development effort on the BEAR accelerator was centered on the Ground Test Stand (GTS) at Los Alamos. The objectives of GTS testing were (1) to provide a facility for the development, testing, and functional flight qualification of
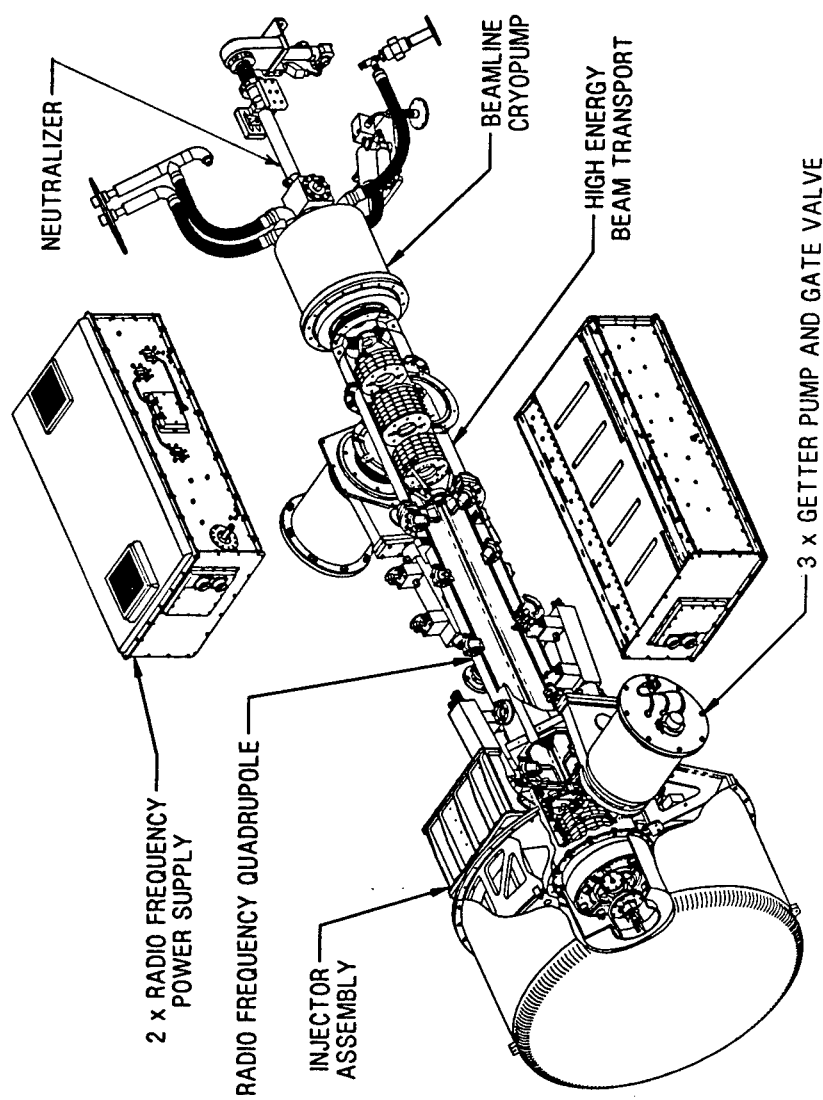
Figure 10. BEAR accelerator design.

NEUTRALIZER

BEAMLINE
CRYOPUMP

HIGH ENERGY
BEAM TRANSPORT

3 x GETTER PUMP AND GATE VALVE

2 x RADIO FREQUENCY
POWER SUPPLY

RADIO FREQUENCY QUADRUPOLE

INJECTOR
ASSEMBLY

TABLE VI

ACCELERATOR OUTPUT BEAM DESIGN PARAMETERS

Parameter	Specification
Particle Energy	1. MeV
Beam Output Currents	
Neutral Atoms (H°), minimum	10. mA (equivalent)
Negative Ions (H^-)	5. mA
Positive Ions (H^+)	5. mA
Angular Divergence	$\pm 1.$ mrad
Diameter	2.5 cm
Pulse Width	50. μs
Repetition Rate	5. pps
Emittance	0.01π cm-mrad

the accelerator components; (2) to demonstrate the detailed performance characteristics of individual accelerator components; (3) to demonstrate the detailed performance of the integrated accelerator system; and (4) to test and calibrate the Beam Diagnostics (BD) Section's beam-sensing systems. The test program was successfully accomplished and provided a flightworthy accelerator ready for integration into the payload system. Each major subsystem of the accelerator is discussed briefly in the following paragraphs.

Injector

The design requirements for the injector—the most ambitious piece of accelerator hardware (Figure 12)—are presented in Table VII. The flight configuration of the injector, which was developed by LANL in conjunction with the McDonnell Douglas Missile System Co., is shown in Figure 13.

The H^- ion source is a cesiated Penning-Dudnikov source that has been highly modified and engineered for flight. Cesium is provided in the form of a mixture of the compound cesium dichromate ($Cs_2Cr_2O_7$) with metallic titanium powder, which is compacted in a small cavity "insert" fitted into the anode. As the anode is heated, chemical reaction of the compacted powder liberates metallic cesium vapor to the plasma arc region,
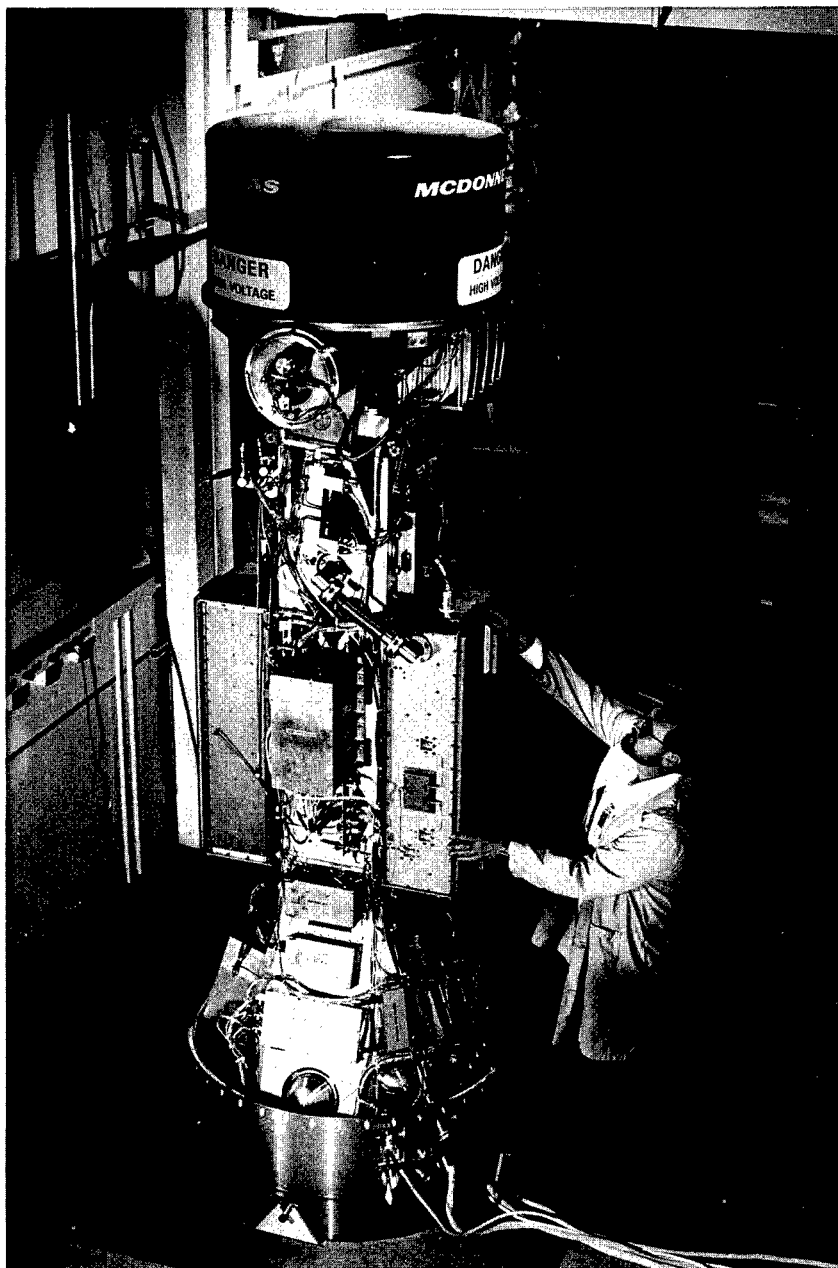
Figure 11. The BEAR accelerator.
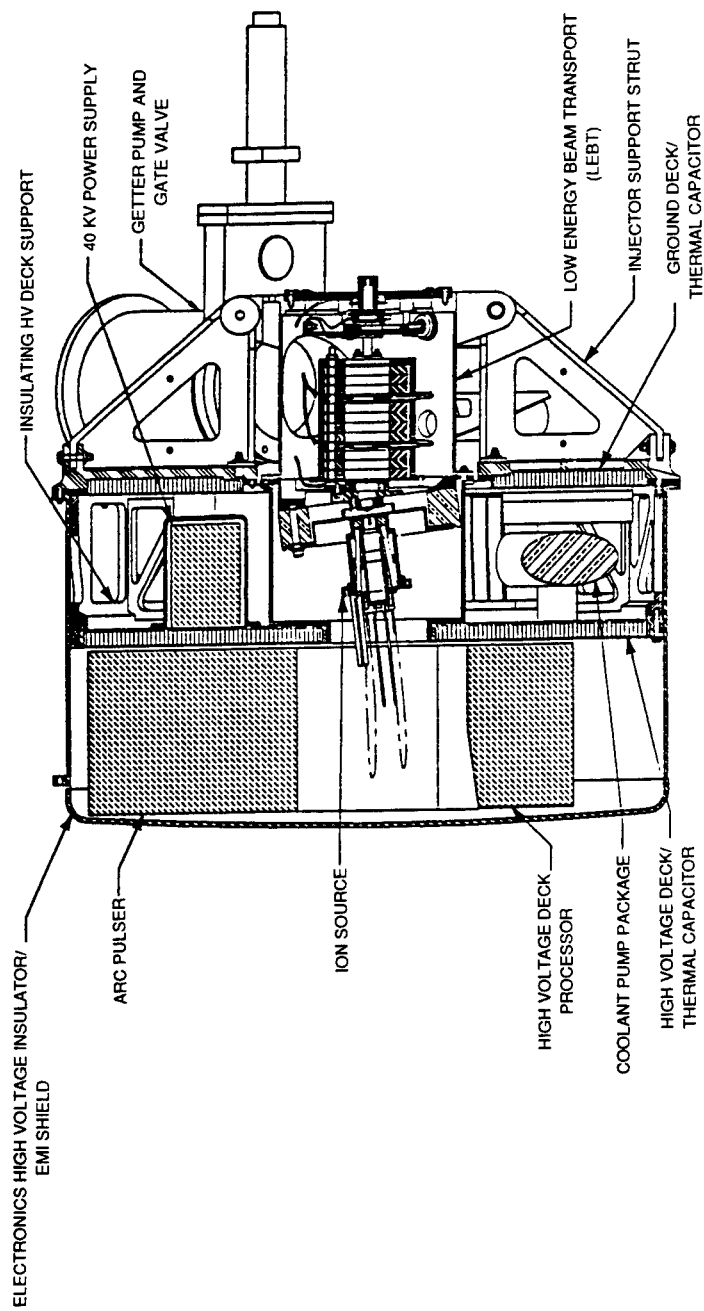
Figure 12. BEAR injector design [McDonnell Douglas].

ELECTRONICS HIGH VOLTAGE INSULATOR/
EMI SHIELD

INSULATING HV DECK SUPPORT

40 KV POWER SUPPLY

GETTER PUMP AND
GATE VALVE

LOW ENERGY BEAM TRANSPORT
(LEBT)

INJECTOR SUPPORT STRUT

GROUND DECK/
THERMAL CAPACITOR

ARC PULSER

ION SOURCE

HIGH VOLTAGE DECK
PROCESSOR

COOLANT PUMP PACKAGE

HIGH VOLTAGE DECK/
THERMAL CAPACITOR

TABLE VII

INJECTOR DESIGN PARAMETERS

Parameter	Specification
Beam Particle	H^-
Output Current	40. mA (minimum)
Particle Energy	30. keV (nominal)
Pulse Duration	130. μs
Repetition Rate	5. pps
Emittance	0.01π cm-mrad (rms)
Beam Alignment Tolerances at LEBT Exit, Maximum	
Positional	±0.25 mm
Angular	$\pm10.$ mrad
Operating Modes	
Startup	Manual
Steady State	Autonomous (programmed)

where it donates electrons to the arc discharge. The TZM molybdenum cathode and stainless steel anode assembly is a self-aligning system contained in an aluminum housing. Both the anode and cathode are actively heated by internal heaters, and both electrodes are temperature controlled. The H^- ions are extracted from the source at about 30 kV across a single 3.5-mm gap.

The LEBT contains a fixed-focus, quadrupole magnet triplet composed of precisely positioned blocks of neodymium-iron-boron permanent magnets. Several iterations of magnet positioning were carried out on the GTS to attain the optimum configuration. Because these magnets are temperature sensitive, the LEBT's supporting structure was designed to minimize variations in internal temperature. The beam match to the RFQ is further optimized by controlling the plasma neutralization in the LEBT through the addition of a small amount of xenon gas.

In addition to the H^- ion source and LEBT, the injector includes the associated structure, electronics, and cooling provisions. The injector

Figure 13. Flight injector with cover removed [McDonnell Douglas].

assembly is 81 cm (32 in.) long, 91 cm (36 in.) in diameter, and weighs 218 kg (481 lb). The actual injector output beam current is typically about 50 mA, and somewhat less than half of this beam is matched into the RFQ. Output currents in excess of 70 mA have been 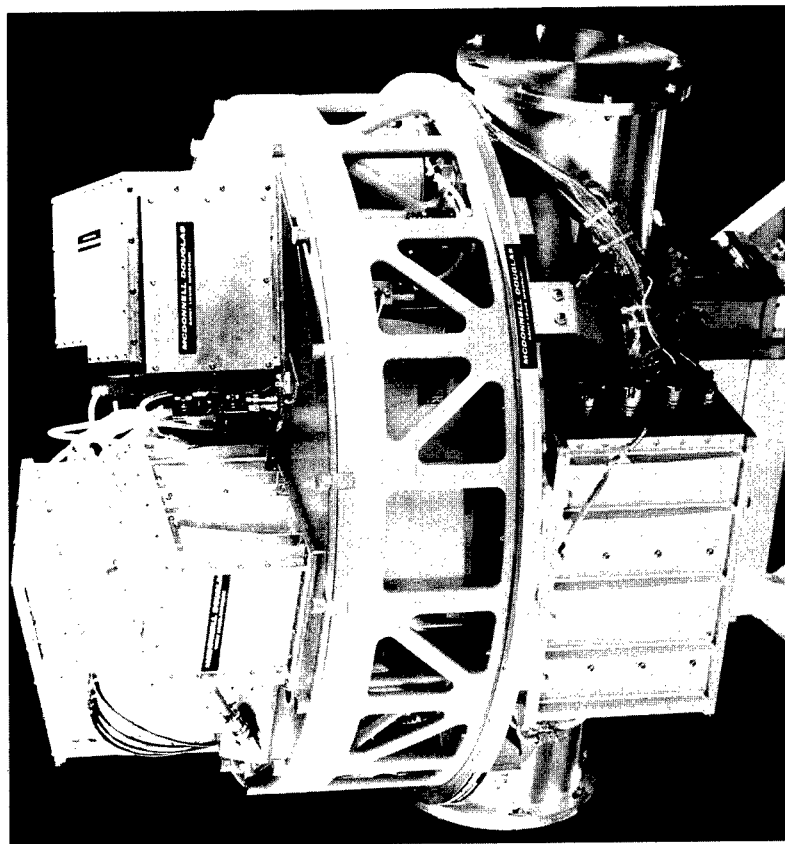observed for operation near the ion source's arc current and arc voltage limits. During tests and the flight, the injector output beam current was measured by a current toroid located at the output end of the LEBT.

RFQ Assembly

The RFQ is the resonant cavity in which the matched fraction of the injector's output current is focused, bunched, and accelerated to its 1-MeV terminal energy level. It is a monolithic structure containing four longitudinal vanes whose inner edges are geometrically modulated in a sinusoidal pattern of increasing wavelength and amplitude and are phased for axial acceleration. The design requirements are summarized in Table VIII, and the unit is illustrated in Figures 14 and 15.

The physics design for the BEAR RFQ represents a significant advance in RFQ design. The BEAR RFQ's power consumption and length were reduced by about 10% from those of a conventional design, with attendant weight savings. The flight RFQ, whose fabrication technology was pioneered by Grumman Space Systems and its subcontractor, GAR Electroform, is 1.02 m (40 in.) long and weighs 54.8 kg (121 lb). The vanes are copper-plated aluminum, with the exception of the vane tips, which are bare aluminum. The minimum aperture diameter is 2.4 mm. The RFQ accelerates 30 mA of matched H^- beam at a power requirement of 1.5 kW/mA, with a copper loss of 70 kW. Because of the low-duty factor, 0.025%, and frequency control of the rf amplifiers, no active cooling is required. The RFQ's intervane voltage was determined from the measured x-ray spectrum to be about 48 kV (twice Kilpatrick limit). Using an energy spectrometer specifically designed for this measurement, the RFQ output beam energy spectrum was determined to be centered at 1 MeV, the design value, with a half-width at half-maximum of about 0.04 MeV. The measured RFQ output beam emittance was 0.012π cm-mrad (normalized rms) at a beam current of 20 mA. During testing and in flight, the RFQ output beam current was measured by a current toroid located at the entrance to the HEBT.

High-Energy Beam Transport Assembly

The primary purpose of the HEBT is to accept the thin, rapidly diverging beam from the RFQ and to magnetically refocus it as an approximately circular beam of the 2.5-cm diameter with a near-zero divergence. The HEBT also contains some of the accelerator internal diagnostic (AID) instruments for monitoring the output beam. Its design parameters are given in Table IX, and the flight unit, which was assembled for LANL by the McDonnell Douglas Missile Systems Co., is illustrated in Figures 16 and 17.

35

TABLE VIII

RFQ DESIGN PARAMETERS

Parameter	Specification
Input Particle Energy	30. keV (nominal)
Matched Input Beam Current	30. mA (nominal)
Output Particle Energy	1. MeV
Output Beam Current	25. mA
Output Emittance	0.01π cm-mrad (rms)
Capture Efficiency	87.%
Resonant Frequency	425. MHz
Instantaneous Power Consumption	100. kW (maximum)
Pulse Width	50. μs
Repetition Rate	5. pps
Intervane Voltage	44. kV (nominal)
Peak Surface Field	31.3 MV/m
Clear Aperture	2.4 mm
Vane Length	99.6 cm
Weight	68. kg (maximum)

Mechanically, the HEBT consists of a housing containing a permanent magnet quadrupole triplet system similar to that of the LEBT. The beam loss through the HEBT is typically 10%. The HEBT output beam diameter is 25 mm (about 9 mm rms), with a divergence of approximately ±0.9 mrad. During its integrated tests and in flight, the HEBT's output beam current was measured by an AID current toriod located at the beam exit end.
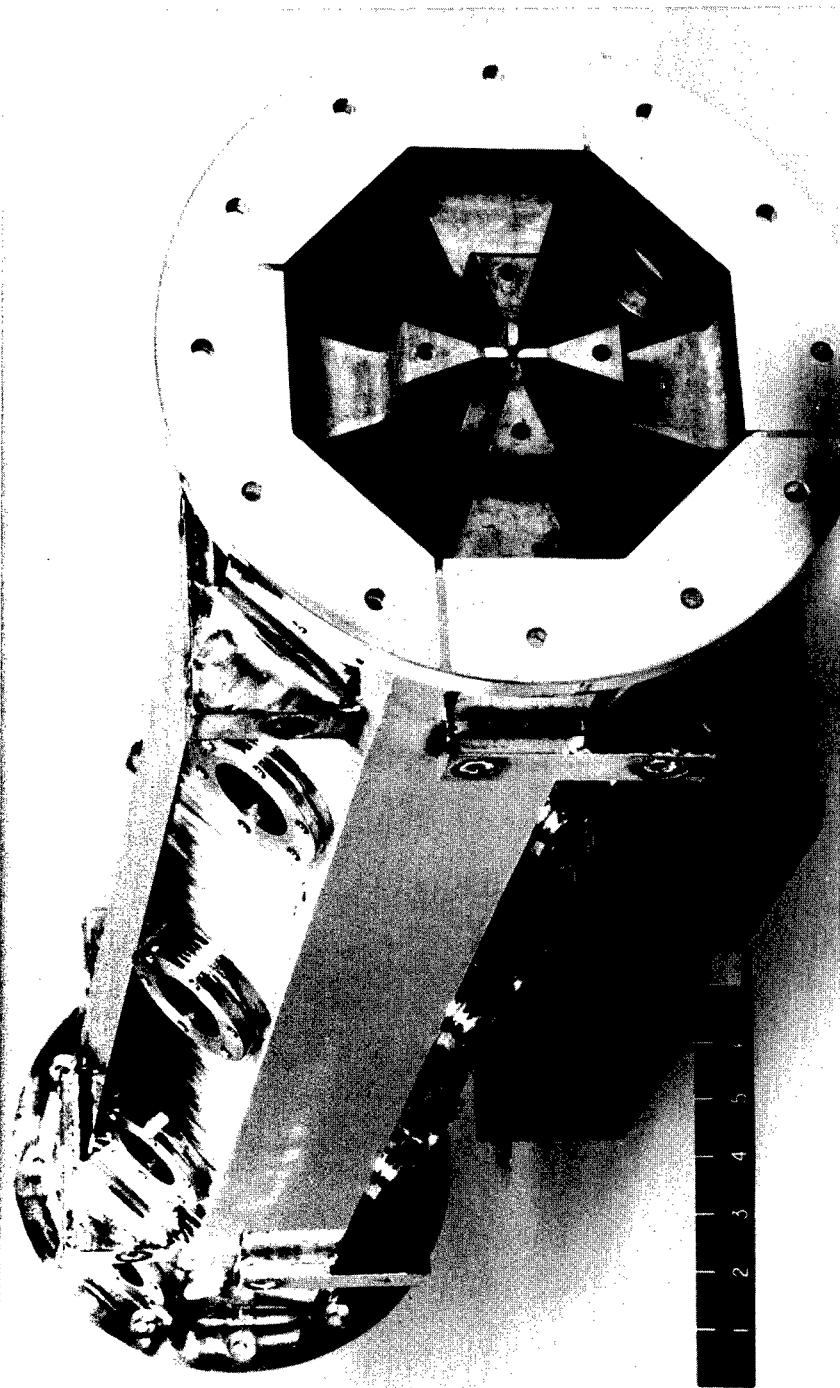
Figure 14. RFQ design [LANL/Grumman].

Figure 15. Flight RFQ [Grumman].

TABLE IX

HEBT DESIGN PARAMETERS

Parameter	Specification
Input Beam Current	25. mA
Input Beam Diameter	2.5 mm
Input Beam Divergence	±30. mrad
Output Beam Current	23. mA
Output Beam Diameter	2.5 cm
Output Beam Divergence	±1. mrad
Output Beam Emittance	0.01 π cm/mrad
Maximum Length	65. cm
Maximum Weight	38. kg

Neutralizer Assembly

The Neutralizer Subsystem was configured to provide maximum neutralization of the beam in its normal mode (over most of the experimental period) and to have the capability of being programmed to operate in an underneutralization mode (shut off) and an overneutralization mode (injection of a preset excess of gas) for prescribed periods. This subsystem embodies a vacuum-monitoring transducer and a sweep magnet assembly that removes free electrons. It also provides an upstream mounting location for the shadow-casting wire, which is functionally part of the Shadow Wire Scanner (SWS) Subsystem. The principal design requirements for the neutralizer are listed in Table X, and the flight unit is depicted in Figure 18.

The flight neutralizer uses xenon gas injected into a 2.54-cm-diameter tube through a pulsed piezoelectric valve. The BEAR accelerator represents the first application of beam neutralization by gas injection at these beam current and brightness levels. The predicted maximum neutralization efficiency of about 50% agrees well with experimental observations (Figure 19). During ground functional tests, beam measurements made 2.5 meters downstream of the neutralizer exit indicated a neutral beam diameter of 1 cm (rms) with a divergence of about ±1 mrad.

Figure 16. HEBT design [LANL/McDonnell Douglas].
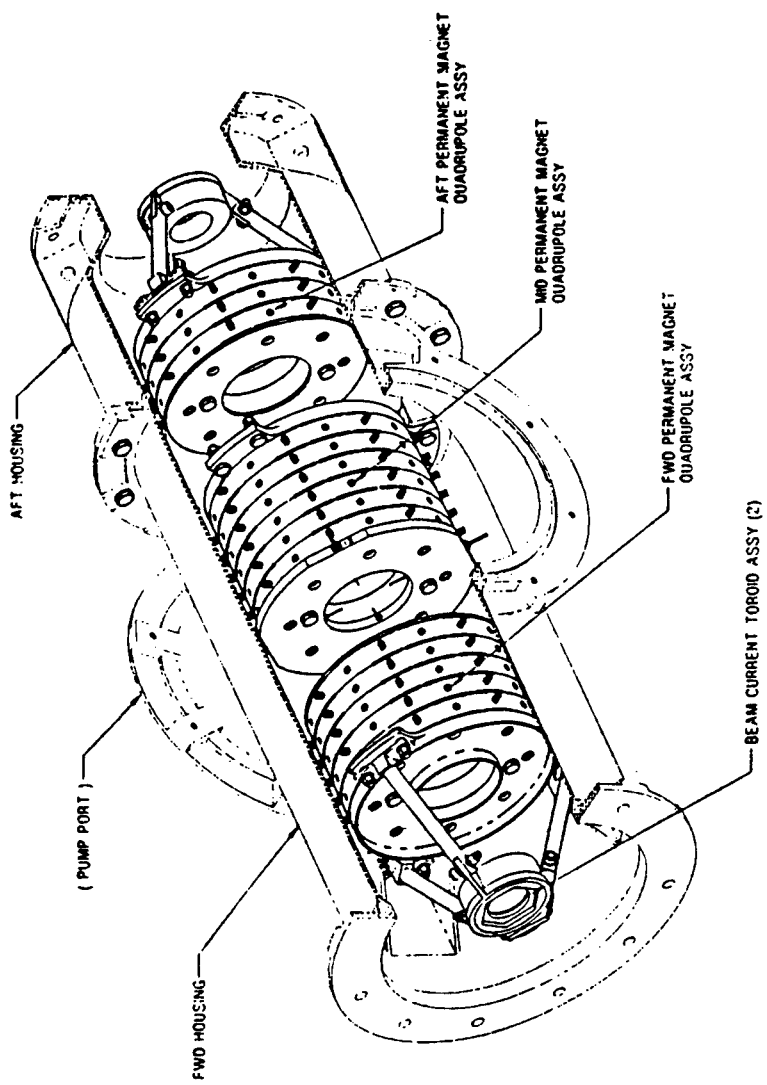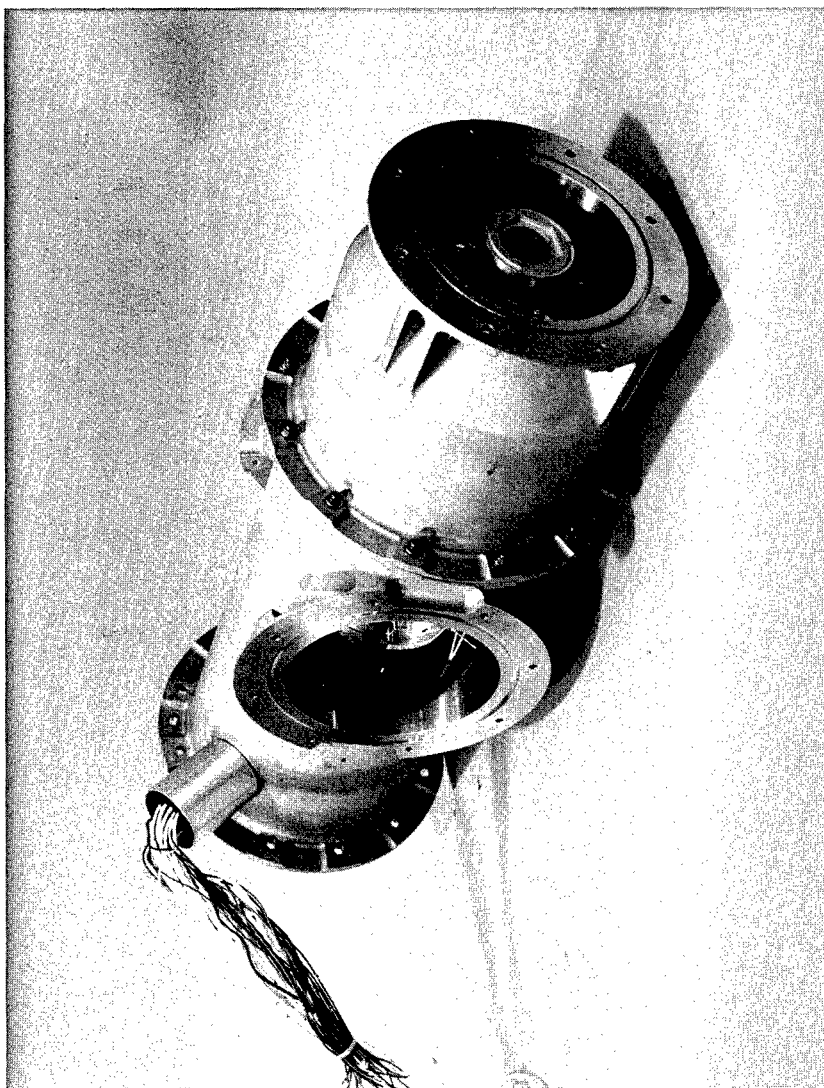
AFT PERMANENT MAGNET QUADRUPOLE ASSY

MID PERMANENT MAGNET QUADRUPOLE ASSY

FWD PERMANENT MAGNET QUADRUPOLE ASSY

BEAM CURRENT TOROID ASSY (2)

AFT HOUSING

(PUMP PORT)

FWD HOUSING

Figure 17. Flight HEBT [McDonnell Douglas].

41

TABLE X

NEUTRALIZER DESIGN PARAMETERS

Parameter	Specification
Type	Gas cell
Injectant	Xenon
Input Beam Energy	1.0 MeV
Input Beam Current	25. mA (H^-)
Output Beam Energy	1.0 MeV
Output Beam Neutral Current, Normal Mode	10. mA, equivalent (minimum)
Output Beam Residual Charged Species Net Currents	
Normal Mode	<1.0 mA (positive or negative)
Overneutralization Mode	3. mA (positive)
Pulse Rate	5. pps
Injectant Backflow Limit to Cryotrap	0.0015 torr-ℓ/sec (maximum)
Maximum Allowable Injectant Valve Leakage	1. $\times 10^{-8}$ torr-ℓ/sec

Radio Frequency Power Subsystem

The driving power for the RFQ is supplied by two solid-state rf amplifiers, which Westinghouse Electric Corp. developed specifically for the BEAR accelerator. Each amplifier weighs 54.4 kg (120 lb) and has demonstrated output power in excess of 60 kW, which represents a weight-to-power ratio of less than 1 g/W. The 5-pps repetition rate rf pulse is 60 μs in duration at a frequency of 425 ± 0.5 MHz. The RF Power Supply and Control Subsystem tracks the RFQ resonant frequency to within 0.02 MHz. The BEAR accelerator is the first NPB accelerator to be driven exclusively by such solid-state rf power amplifiers, one of which is shown in Figure 20. The amplifiers are controlled by an rf controller unit, as indicated in Figure 21, which provides the required commands to, and acquires performance and state-of-health data from, the rest of the RF Subsystem.
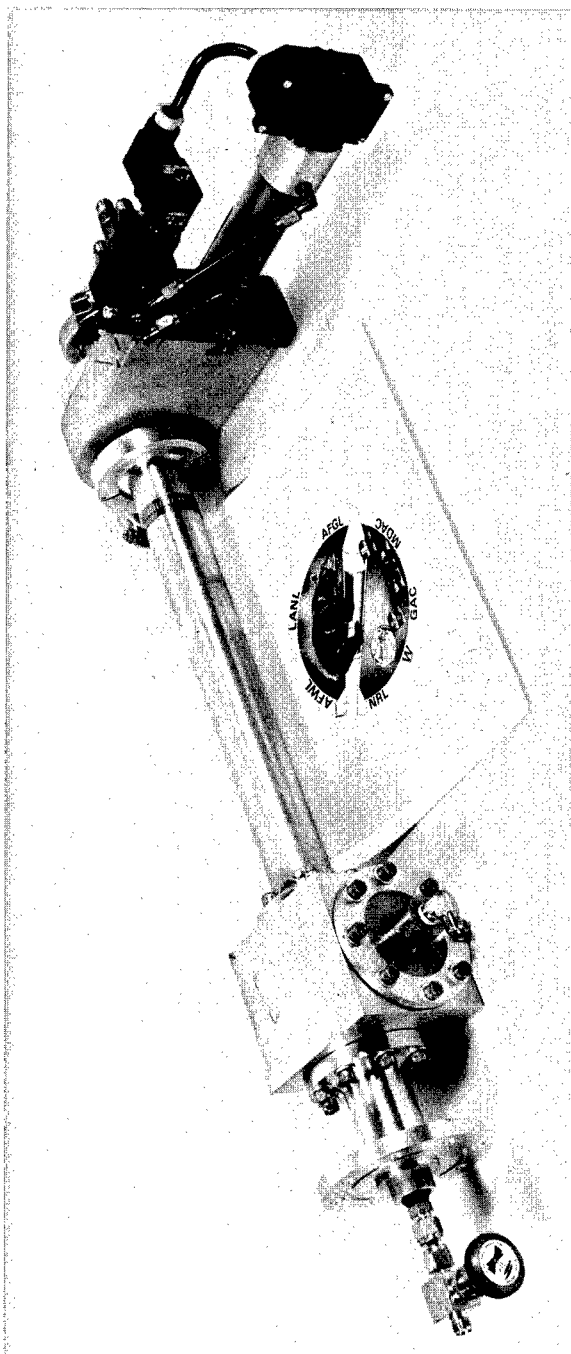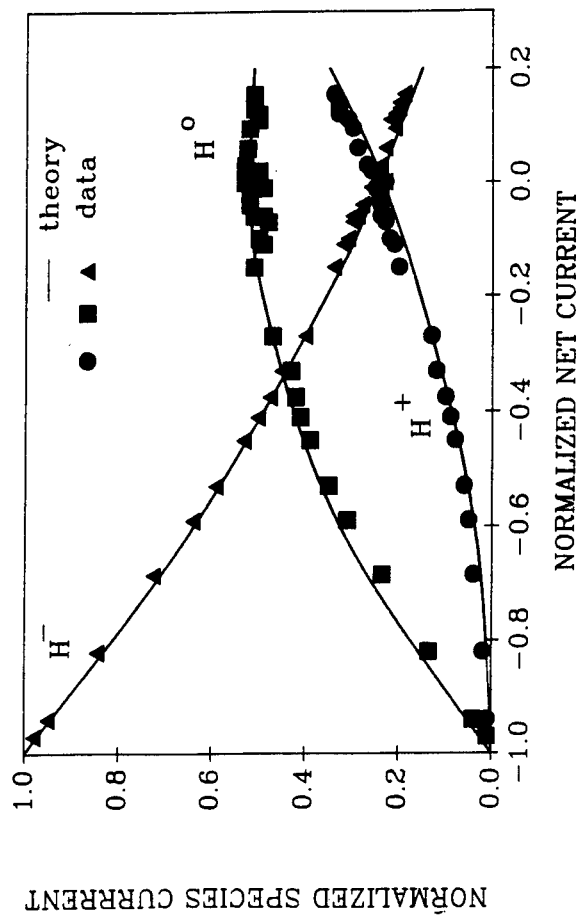
Figure 18. Flight neutralizer.

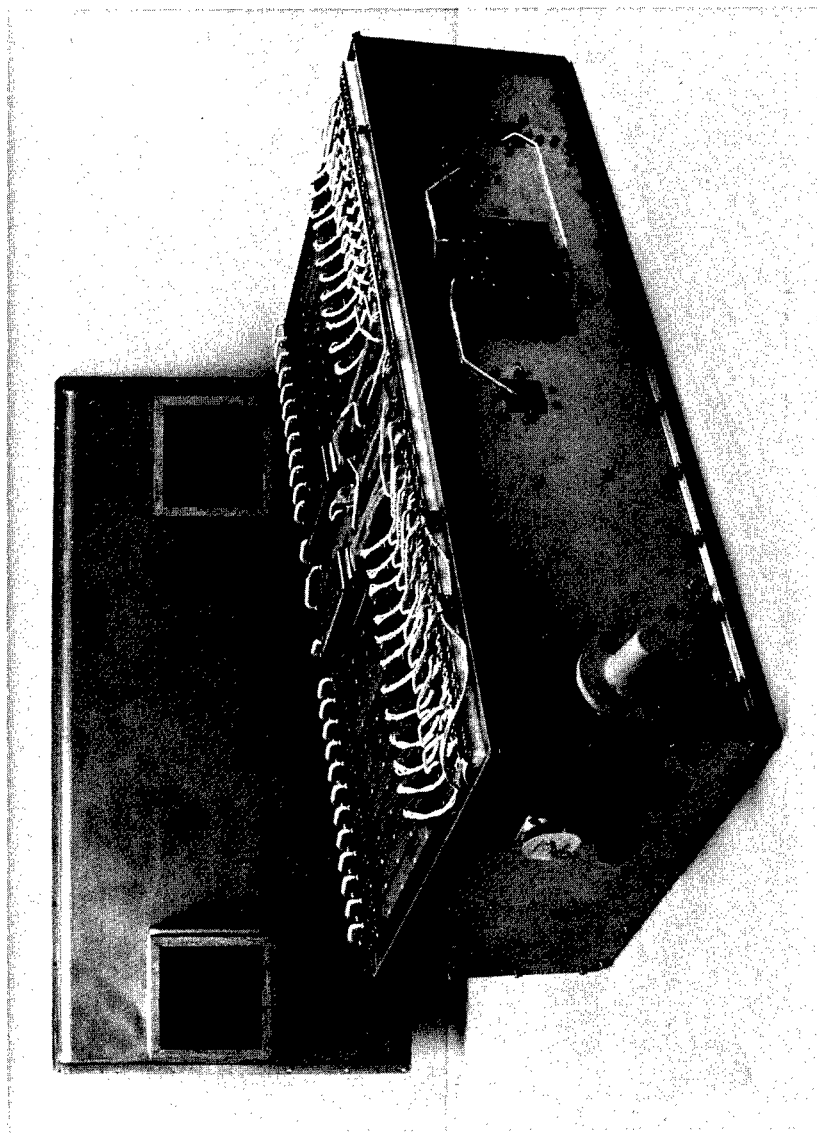Figure 19. Predicted vs. measured neutralization efficiency.

44

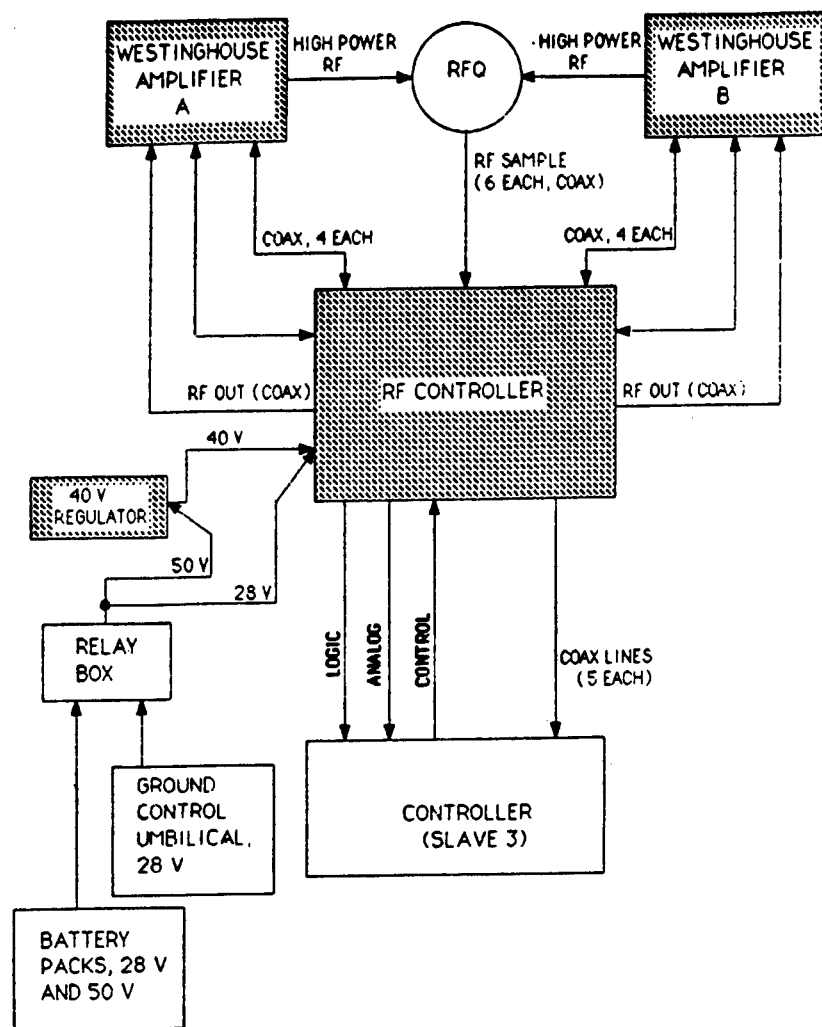Figure 20. Solid-state rf amplifier unit [Westinghouse].

Figure 21. RF Power Supply and Control Subsystem logic.

Vacuum Subsystem

The Vacuum Subsystem, which maintains an acceptable vacuum level inside the beamline during integrated ground testing and the actual flight mission, comprises a set of noncontiguous components connected to the beamline, as shown schematically in Figure 22. These components include three getter pumps with their associated isolation gate valves, one cryocondensation pump, and the beamline exit gate valve. Two of the getter pumps are located on the LEBT, and the third is on the HEBT. The cryocondensation pump (Figure 23), called the beamline cryotrap or cryopump, was developed specifically for BEAR by Janis Research Corp. It is positioned between the HEBT and the neutralizer. Commercially available SORB-AC^{TM} getter pumps were significantly modified to improve their structural stability and were subsequently flight-qualified at Los Alamos. These pumps (Figure 24) have an effective pumping speed of 600 ℓ/sec for hydrogen and zero for xenon. The only xenon pumping for the LEBT is 0.6 ℓ/sec through the 5-mm-diameter RFQ orifice (at the LEBT/RFQ interface) to the 200-ℓ/sec cryocondensation pump. This configuration provides a high partial pressure of xenon and low partial pressure of hydrogen between the H^- source and the RFQ, which is necessary for optimum operation of the accelerator. The beamline cryotrap is a hollow coaxial dewar configuration containing supercritical helium in the annulus. This cryotrap pumps all gases except hydrogen and helium. The HEBT getter pump provides additional hydrogen pumping in the HEBT.

Accelerator Control and Data Acquisition Subsystem

During integrated testing and in flight, all the payload functions were controlled by the Accelerator Control and Data Acquisition Subsystem. The heart of this system is the Master Controller, which provides autonomous flight control, sequencing, and data acquisition for all payload subsystems. Supporting the Master Controller are five distributed slave processors: two dedicated to the injector; one for the Neutralizer and RF Power subsystems; one for the Vacuum Subsystem, electrical power, and environmental diagnostics; and one for the BD Section. The AID instrumentation, under the command of the Master Controller, was designed to monitor the operating parameters of the accelerator components (Injector, LEBT, RFQ, HEBT, Neutralizer, RF, and Vacuum subsystems). Currents, voltages, frequencies, pressures, temperatures, set points, and many housekeeping functions were determined on a pulse-by-pulse basis. The more critical data were taken as pulse waveform measurements, including the source arc current and voltage, the extractor pulser voltage, all the accelerator beam currents, the RF Power Supply and Control Subsystem forward and reflected powers, and the BD instrument signals.

Space Frame

The nontrivial problems of supporting the more massive accelerator components (e.g., rf amplifiers, injector, and RFQ) and of maintaining the critical alignment of the beamline were solved by assembling the beamline

47

Figure 22. Flight Vacuum Subsystem.

COPPER-MYLAR MATRIX

TENSION CABLES

VENT GAS COOLED HEAT EXCHANGER

GOLD PLATED CRYOPUMPING SURFACE

GHe PRESSURE RELIEF VENT

GHe EMERGENCY RELIEF VENT

LHe FILL

LHe VENT

BEAR   BEAMLINE CRYOPUMP
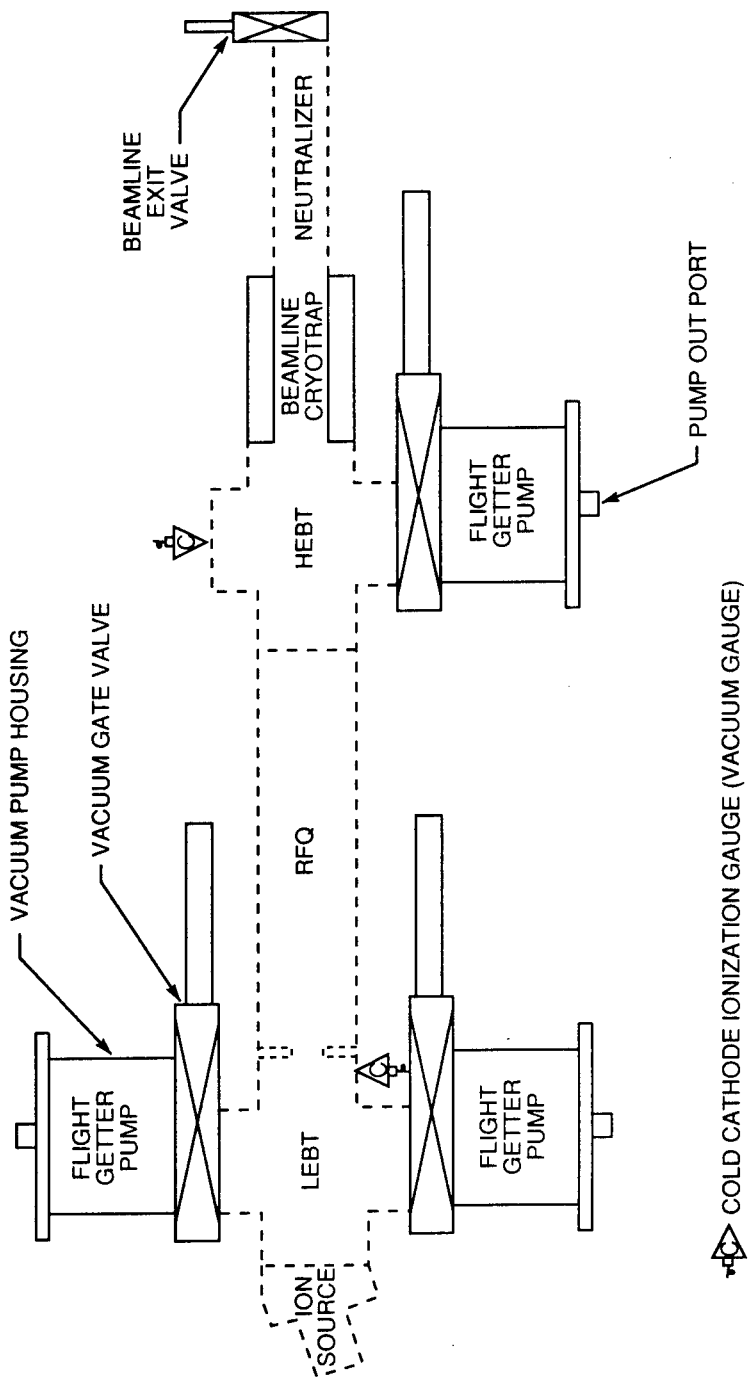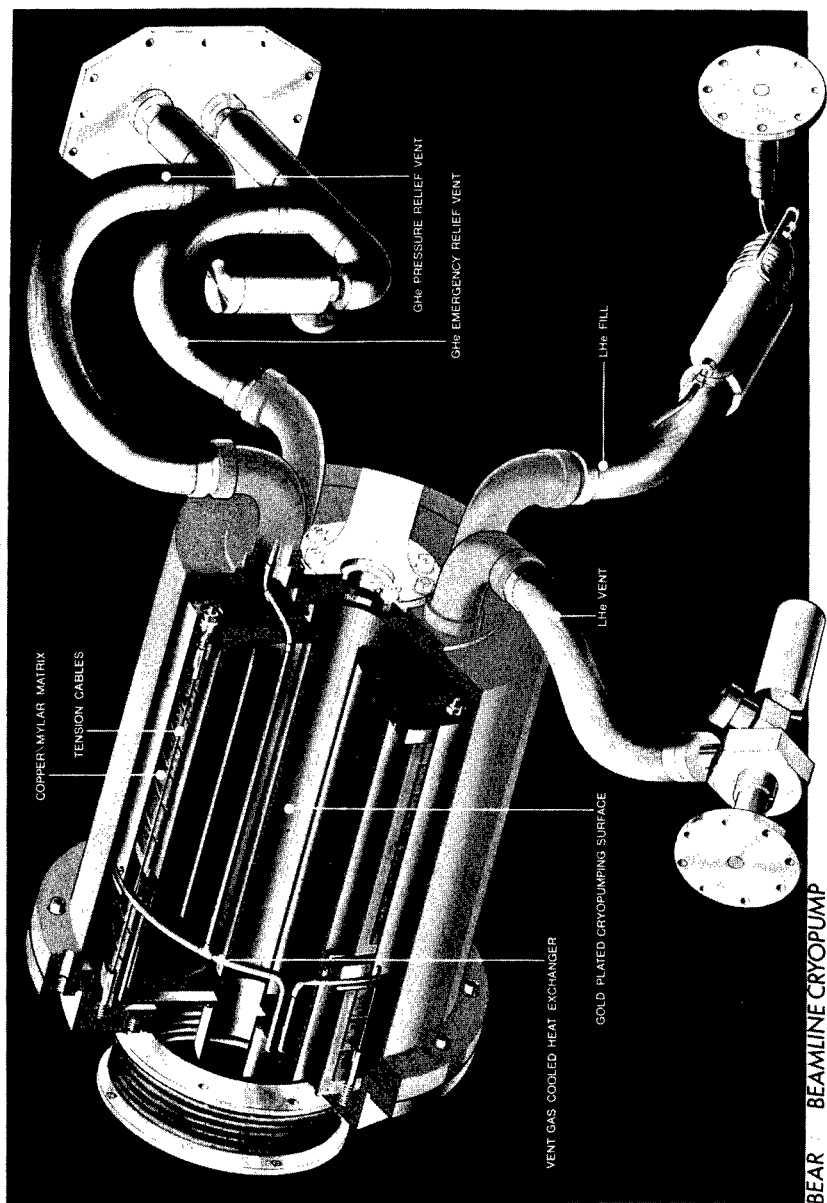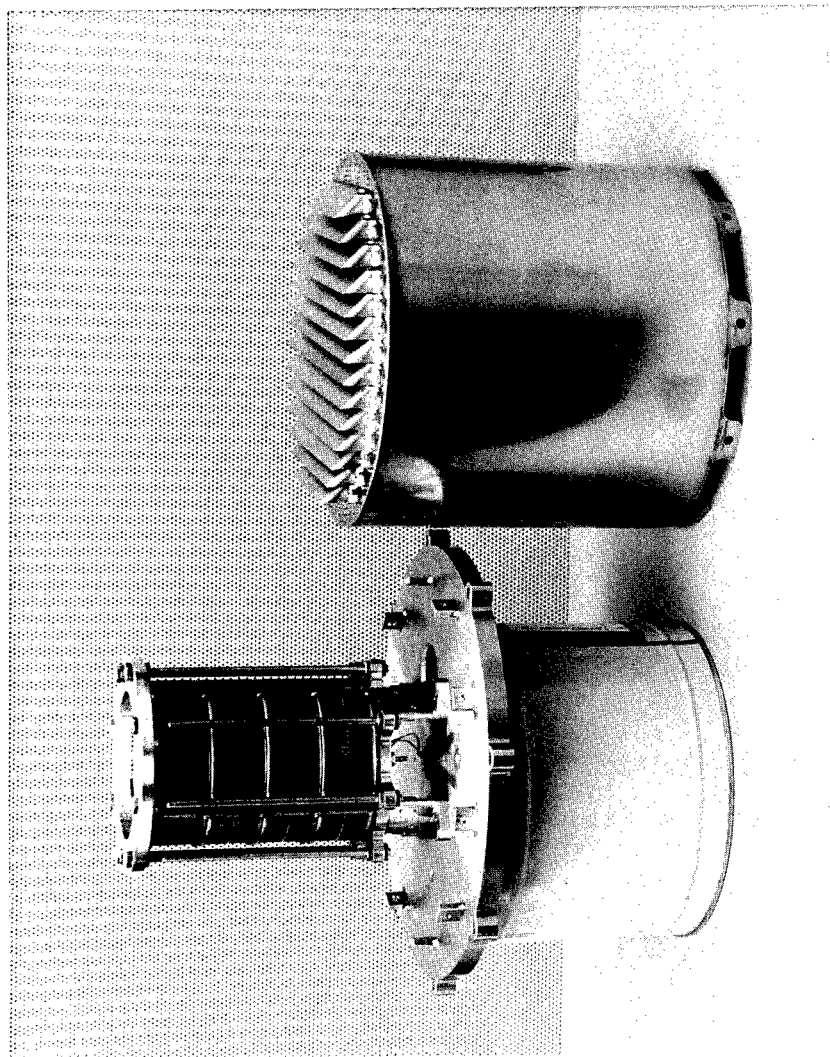
Figure 23. Beamline cryotrap [Janis Research].

49

Figure 24. Flight getter pump subassembly.

and its supporting subsystems to the Space Frame, the rigid, Eiffel-Tower-like structure shown in Figure 25. This structure was designed to accommodate the accelerator's axial loads (Figure 26) and to prevent any radial loads on the beamline. In flight, the annular space containing the Space Frame and enveloping the beamline was pressurized to about 17 psia.

BEAM DIAGNOSTIC INSTRUMENTATION

The BD Section of the BEAR vehicle is a physically discrete section just aft of, and sharing a common isolation bulkhead with, the APS. This section houses the BD instruments, as well as two of the plasma physics instruments. The BD Section is axially traversed by the beam as it exits the payload. A drawing of the BD Section is presented in Figure 27. This section is 62 cm (24.4 in.) long and has the same outside diameter as the rest of the payload. The instruments in the BD Section that specifically measure the characteristics of the beam emerging from the accelerator are the Beam Current Monitor (BCM), the SWS unit, and the two video cameras. These instruments are described briefly in the following paragraphs; greater detail is provided in Volume II.

Beam Current Monitor

The BCM is an encapsulated, toroidal, Rogowski-type coil (Figure 28) located at the output end of the neutralizer assembly. It nonintrusively measures the *net* beam current exiting the accelerator. The BCM samples the beam current 50 times in a 100-μs interval surrounding each pulse.

Shadow Wire Scanner Assembly

The SWS consists of a 1.5-mm-diameter shadow-casting wire centrally located in the neutralizer tube and of a movable sensor assembly (Figure 29) consisting of three 1-mm-diameter shadow-scanning wires that are separated from each other by 0.050 in. and are located at the exit plane of the BD Section. The shadow-casting wire absorbs all the impinging beam particles. The sensor wires measure the secondary electron emission resulting from beam particles striking the wires. The secondary-driven current is measured 50 times in the 100-μs interval surrounding the beam pulse. Beam profiles (Figure 30) are generated as the cam moves the sensor wires across the beam through the umbra and penumbra formed by the shadow-casting wire. Beam pointing, divergence, and particle flux are then derived from the sensor wire signals when all three are in shadow. The inter- and intrapulse jitter of these beam quantities is also derived.

Video Imaging Subsystem

Particle beam propagation is observed by the two video cameras in the Video Imaging Subsystem (Figure 31), which was developed for LANL by EG&G. One of these is a visible-light, unfiltered, intensified video camera (visible TV), and the other is an ultraviolet- (uv-) filtered, intensified, time-gated video camera (uv TV). Both TVs are aligned to observe the beam
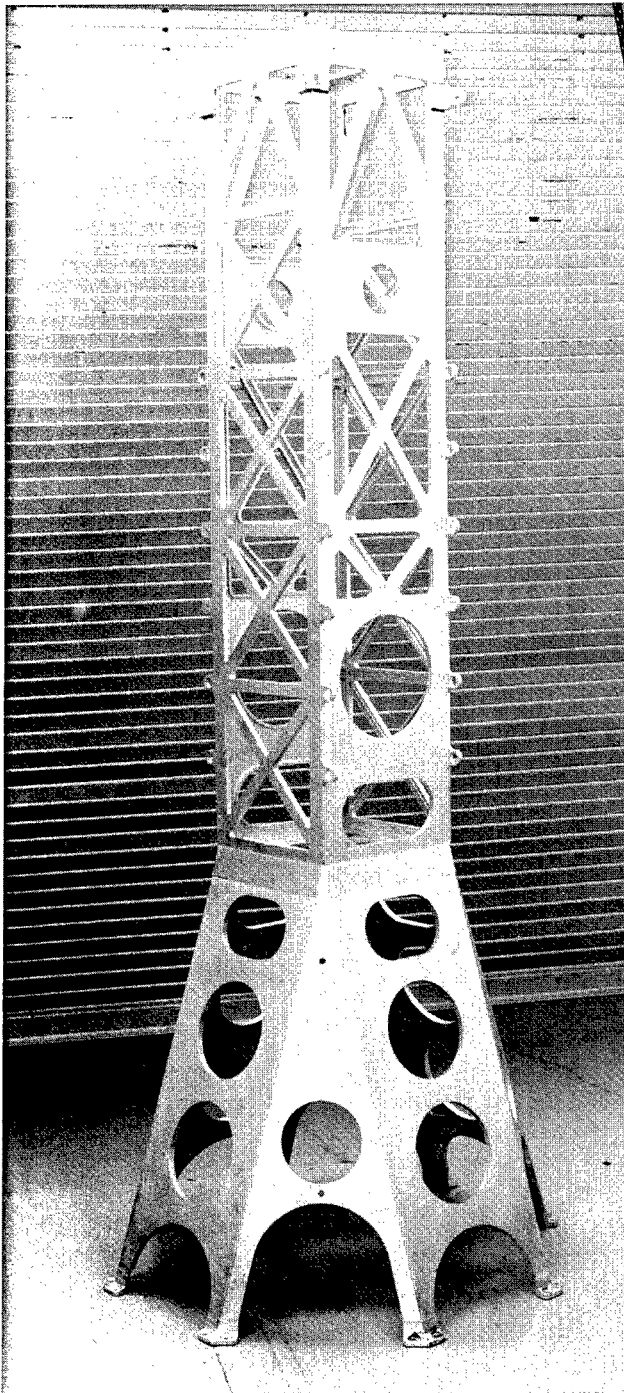
Figure 25. Space Frame.

VON MISES STRESS

LOAD CASE 1.

TOWER2, 8/86

abaqus results
element stresses
patran format

1.47+04
1.38+04
1.28+04
1.18+04
1.09+04
9.90+03
8.93+03
7.96+03
6.99+03
6.02+03
5.05+03
4.09+03
3.12+03
2.15+03
1.18+03
2.13+02
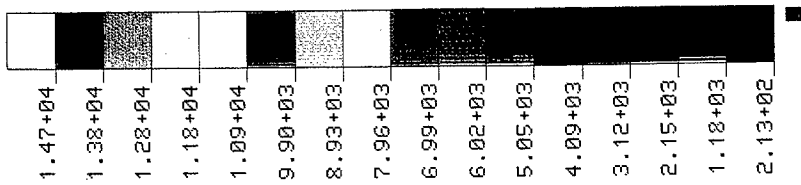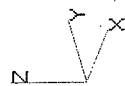
Figure 26. Stress analysis of Space Frame.

BEAM DIAGNOSTICS (BD) SECTION
BEAR PAYLOAD

SSD Electronics
BD Battery Pack
Beam Current Monitor
Transition Structural Module
Power Control Relay Box
Video Electronics
"Visible" Video Camera
Mirrors
Solid-State Detector(1of3)
Langmuir Probe Electronics
Langmuir Probes(1of4)
"Ultraviolet" Intensified Video Camera
Shadow Wire Scanner Sensor Unit
Cold-Cathode Ionization Gauge(1of2)
BCM and Shadow Wire Scanner Electronics
BD Section Slave Controller

Figure 27. Beam Diagnostics Section.

Figure 28. Beam Current Monitor.

Figure 29. Shadow Wire Scanner sensor assembly.
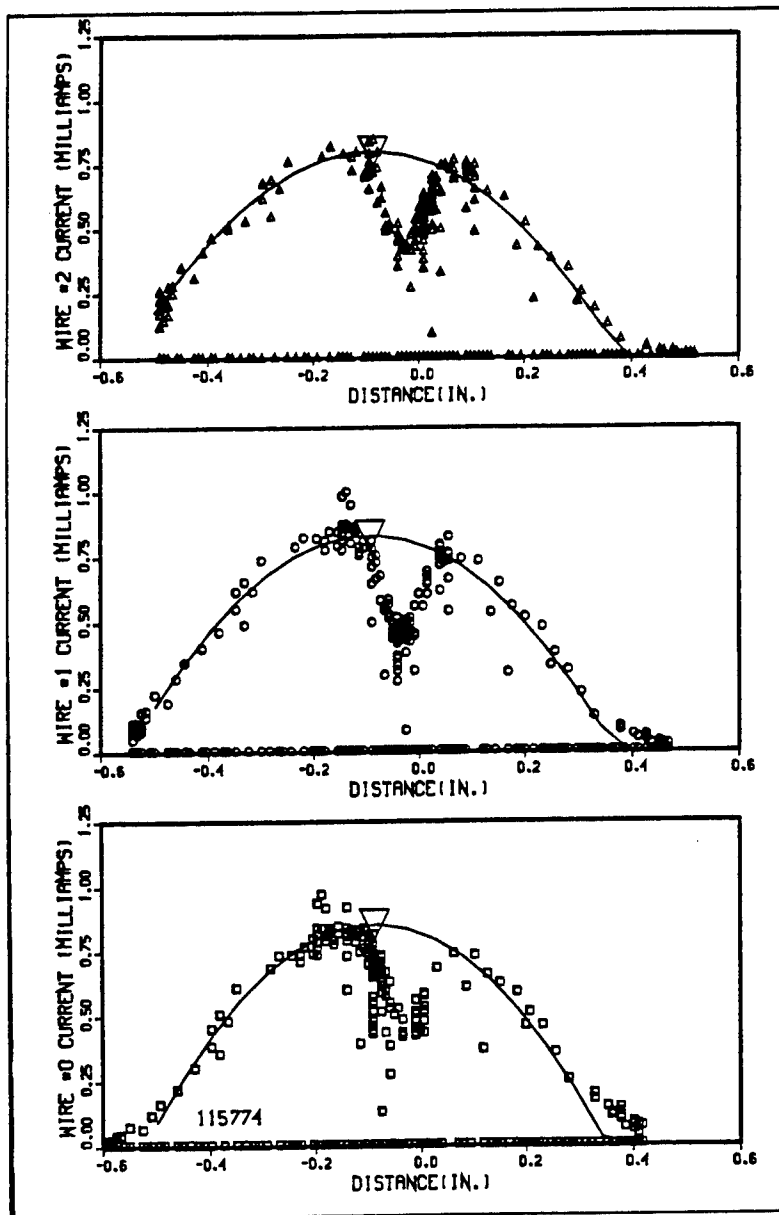
Figure 30. SWS sensor current beam profiles.
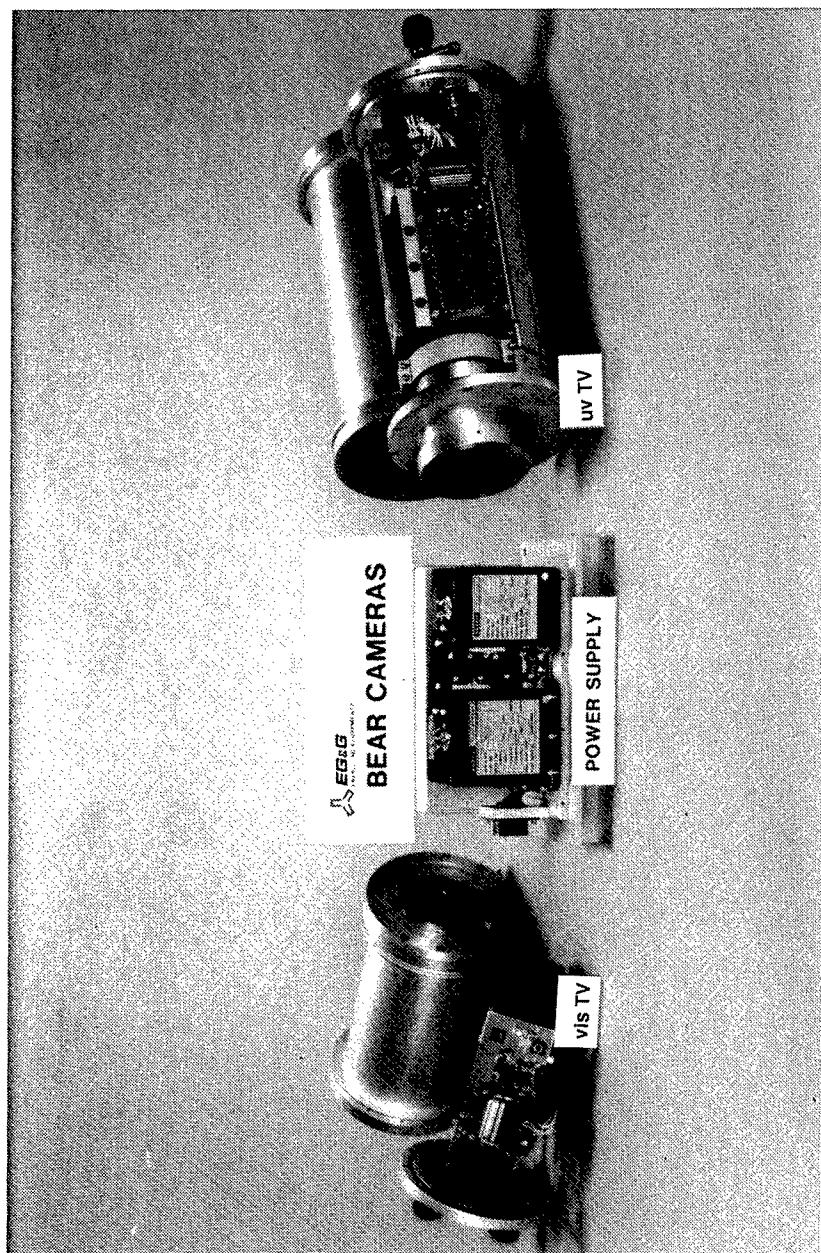
Figure 31. Video Imaging Subsystem cameras and power supply [EG&G].

parallel to the payload spin axis, which is the direction of beam propagation. The visible TV is a documentary camera that not only views the beam but also observes motor separation, sensor deployment, attitude control maneuvers, etc. This camera also has two "rear-view mirrors" in its field of view to observe the beamline gate valve area and the SWS sensor assembly area. The uv TV is designed to observe at 391.4 nm the air fluorescence produced by beam interactions with ambient nitrogen. The intensifier's high voltage is gated on and off synchronously with the beam pulse. The uv TV was aligned parallel to the beam axis and was positioned approximately 5 in. away from the beam axis.
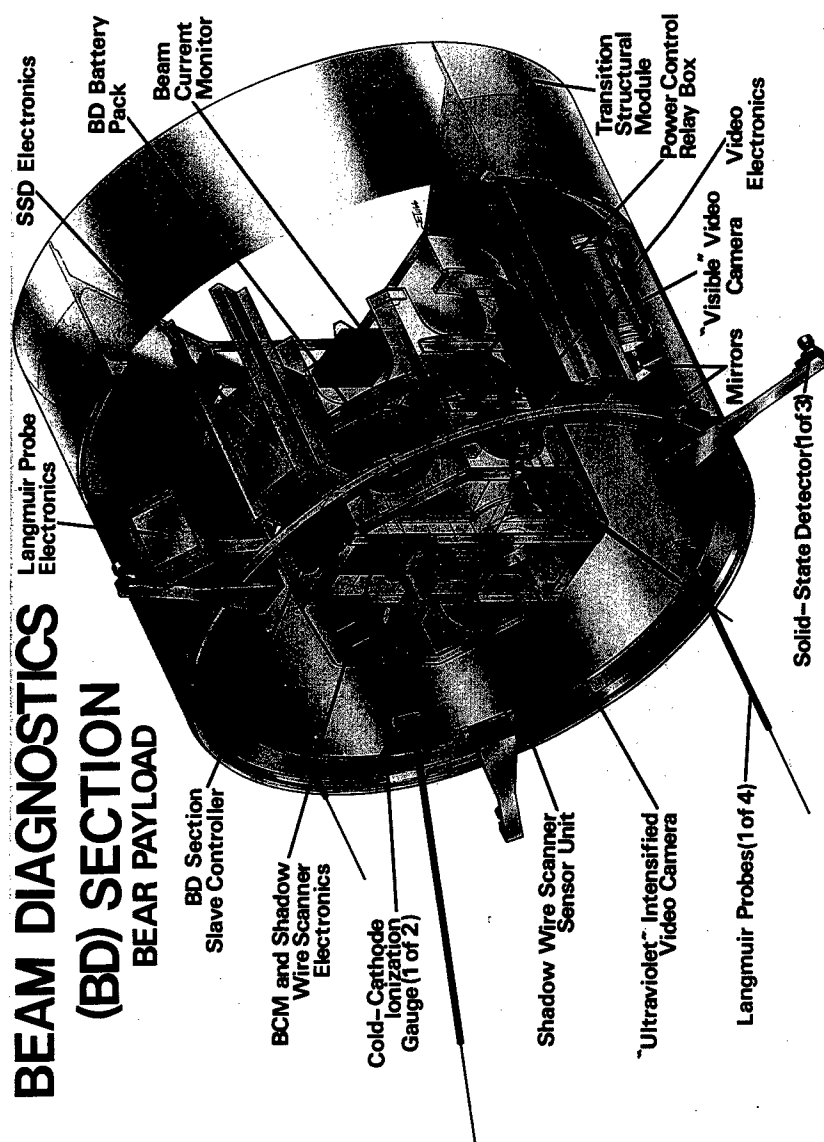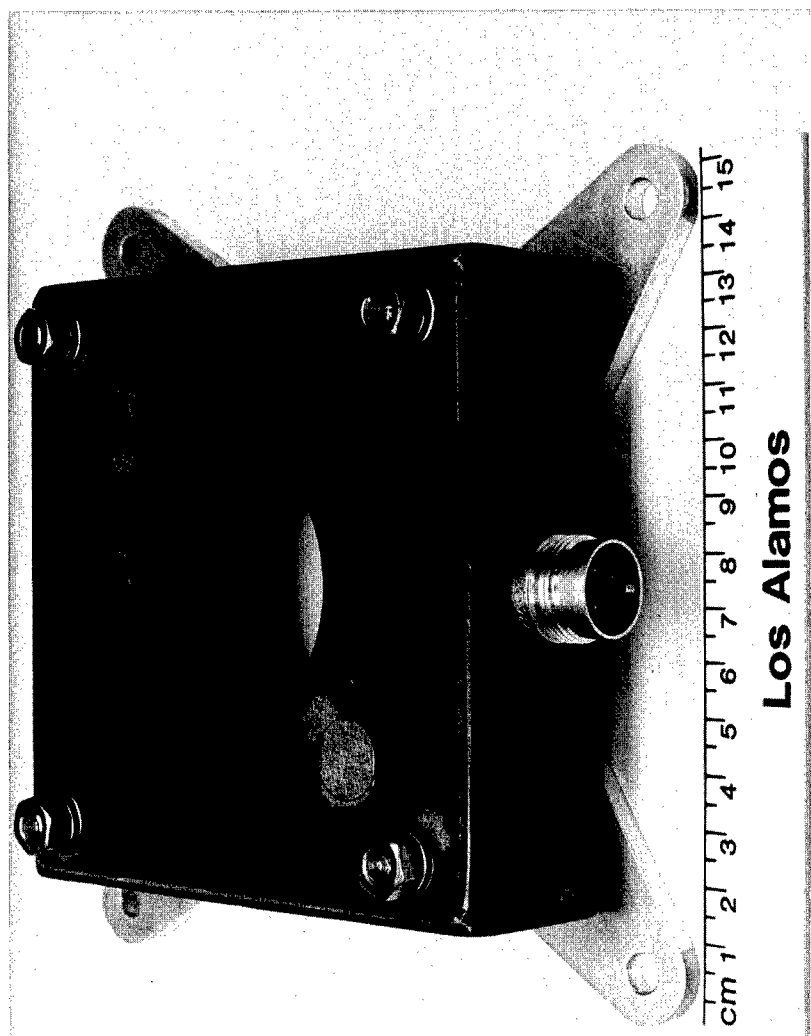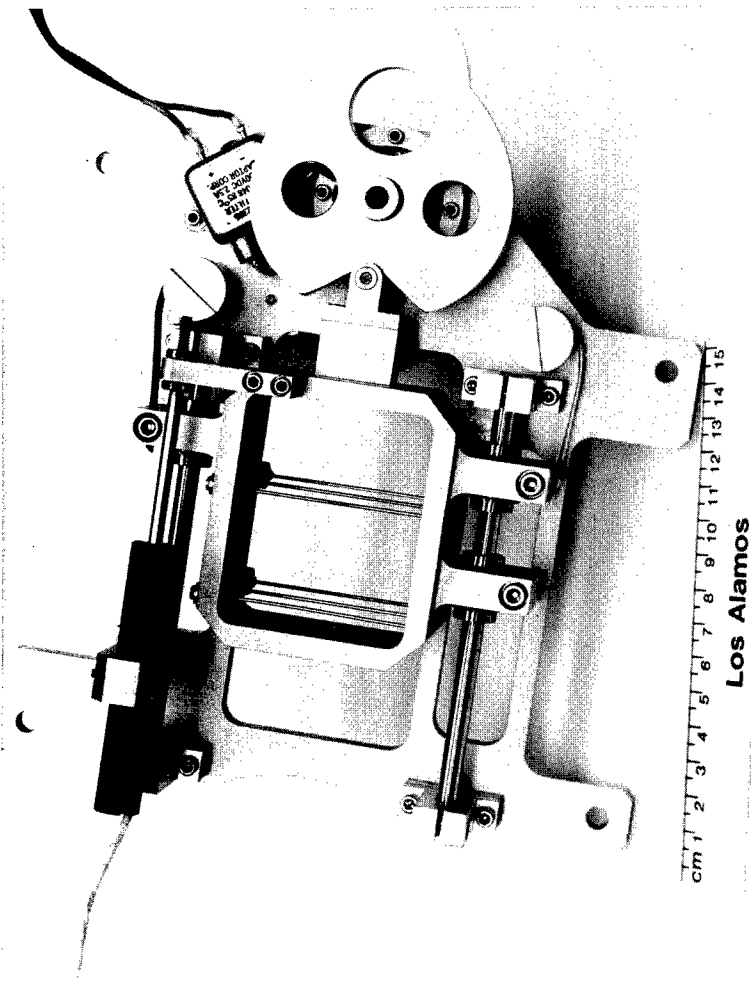
PLASMA PHYSICS DIAGNOSTIC INSTRUMENTS

The plasma physics diagnostic (PPD) instruments are situated at several different locations along the payload's axis. The boom-mounted Plasma Wave Receiver (PWR) and high-voltage detector (HIV) probes, as well as the Electrostatic Analyzer (ESA), are located in the TP Section, while the cold-cathode ionization gages (CCIGs), solid-state particle detectors (SSDs), and Langmuir probes are mounted on the BD Section. The deployable sensors were released just after booster separation.

Plasma Wave Receiver

The Naval Research Laboratory (NRL) provided the PWR. The PWR has two spherical sensors at the ends of Weitzman booms extended radially from the TP Section (Figure 8). The PWR measures the voltage between the two sensors and between the sensors and the payload skin. A key feature of the voltage difference is the frequency band over which the measurement is made. The PWR measures this voltage over a wide range of frequencies from direct current to 50 MHz. The voltage difference is interpreted in terms of spacecraft charging and electric fields. PWR data consist of 14 discrete signals plus one continuously modulated signal.

High-Voltage Detector

NRL also produced the HIV. The HIV has one spherical sensor deployed radially from the SPS on a Wentworth boom (Figure 8). The voltage between the payload skin and the HIV sphere is adjusted three times during each pulse in the sense needed to null the current collected by the sphere. In principle, the sphere should float near the plasma potential at some distance from the payload. The current-nulling voltage will then indicate the potential of the spacecraft with respect to the distant plasma, i.e., spacecraft charging.

Electrostatic Analyzer Assembly

SAIC, Inc., provided five electrostatic analyzers to measure, with microsecond time resolution, the energy spectrum of electrons and positively charged ions striking the payload. Four separate spherical-plate sensors measure the differential low-energy (20- to 300-eV) and high-energy (200-

59

to 3000-eV) spectra of particles of each charge sign. A fifth sensor is configured as a retarding potential analyzer to measure the integral spectrum of electrons with energies above 25 eV. Plasma chamber tests confirmed that the sensor potential with respect to the distant plasma could be inferred from the energy spectrum of the incident particles. Hence, this instrument provides a measure of spacecraft charging.

Cold-Cathode Ionization Gages

Of the two CCIGs in the BD Section, one was located as close as possible to the beamline gate valve—the valve that isolates the accelerator beamline from the BD Section. The other CCIG was positioned to be as far as possible aft of the beamline gate valve, near the SWS sensor assembly and ARIES motor adapter (Figure 27). The CCIGs were designed to measure pressure over the range 10^{-3} to 10^{-6} torr. The CCIG pressures are measured twice per pulse.

Solid-State Detector Assembly

The SSD instrument (Figure 32) consists of three solid-state detectors designed to measure protons in five energy channels between 200 keV and several million electron volts. Energetic electrons are detected in the lowest energy channel. Channel A3 is centered about 1 MeV, and the count accumulations are measured with 20-ms resolution over the 200-ms interval between beam firings. Two detectors have a sensitive area of 100 mm^2, and the third detector's sensitive area is only 10 mm^2. Their effective areas, limited by collimators, are actually 20.3 mm^2 and 1.98 mm^2, respectively. The three sensors are deployed on arms from the BD Section. In the deployed configuration, they are oriented to view backward with respect to the injected beam to observe particles as they return on their helical orbit within the geomagnetic field.

Langmuir Probe Subsystem

The Langmuir Probe Subsystem (LPS), also supplied by the NRL, used four pulsed Langmuir probe sensor elements deployed from the open aft end of the BD Section (Figure 27). The Langmuir probe sensors operate as pairs. One pair is located at a larger radial distance from the beam than the other and is thus less likely to be affected by the vehicle's wake. The pulsed designation refers to the fact that the classic Langmuir probe voltage sweep is interrupted at regular intervals by a return to a fixed-bias voltage—effectively a combined squarewave/sawtooth profile. Internal electronics alternatively treat each pair as predominantly electron collecting or predominantly ion collecting. This nomenclature refers to the bias voltage to which the probe returns at regular intervals. If that reference bias voltage is positive, electron collection will result; when negative, it causes (positive) ion collection. Current measurement on the electron-collecting pair was synchronized with the beam pulse. The LPS measures plasma
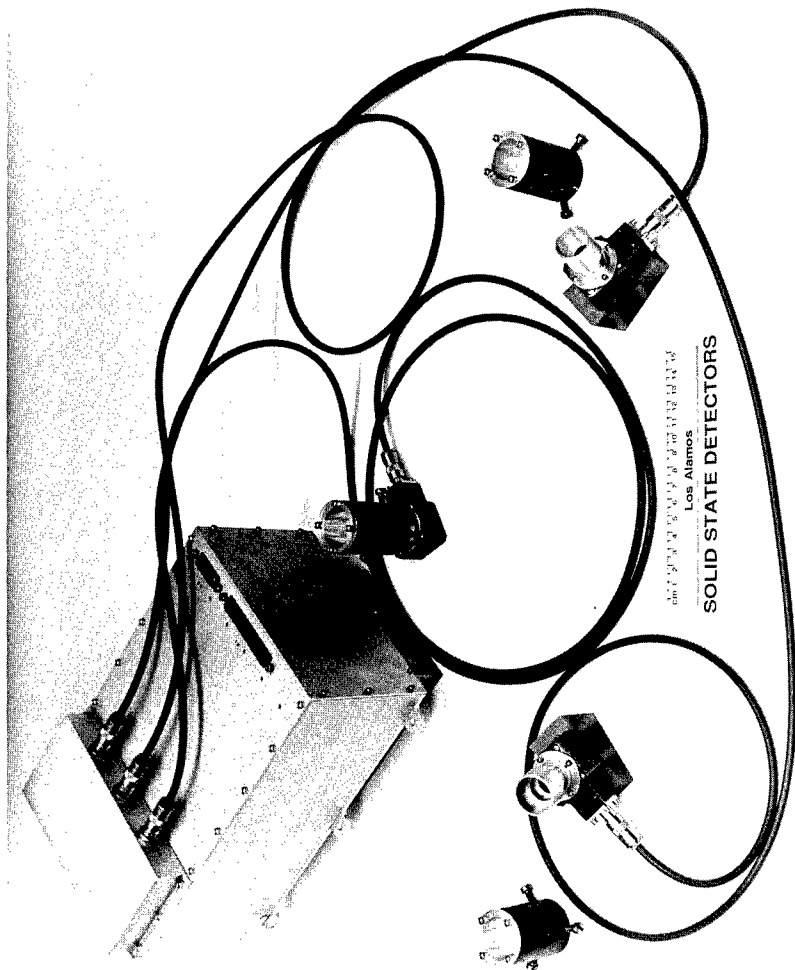
Figure 32. SSD instrument.

61

electron and ion density and temperature and the potential of the space-craft with respect to the surrounding plasma, provided that the potential difference is less than about 100 volts.

DYNAMICS INSTRUMENTS

The set of instruments loosely grouped here under the heading of dynamics instruments was of two classes: those that provided information on the external dynamics (attitude and trajectory) of the vehicle itself and those that monitored (in selected locations) the internal dynamics of specific vehicular structures in response to separation- and thruster-induced disturbances.

External Dynamics Instruments

The Attitude Control System supplied by Space Vector Corp. includes a stabilized platform with two positional gyros and one rate gyro. The gyro outputs, coupled with tracking data, provide instantaneous position, velocity, and attitude data for the vehicle. In addition, the Air Force Geophysics Laboratory supplied a magnetometer to measure the component of the geomagnetic field along each of three orthogonal axes. The magnetometer data are used to determine the pitch angle of the beam injection.

Internal Dynamics Instruments

Northeastern University incorporated three single-axis accelerometers in the TP Section to measure the transient, unidirectional, and low-frequency vibrational accelerations along three orthogonal axes in this part of the payload. LANL installed additional accelerometers at various points in the APS. A triaxial assembly at the top of the Space Frame measures high-frequency (up to 750 Hz), high-amplitude, structural accelerations at that key location. Four other single-axis accelerometers are used to measure low-frequency acceleration along the payload's x-axis, the transverse dimension in which beam pointing and pointing jitter were measured. These sensors were located at the top of the Space Frame, on the RFQ, on the Space Frame near the top of the beamline cryopump, and near the SWS sensor assembly.

4. RESULTS

The BEAR payload was successfully launched on July 13, 1989, after one prior attempt aborted by a booster malfunction. It gathered a wealth of data in the course of its flight, some still awaiting detailed analysis. The material that follows describes the flight and presents a brief, preliminary assessment of the results.

FLIGHT AND RECOVERY

Prelaunch Payload Testing

Flight simulation tests were carried out on the integrated Accelerator Payload Segment (APS), both at Los Alamos and at White Sands Missile Range (WSMR). To functionally test the accelerator with its flight set of beam diagnostic (BD) instrumentation, a ground test vacuum bell jar was fitted into the aft end of the APS, providing an evacuation capability in the BD Section. For some tests, another ground test unit—a specialized accelerator performance diagnostic unit—was then attached to the opposite end of the bell jar. This diagnostic unit contains a magnet that separates the H^-, H^+, and H° beam components and directs them to three separate magnetically and electrostatically suppressed Faraday cups. (The magnitude of the neutral current was measured by stripping the H° beam to H^+ through a thin nickel foil and measuring the resulting H^+ current.) The unit also contains beam-emittance-measuring probes.

A representative sample of the performance data thus obtained for the integrated flight hardware is shown in Figure 33. The composition of the beam was calculated from the beam current data obtained from the accelerator's High-Energy Beam Transport (HEBT) current toroid and the Beam Current Monitor (BCM) in the BD Section. Excellent agreement was obtained between the data obtained using this technique and the measurements made downstream of the BD Section with the three Faraday cups. Accordingly, the beam composition in flight could be determined directly from the HEBT current toroid and BCM measurements.

The output beam emittance and divergence were also independently measured with the ground diagnostic unit and with the BD Section's Shadow Wire Scanner (SWS) instrument. Again, the agreement between ground and flight instrument data was excellent. During the flight simulation tests, the SWS also measured beam pointing, divergence, and jitter.
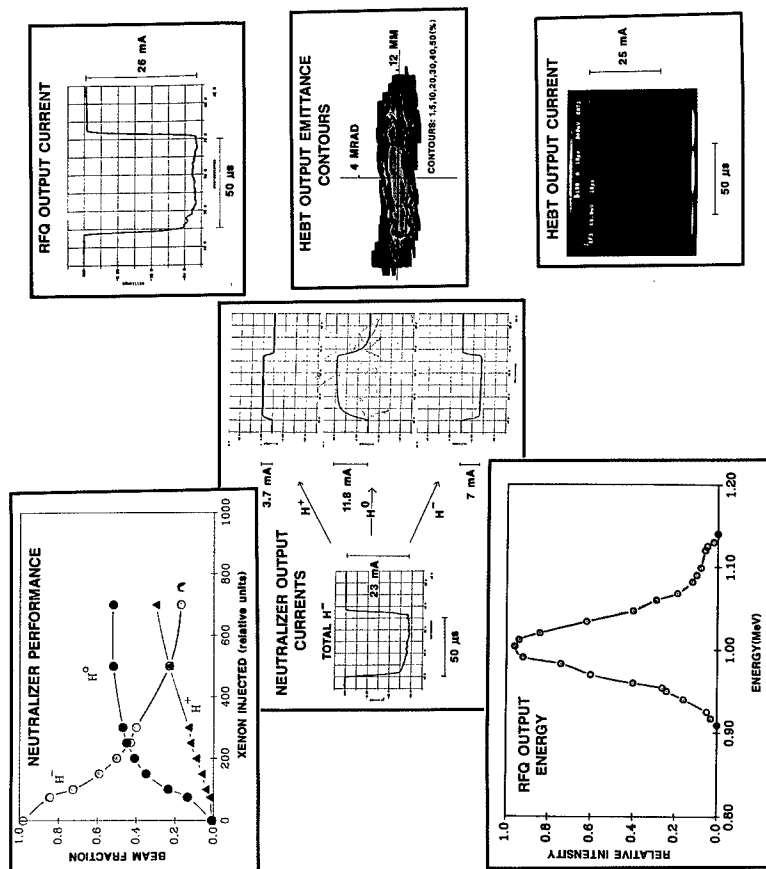
Figure 33. Accelerator performance in flight simulation tests.

64

All of these ground-vs-flight measurement correlations obtained during the flight simulation tests provided a basis for confidently determining accelerator performance during the actual BEAR flight.

The flight simulation tests also included integrated payload (APS/ Support Payload Segment [SPS]) system-level environmental shock and vibration tests. These tests were done on massive shock and vibration test tables, which the US Army Test and Evaluation (ARMTE) unit obligingly relocated to NASA's vehicle assembly building at WSMR. The bell jar/ diagnostic unit assembly was not attached during these tests. The shock and vibration loads imposed conformed to the ARIES booster specifications: the vibration loads covered the range of those anticipated during booster ignition and the boost phase, and the shock load simulated the most severe shock expected, i.e., that anticipated during booster/payload separation. By mid-May 1989, the payload had passed all environmental tests.

Aborted Launch Attempt of June 13, 1989

The first attempt to launch BEAR took place on June 13, 1989. The launch countdown began at noon on June 12 and proceeded smoothly until about 2:00 a.m. (T* minus 1 hour) on June 13, when a total loss of power to the accelerator's beamline cryotrap vent heater was detected. Sustained loss of heater power would have resulted in rupture of the cryotrap's burst disk, necessitating abort of the launch. However, through the efforts of the launch pad crew under the pressure of extremely severe time constraints, this problem was identified and overcome, and the countdown continued— the power failure was traced to an electrical short within the external vacuum system umbilical cable. The launch crew obtained a substitute power supply for the vent heater by patching together several electrical extension cords and an ordinary laboratory power supply, providing voltage directly to the pins of the umbilical receptacle at the payload skin. Diagnosing the problem, "jury-rigging" an appropriate substitute power system, and demonstrating the fix, all took less than an hour.

After the vent heater problem had been solved, the countdown was resumed and proceeded smoothly to zero time. However, because of a failure of a timing circuit located in the Launch Vehicle Segment (LVS), the booster did not ignite as programmed and the launch operations were aborted at T plus 16 sec (at about 3:30 a.m. MDT, June 13).

Although the booster did not ignite, the accelerator's control system did receive the $T = 0$ signal and mindlessly executed the programmed accelerator flight sequence on the launch pad. This response, of course, resulted in the opening of the beamline exit gate valve at T plus 128 sec and the presumably disastrous exposure of the operating accelerator (at vacuum conditions) to atmospheric pressure. As designed, the cryotrap's burst disk ruptured almost immediately. To assess the extent of the damage

---

* In a formal launch countdown, all times are reckoned, minus or plus, from the planned moment of liftoff, $T = 0$.

to the accelerator and to carry out any required repairs, the payload was returned to the vehicle assembly building on June 14.

Within 24 hours of replacing the burst disk and evacuating the accelerator beamline, the accelerator systems were reactivated. Accelerator startup was normal, all systems functioned properly, and the rf quadrupole (RFQ) needed essentially no rf conditioning before nominal accelerator output beam currents were obtained. Accordingly, the abrupt exposure on the launch pad of the operating accelerator to atmospheric pressure did *not* result in any damage to the accelerator (with the anticipated exception of the ruptured cryopump burst disk), clearly demonstrating the robustness of this design.

A detailed analysis of the malfunctioning booster ignition timing circuit uncovered a TTL/CMOS element incompatibility and resulted in a design modification that included incorporation of pull-up resistors and additional filtering. The modified circuit was subjected subsequently to functional and environmental tests and qualified for the BEAR mission. The M56A-1 rocket motor itself was replaced with an alternate unit. On July 6, the booster and payload segments were again mated on the launch pad, and the appropriate tests were carried out in anticipation of launch on July 13, 1989.

Final Countdown and Flight

The final countdown was initiated at T minus 15 hours: 11:30 a.m. MDT, July 12, 1989. During the first 8 hours of the countdown, the accelerator Vacuum Subsystem was configured for flight. This activity involved precooling and charging the beamline cryotrap and replacing the commercial ground support cryopumps with activated flight getter pumps. At T minus 6 hours, the first of two accelerator functional tests was initiated and the accelerator performed flawlessly. The second functional test was initiated at T minus 1.5 hours and, again, operation was virtually perfect. The accelerator systems were maintained in the fully operational state with the contained beam at nominal current level until about T minus 155 sec. At that time, the Radio Frequency (RF) Power Supply and Control Subsystem and the injector's high voltage were turned off, and only the H^- ion source remained on.

Booster ignition and liftoff occurred at precisely 2:30:00.69 a.m. MDT (T = 0) on July 13, 1989. The flight profile, as discussed in the following paragraphs, is presented in Figure 34. The actual flight trajectory was somewhat lower than predicted. Booster burnout occurred at T plus 63 sec at an altitude of about 44 km. Payload separation was effected 22 sec later at approximately 78 km altitude.

The flight's experimental phase began with the initiation of the first pitchover maneuver at T plus 87 sec (at 81 km). This 8-sec maneuver aligned the payload's longitudinal axis with the geomagnetic field vector, directing the beam downward along the magnetic field lines. During the

66
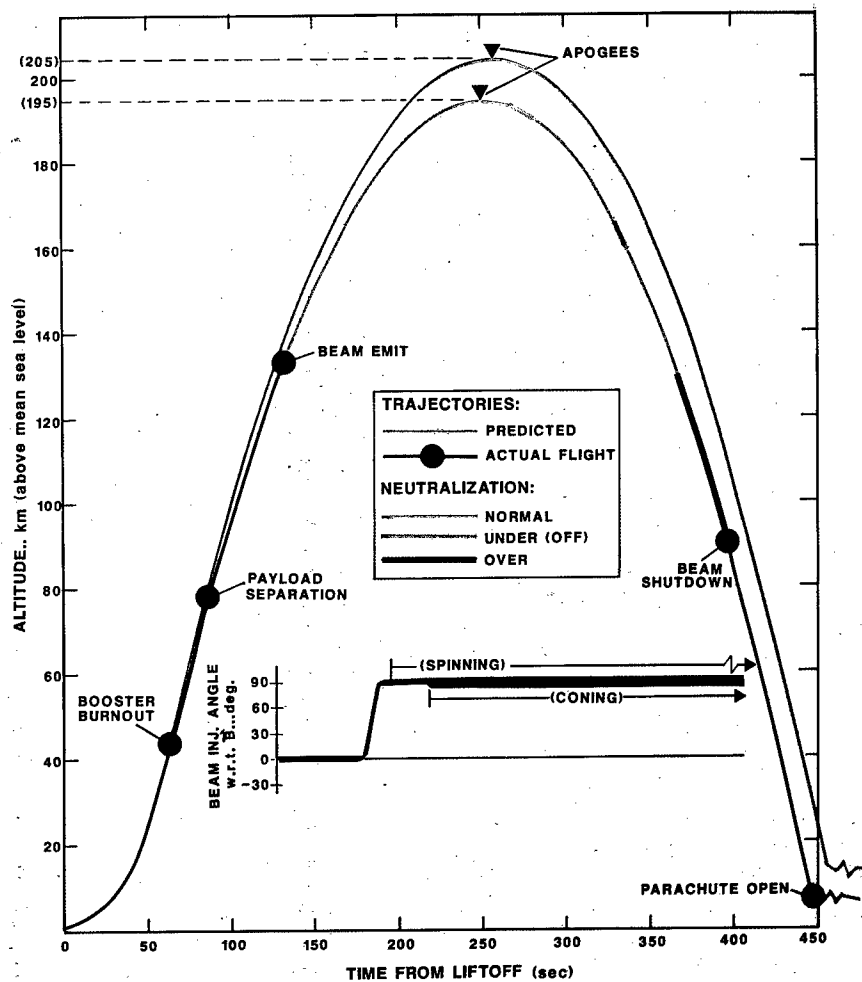
BEAR FLIGHT TRAJECTORY

Figure 34. BEAR flight trajectory. The beam injection angle plot shows spinning and coning (4°-half-angle) motions.

67

maneuver, at T plus 91 sec, the injector's high-voltage extractor was turned on and, 16 sec later, the RF Power Supply and Control Subsystem was enabled. Neutralizer gas pulsing was initiated at T plus 127 sec and, 1 sec later, at an altitude of 133 km, the accelerator beamline exit gate valve was opened, emitting the beam into space.

The second payload maneuver, which was initiated at T plus 176 sec, rotated the payload's longitudinal axis nearly perpendicular to the geomagnetic field to point 155° SSE. Next, beginning at T plus 193 sec, the Attitude Control Subsystem (ACS) thrusters were fired to increase the payload spin rate stepwise, ultimately to about 20 rpm. Finally, at T plus 212 sec, a nutational coning motion was induced to cause the payload's longitudinal axis to precess, varying the angle of the injected beam with respect to the geomagnetic field periodically from about 82° to about 90°. The payload reached apogee 245 sec into the flight at an altitude of 195 km.

To measure the effects of ejecting a grossly underneutralized beam from the payload (especially spacecraft charging), the neutralizer was turned off (producing a pure H^- beam) during the intervals from T plus 260 sec to T plus 270 sec and from T plus 322 sec to T plus 332 sec. Near the end of the experiments, at T plus 360 sec and 133 km, a programmed excess of xenon gas was added to the neutralizer, overneutralizing the beam (producing a net positive current) for the remainder of the flight.

The experimental phase of the flight was concluded after 394.5 sec at 90 km, when the beamline exit gate valve was closed and all accelerator systems were shut down. The recovery parachute, which was released when the payload reached an altitude of 5.9 km, retarded the payload's terminal rate of descent to about 20 ft/sec. Impact occurred approximately 77 km (48 miles) uprange, nearly due north of the launch pad.

During the flight, all instrumentation functioned normally and the resulting data streams were successfully telemetered to the ground stations and were also recorded by the on-board recorder. The discrepancy between the predicted and actual flight trajectories (Figure 34) was attributed largely to underestimation of drag coefficients, since there were no prior empirical data for a payload of these dimensions.

Flight System Recovery

The payload system was located and recovered[7] by the recovery team at about 6:30 a.m. MDT on July 13. Apparently the payload assembly had impacted the earth vertically and had then fallen over on its side, the forward end striking a slightly higher, mounded area in the process. The resultant shear forces caused the clamp that holds the APS and SPS together to part, separating the two segments (Figure 35). The APS and SPS were brought back to the vehicle assembly building for cursory inspection and evaluation, and it was found that the accelerator beamline could still hold a vacuum.
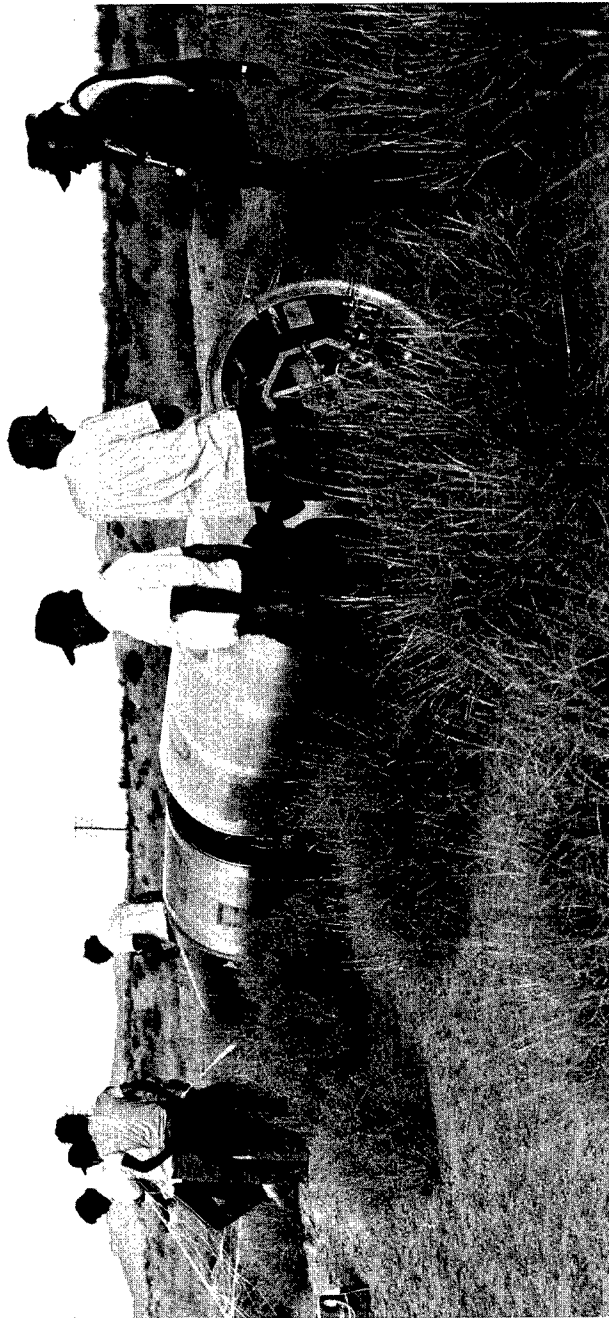
68

Figure 35. Recovered payload at the site of impact.

The APS was returned to Los Alamos on July 21, partially disassembled, and inspected. Mechanical damage to the main structure on the APS was found to be limited to a few pieceparts. Some subassemblies near the aft end of the BD Section sustained significant damage, but, in general, most instrumentation was operable with little or no restoration.

This minor damage was easily and quickly repaired. After the detailed inspection of the accelerator, the two ground support cryopumps were installed, one on the Low-Energy Beam Transport (LEBT) and one on the HEBT. The accelerator vacuum reached the 10^{-6}-torr range after only a few hours of pumping. It is especially noteworthy that the one LEBT flight getter pump remaining on the accelerator was reactivated and continued to pump successfully on the beamline.

On July 26, the accelerator was operated at Los Alamos. All the accelerator systems came on rapidly and operated normally and stably, with the exception of a slight decrease (from 95% to 90%) in the rf field level of the RFQ. No rf conditioning of the RFQ was required, and nominal HEBT output beam currents were obtained shortly after full operation was initiated. This result is another testimonial to the ruggedness of the BEAR NPB accelerator system.

ACCELERATOR PERFORMANCE

Flight Vibration and Shock Loads

To provide a better understanding of the accelerator's flight performance, it is relevant to discuss first the vibration and shock loads experienced by the payload during the launch and booster separation phases. The accelerometer data obtained at the top of the Space Frame (the bottom of the injector) indicate that the random vibration levels experienced during the launch were quite low. In fact, the overall rms acceleration level was less than one-third of that experienced at the same location during the system-level random vibration test at WSMR.

However, the shock loads experienced during booster/payload separation were significantly different from the 11-ms, half-sine pulse of the ARIES specification. The accelerator shock response data, obtained at the top of the payload Space Frame, indicate an initial spike, rising in less than 1.5 ms, that could only be produced by a very rapidly rising separation load (approximated by a step rise followed by exponential decay). This initial spike is followed by a higher and broader peak that is characteristic of the system's fundamental frequency response. The calculated shock spectrum, based on accelerometer data from the top of the Space Frame, has a 22-g peak at about 75 Hz (as expected and observed during flight simulation tests) but also has an additional *unexpected* 23-g peak centered at approximately 260 Hz.

Intermittent erratic behavior of the accelerator ion source was observed immediately after booster separation and persisted for the duration of the

flight. The cause of this abnormal behavior was probably a shock-induced malfunction of the pulsed piezoelectric hydrogen flow control valve located on the ion source body. A generically identical hydrogen valve assembly had been successfully shock tested as part of the ion source/LEBT subassembly with a 25-g peak, decaying sinusoidal transient. For the test, the subassembly shock spectrum had a single peak at about 70 Hz. However, during the flight, the hydrogen valve assembly was also subjected to at least a 23-g shock load that peaked at about 260 Hz. Recent (postrecovery) tests indicate that the valve assembly has a fundamental frequency of approximately 250 Hz. Accordingly, the hydrogen valve assembly experienced a significant and unanticipated shock load during booster/payload separation, which appears to have disrupted the valve's operation.

Pulse-to-Pulse Performance in Flight

The detailed pulse-to-pulse accelerator performance obtained during the flight is best summarized by the data presented in Figures 36, 37, and 38. Once again, in these figures, T = 0 sec corresponds to booster ignition; at T = 128 sec, the beamline gate valve was opened; and, at T = 394.5 sec, the beamline gate valve was closed and the accelerator systems were shut down. The accelerator produced relatively normal beam pulses (in excess of 10 mA) for about 300 of the total 1,310 pulse commands. A more comprehensive discussion of the erratic behavior of the ion source (and, hence, of the accelerator) caused by the shock-induced malfunctioning of the hydrogen flow valve is presented in Volume II.

The time history of the injector's operating characteristics during the flight is illustrated in Figure 36, which presents the ion source arc current, the pulsed extractor voltage, and the H^- beam current measured at the output of the LEBT. The ion source pulsed continuously with a repeatable arc current of about 126 amperes during the ignition and boost phase. Immediately after separation (T = 85 sec), ion source operation became intermittent, the arc current magnitude varying sporadically between zero and some level above instrument saturation (166 amperes). Good beam pulses (>10 mA) were observed for arc currents between about 70 and 140 amperes (the nominal arc current was about 120 amperes). The extractor's high voltage was turned on at T = 91 sec. The intermittent behavior of the ion source resulted in associated extractor breakdowns in which normal extractor voltage (about 35 kV for good pulses) decreased to a mean value of about 25 kV. During extractor breakdowns, the LEBT current toroid electronics were driven into saturation (spurious LEBT current of 76 mA [Figure 36]). During good beam pulses, the mean actual LEBT current was about 42 mA.

The operating characteristics of the accelerating elements (RFQ and RF subsystems) and the HEBT during flight are presented in Figure 37. The top trace in Figure 37 shows the time history of the rf field level in the RFQ in percent of the nominal level required for acceleration of the H^- beam to 1 MeV; in actuality, beam acceleration to 1 MeV is obtained at values as low as 80% of nominal. Before launch, the rf field-level set point

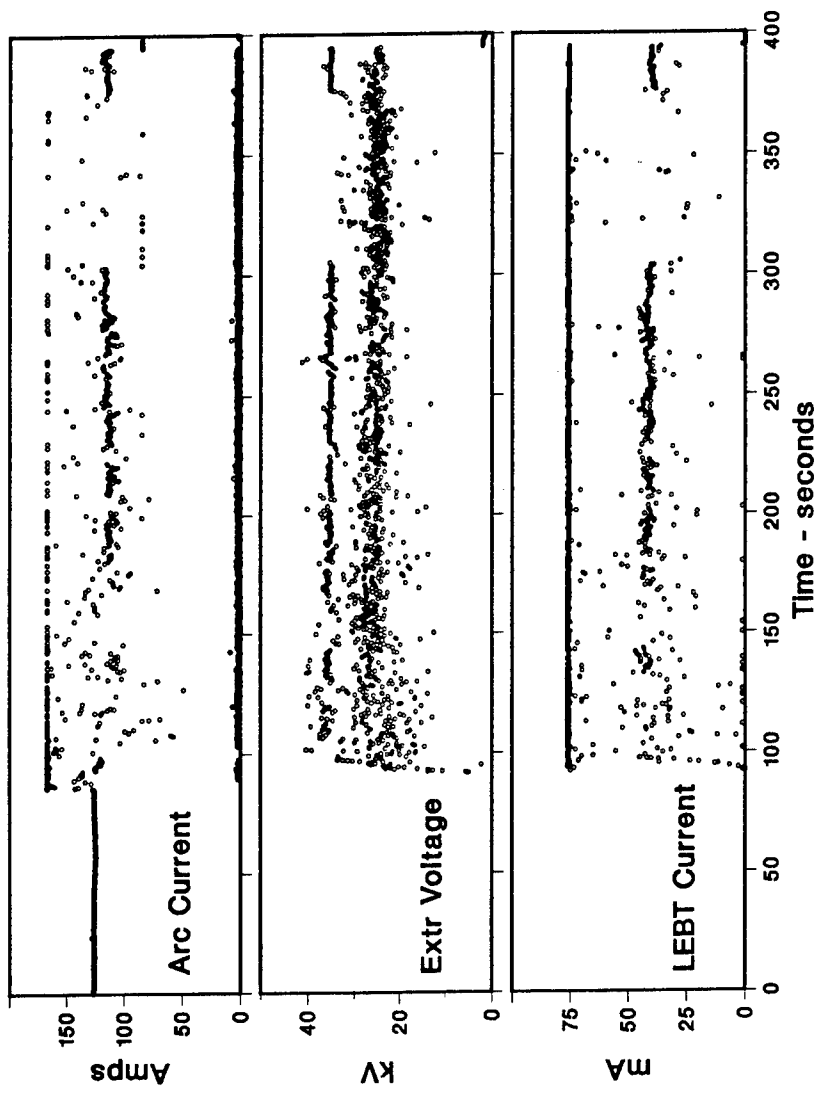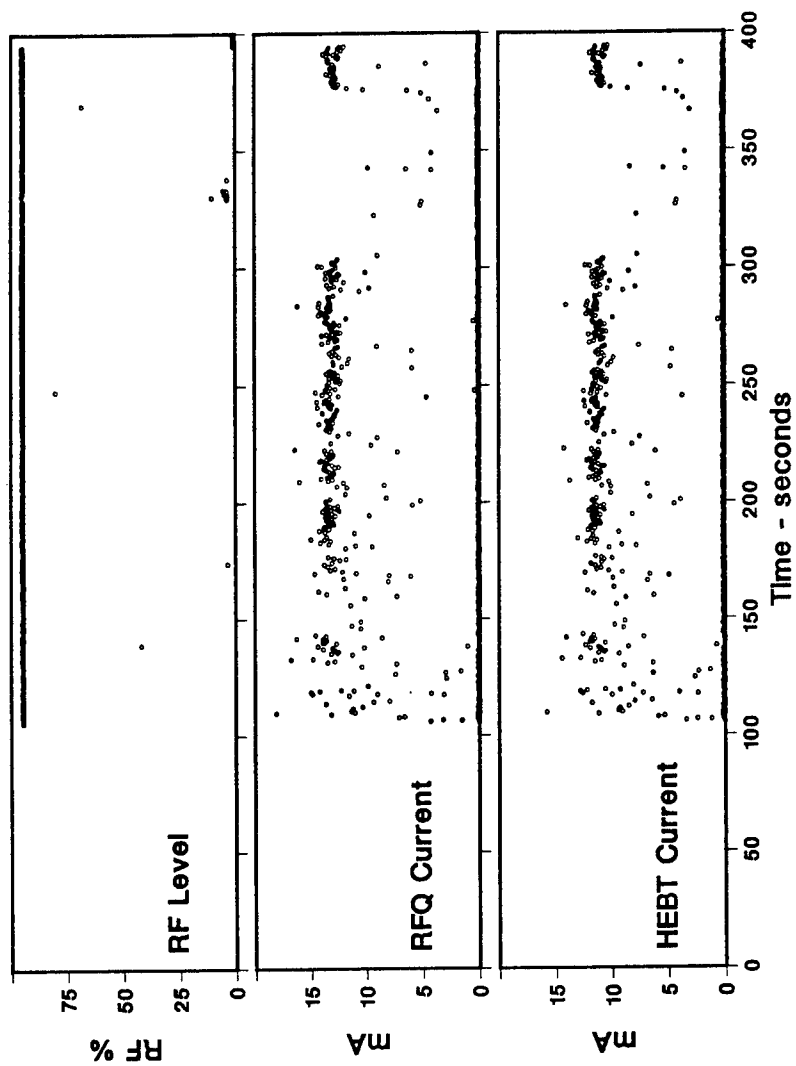Figure 36. Time histories of injector's operating characteristics during flight.

72

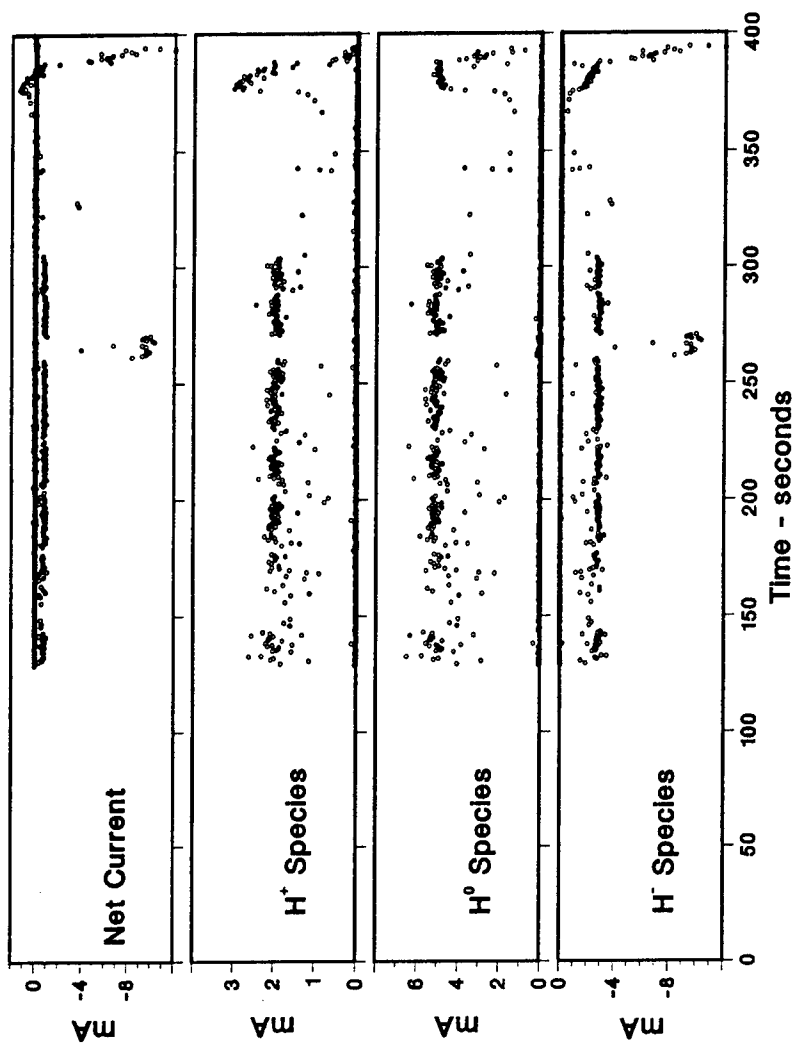Figure 37. Time histories of rf field level and of RFQ and HEBT output beam currents.

73

Figure 38. Time history and composition of neutralizer output current.

was adjusted to its typical operating value of 95%. This value minimizes the possibility of arcing in the RFQ cavity. The RF Subsystem was activated 15 sec after the high-voltage extractor was turned on. Figure 37 shows that the rf field level in the RFQ rose from zero to its full operating value in less than one interpulse interval (200 ms), i.e., no rf conditioning was required. The essentially flat rf-field-level trace demonstrates extremely stable and consistent operation of the RFQ and RF subsystems for the duration of the flight, despite drastic pulse-to-pulse beam-loading variations from 0% (when the arc current was lost) to as much as 40% at peak output beam current. The lower two traces of Figure 37 show the time histories of the RFQ and the HEBT output beam currents. As expected, these two traces are essentially identical, allowing for the normal beam current loss (approximately 10%) in the HEBT. The RFQ output beam current magnitude varied from 0 mA to a maximum of 18 mA, compared with the nominal RFQ output current of 13 mA.

The characteristics of the final beam exiting the neutralizer, as observed by the BCM in the BD Section, are presented in Figure 38. The shadow-producing wire (located in the neutralizer) of the SWS diagnostic reduced the neutralizer's output beam current by absorbing about 10% of the beam. Thus, although the nominal current out of the HEBT was about 11 mA, the H^- beam current (as recorded by the BCM between T = 260 and 270 sec, when the neutralizer was turned off) was about 10 mA. The BCM measures the net charge component of the output beam current, which is constituted of H^+, H^o, and H^- particles. With the neutralizer on, a net negative beam current of about 0.8 mA exited the payload. The magnitudes of the nominal species currents were $H^+ \approx 2.1$ mA, $H^o \approx 5$ mA, and $H^- \approx 2.9$ mA.

Between T = 303 and 375 sec, the accelerator did not produce any HEBT output beam pulses in excess of 10 mA. However, between 375 sec and accelerator shutdown at 394.5 sec, nominal HEBT output currents of about 11 mA were generated on essentially every other accelerator pulse. During this interval, the xenon gas pressure in the neutralizer had been about doubled, as programmed, resulting in overneutralization of the accelerator output beam. In this case, the net output beam current was positive, as desired, with a peak magnitude of 1.4 mA at T $\approx$ 376 sec. The corresponding magnitudes of the species currents were $H^+ \approx 3.2$ mA, $H^o \approx 5.2$ mA, and $H^- \approx 1.8$ mA. Between 376 sec and the closing of the beamline exit gate valve, what appear to be anomalously large (up to 24 mA) negative net output beam currents are indicated. This observation is not yet completely understood but is associated with the production of secondary electrons at the relatively low altitude (115 to 90 km) of the payload during this time interval.

Comparison of Flight Versus Ground Test Performance

An important objective of the BEAR flight was to determine the effects of the space environment on the NPB accelerator's operation. The magnitude of the beam current generated by the accelerator in space has already

been discussed. Given the operating parameters of the injector during the flight, the magnitude of the measured H^- beam out of the HEBT is consistent and compares very well with the results of functional tests carried out on the ground with the same set points.

A more global comparison of accelerator performance is that between the beam divergence, pointing, and their jitter, as determined on the ground during flight simulation tests with the corresponding values obtained during the flight. The beam divergence and pointing were measured in both cases with the SWS instrument located in the BD Section. Figure 39 shows the beam divergence determined during flight simulation tests carried out at Los Alamos and at WSMR between March 15 and June 20, 1989. The single data point for July 13 is the flight value, which represents measurements obtained between the opening of the beamline exit valve (T = 128 sec) and turning off the neutralizer (T = 260 sec). The flight data point is an average of all the good accelerator beam pulses during this time interval, when the sensor wires were in shadow. The jitter in divergence, corresponding to the data points of Figure 39, is shown in Figure 40. Clearly, within the data scatter, the flight data and the ground data are indistinguishable. The beam pointing and jitter in beam pointing are shown in Figures 41 and 42, respectively. Again, the flight and ground data are comparable. It may therefore be concluded that the space environment did not significantly affect the beam divergence, pointing, or jitter in these parameters.

SPACE PHYSICS RESULTS

This section of the report summarizes what has been learned to date concerning the space physics issues—the questions that have arisen with regard to the mutual interactions among the emergent partially neutralized particle beam, the spacecraft itself, and the local space plasma environment. These issues were addressed by the five secondary objectives of the BEAR mission. Some of the enormous data set collected from the BEAR flight has not been fully analyzed, correlated, or interpreted at this writing; hence, some of the space physics results subsequently presented are preliminary. However, they are sufficiently definitive to provide immediate guidance to a follow-on NPB space experiment.

Beam Propagation

The NPB propagation issue concerned potential anomalous stripping processes and far-field, beam magnetic optics distortions. BEAR did not address the latter issue, but the BEAR beam was sufficiently energetic to test Born-approximation descriptions of stripping processes. The relevant parameters and effects that were observed directly with the flight instrument package were the neutral and plasma density in the NPB path, airglow (resulting from particle collisions with ambient neutrals), and the return flux of energetic protons.

76
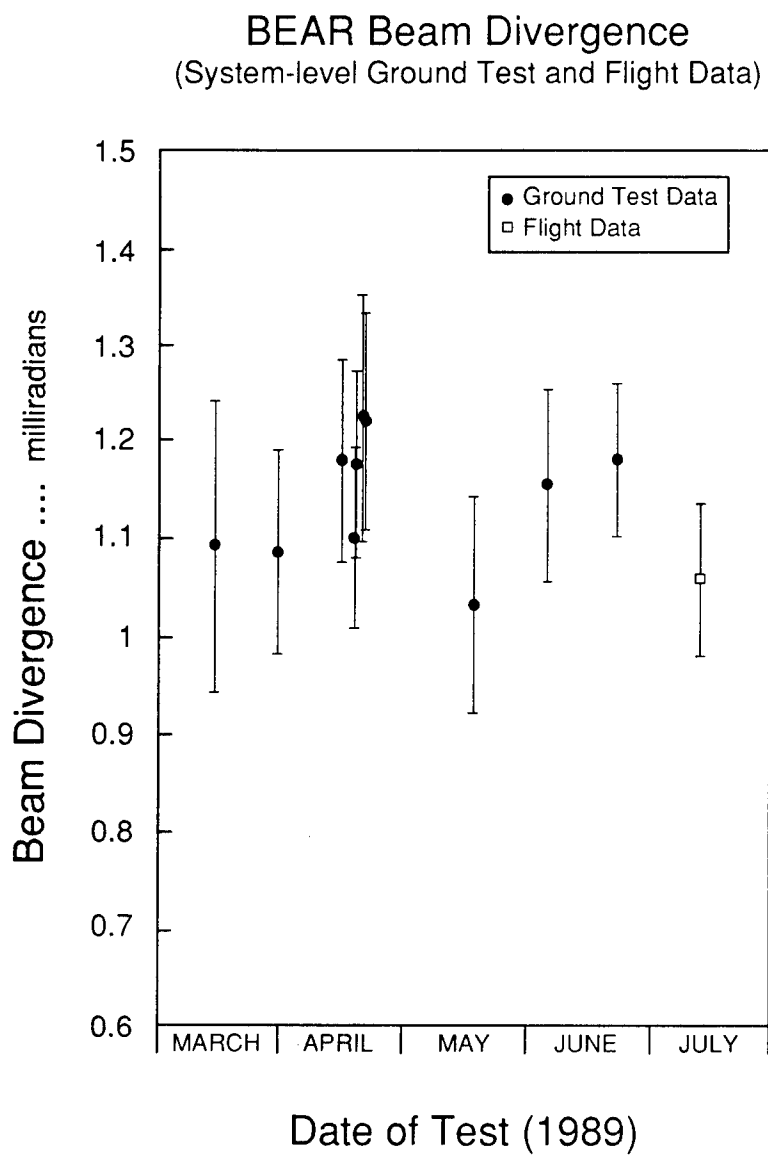
Figure 39. History of beam divergence.

BEAR Beam Divergence Jitter
(System-level Ground Test and Flight Data)
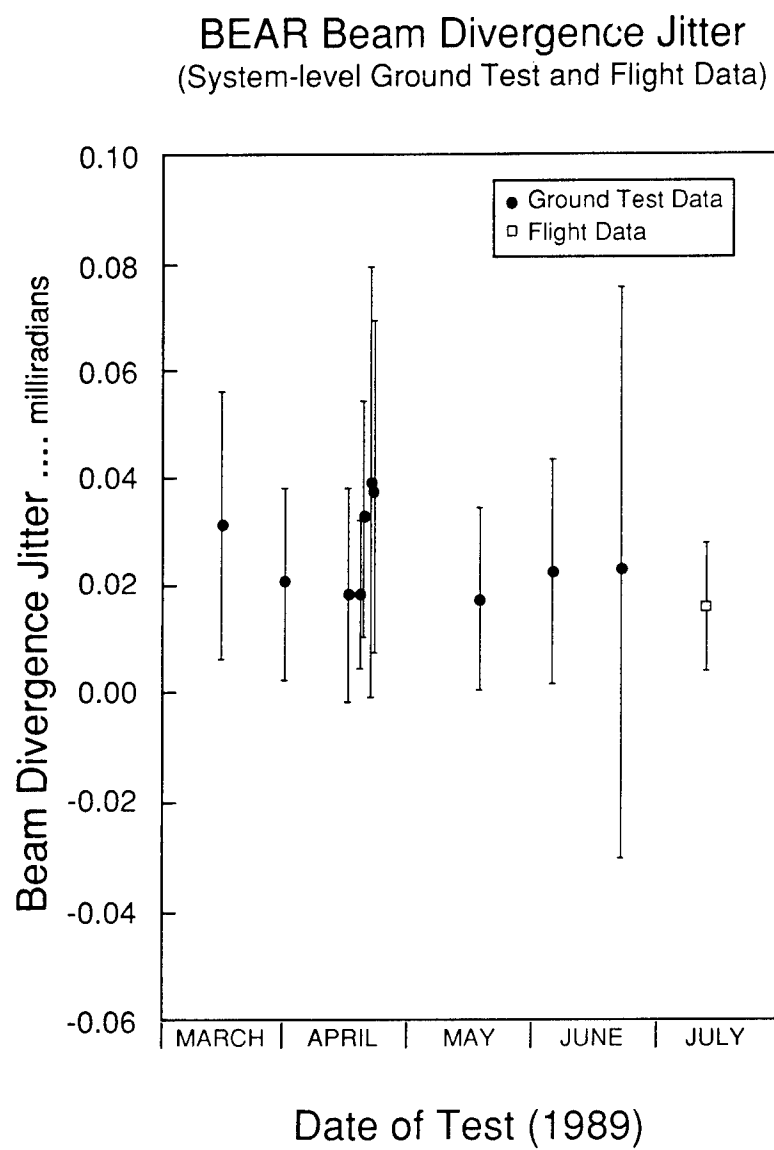
Figure 40. History of jitter in beam divergence.

BEAR Beam Pointing
(System-level Ground Test and Flight Data)

Figure 41. History of beam pointing.

BEAR Beam Pointing Jitter
(System-level Ground Test and Flight Data)

Figure 42. History of jitter in beam pointing.

The neutral density of the beam path was automatically varied by the continuously changing payload altitude and, additionally, by programmed variation of the NPB injection angle with respect to the geomagnetic field vector, **B**.

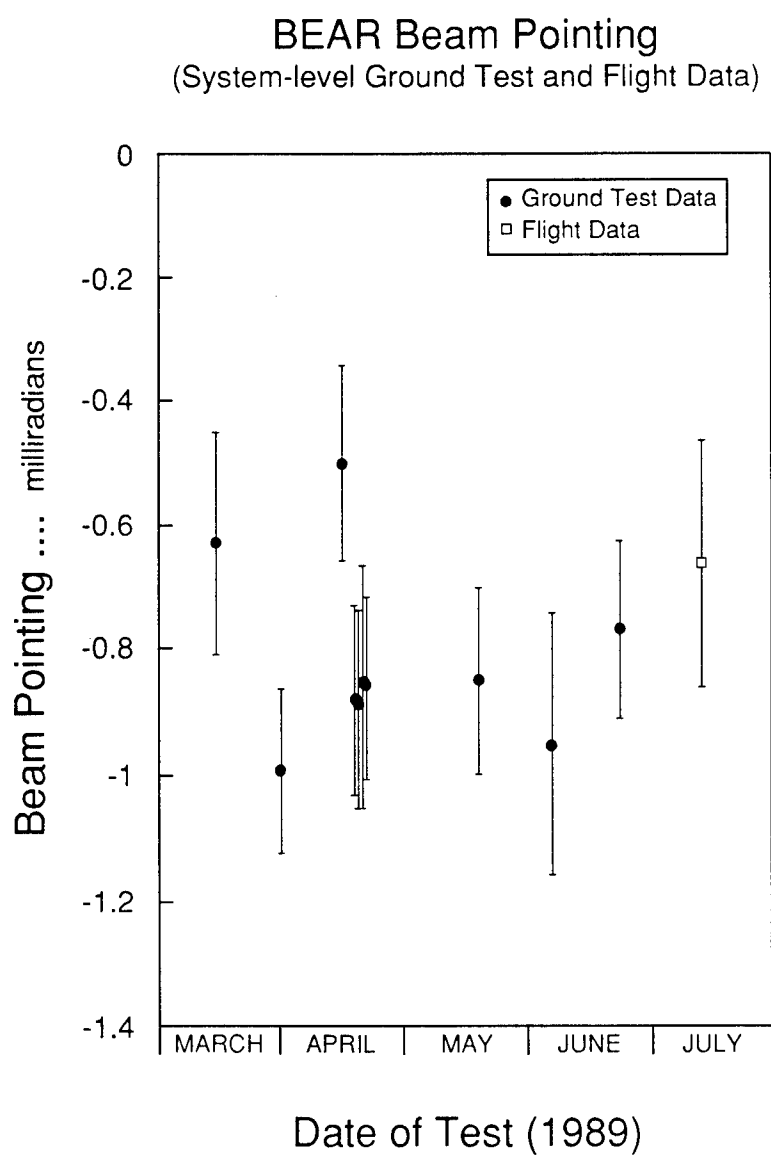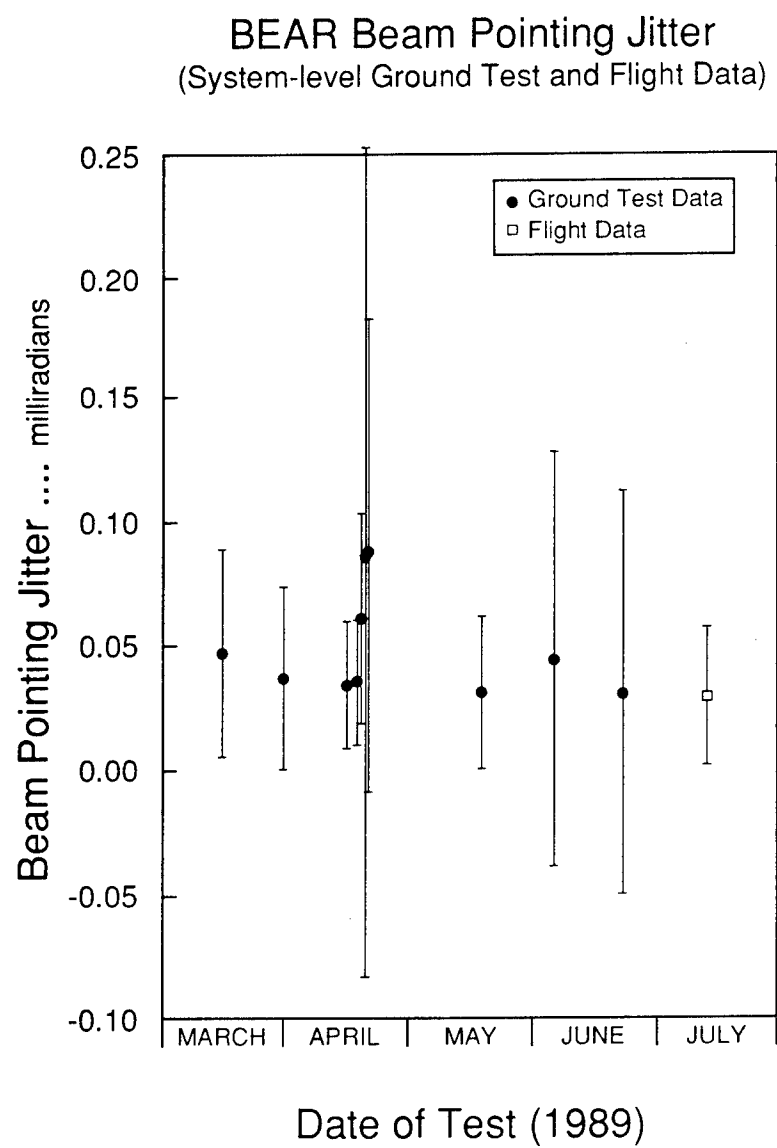The neutral hydrogen atoms were injected south and east (magnetic) before the occurrence of the stripping collisions that converted them to protons. Gradients in the geomagnetic field caused the resultant protons to drift westward as they gyrated. If the protons are initially moving downwards with respect to the magnetic horizon, the amount they drift before returning to the payload altitude is determined by the time taken for them to bounce back from the geomagnetic field "mirror." There is a one-to-one relationship between the pitch angle of an observed proton and the distance it traveled as a hydrogen atom before stripping. Therefore, the solid-state particle detector (SSD) measurements of the fluence of returning protons can be used to estimate the NPB stripping cross section. The NPB injection angle was varied periodically from about 82° to about 90° by an induced coning motion of the payload's spin axis, i.e, precession about the angular momentum vector. The attitude control thrusters were used to augment the natural perturbation in the spin motion.

Data from the cold-cathode ionization gages (CCIGs) (Figure 43) in the BD Section indicate that outgassing was a negligible contributor to the neutral density along the NPB path. The SSD instrument measured (Figure 44) up to 100 counts/pulse in the 1-MeV channel during three time intervals centered on the 200-, 270-, and 340-sec points. These were the times when maximum count rates were expected because the injection was closest to being orthogonal to **B**. In terms of count rates and time of observation, all the SSD measurements are consistent with prelaunch Monte Carlo predictions (Figure 44), based on classical hydrogen atom stripping processes. A more comprehensive quantitative analysis of these data awaits correlation with an accurate payload attitude tape, which uses the three-axis magnetometer and the ACS gyro data to determine the injection pitch angle to ±0.5°.

Video images that show beam propagation by airglow along the path are also being analyzed. On the downleg portion of the flight, the TV beam observations are from altitudes below 120 km, where the stripping mean free path is less than 200 meters. As a result of the relatively high nitrogen density at these low altitudes, the uv TV camera, viewing over a narrow band of wavelengths near 391.4 nm, recorded spectacular beam images during the late stages of the flight. Figure 45, from a perspective almost parallel to the beam axis, shows the beam propagating away from the payload and subsequently turning in the geomagnetic field. The upper photo (Figure 45[a]) is the airglow image as recorded by the uv TV camera. In the lower one (Figure 45[b]), *faux* color has been added to display the variation in intensity across the beam and clearly shows its relative uniformity. This image was taken at 393 sec, when the altitude was sightly greater than 90 km. The beam-stripping distance at this altitude is about 1 meter.

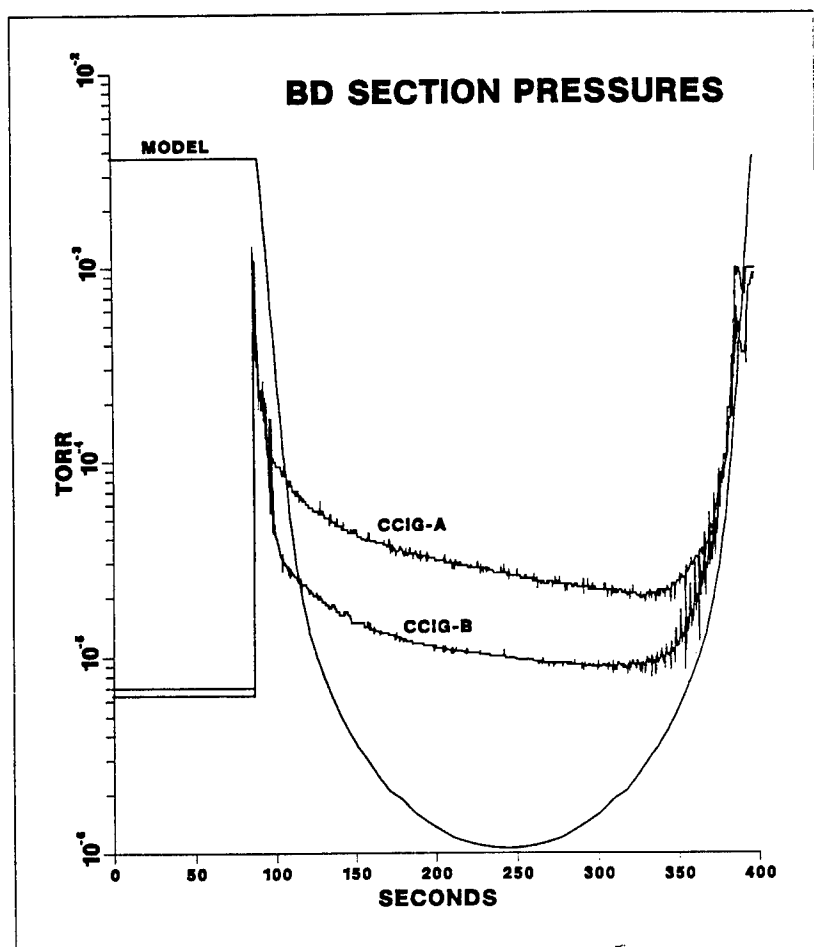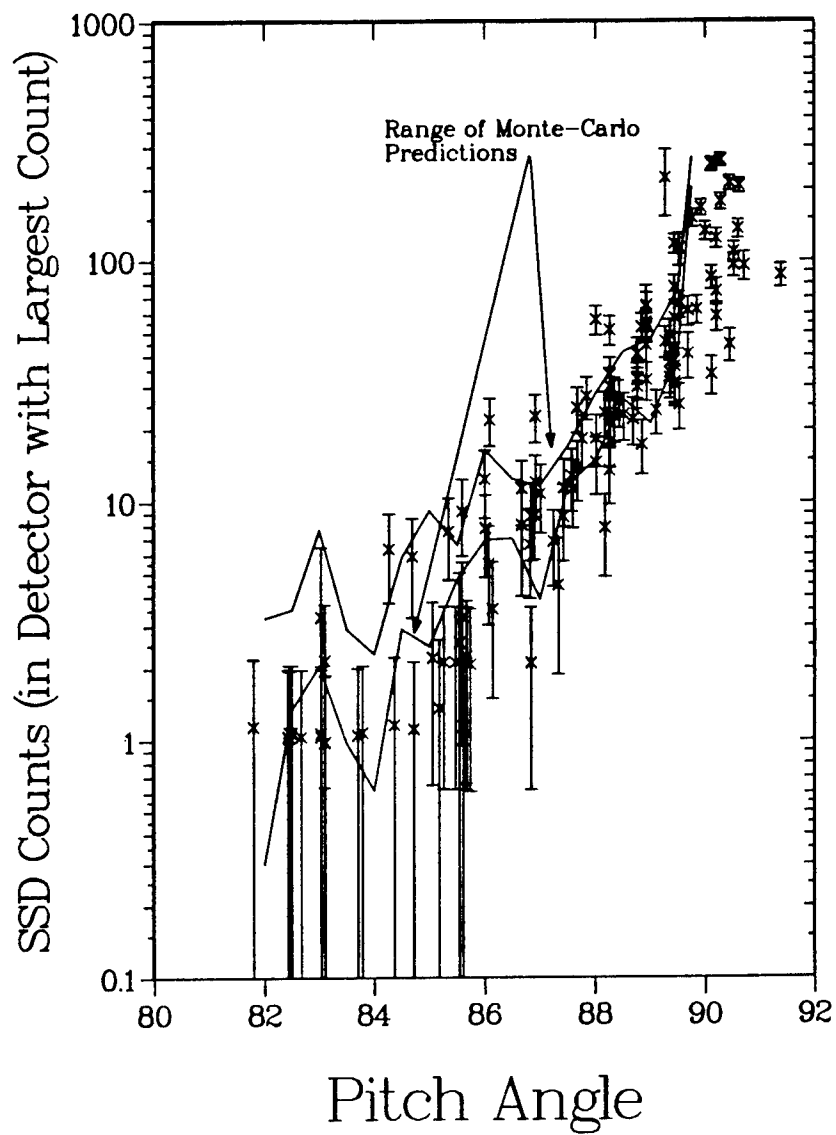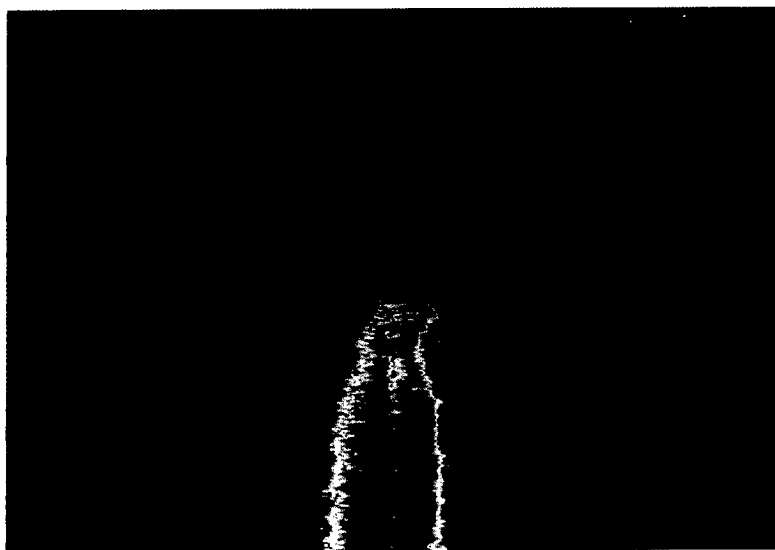Figure 43. CCIG flight data and ambient pressure history from model.

Figure 44. SSD flight data and range of Monte Carlo predictions.

(a)

(b)

Figure 45. Ultraviolet airglow image of beam propagation (ca. 90 km altitude), [a] as observed, [b] colorized to show intensity.

During the upleg portion of the flight, when the beam was oriented parallel to **B**, video images of the beam were obtained from the uv TV between 138 and 145 km altitude. These images were analyzed in terms of the spatially resolved radiance of the beam airglow emission and were compared with model predictions. The results of this analysis indicate that the beam divergence remained at 1 ± 0.3 mrad, at least out to about 1 km, which was the effective range observed by the camera. A comparison of the model-predicted beam radiance versus the measured radiance is shown in Figure 46. The beam radiance increased noticeably for distances greater than 10 meters. This effect is partially attributable to the geometric effect of integrating the emission from longer beam pathlengths and partially to the contribution from the airglow produced by electrons stripped from, and continuing to travel (parallel to **B**) with, the beam.

Based on SSD and video data, there appear to be no anomalies associated with the propagation of the neutral beam; that is, beam propagation was controlled by the expected single-particle collision processes (stripping and ionization/excitation) of the tenuous background atmosphere.

Spacecraft Charging

Spacecraft charging would be extremely difficult to measure directly and, for practical reasons, is inferential. The pertinent observables with the BEAR instrumentation were the energy spectrum of particles striking the payload; the sign (positivity or negativity) of probe currents collected as a function of probe bias voltage; arcs, sparks, discharges, etc., between payload elements; plasma waves; and the ambient plasma density and temperature.

The ambient plasma density and temperature delimit the current available at zero potential difference ("thermal" current) for neutralizing net current emission. The altitude variation in the BEAR trajectory provided a change of about a factor of 10 in the thermal current to the payload. Thermal electron collection is dominated by flow along the magnetic field; therefore, changing the payload's effective collecting area normal to the **B** vector can result in a significant variation in spacecraft charging. BEAR was initially oriented along **B**, exposing an area of about 2 m^2 for electron collection. When the payload was pitched to inject perpendicular to **B**, this area increased to about 20 m^2. Probably the most important control exercised over spacecraft charging during the BEAR experiment was the ability to vary the sign of the net current emitted by modifying neutralizer operation. Gases emitted during ACS thruster firings also affected spacecraft charging.

Preliminary flight data analysis indicates that the payload did indeed experience charging. The sign of the charge and the temporal variation of the potential with respect to the ambient plasma differ over the course of the experimental period. The most obvious indication of spacecraft charging is the increase in the flux and average energy of electrons collected (Figure 47) by the electrostatic analyzer (ESA) sensors in the first interval during which
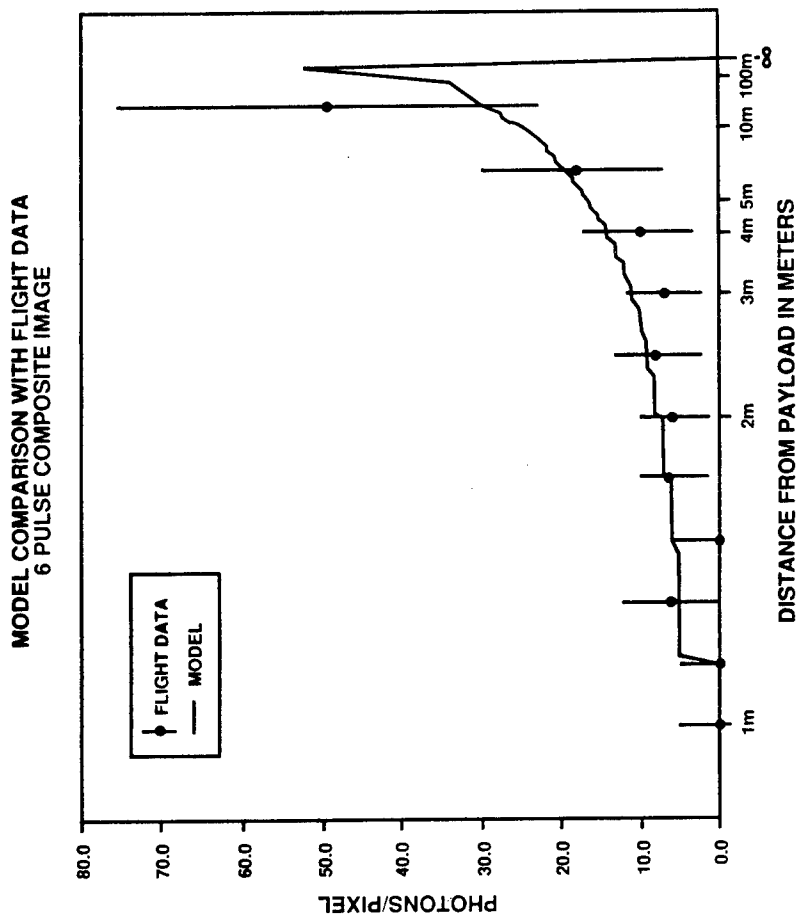
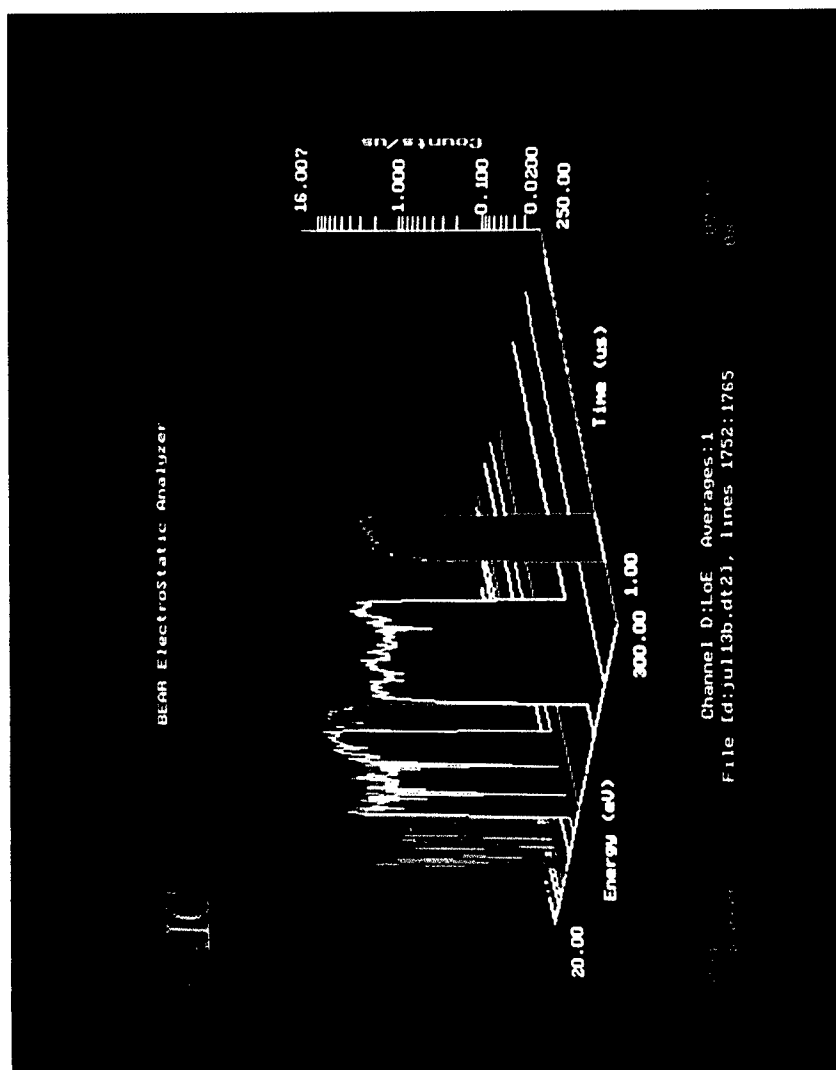Figure 46. Comparison of measured and modeled beam radiance profiles.

Figure 47. Electron current measurement by ESA [SAIC/NW].

the neutralizer was shut off. Increases in the flux of electrons at all energies observed (up to 3000 eV) suggest charging levels up to 1 kV. The high-voltage detector (HIV) instrument, which was designed to acquire data over a cycle that contained a string of repetitive pulses, was unfortunately inhibited in its operation by the missing pulses, which prevented the stepping function—designed to zero in on the voltage level—from ever converging. However, the Naval Research Laboratory's (NRL's) analysis of the available HIV data (Figure 48), in conjunction with Langmuir probe measurements, tends to confirm the foregoing tentative result from the ESA data.

LANL's computer simulations of spacecraft charging suggest that the sign of the skin potential oscillates in time with respect to the distant plasma. The ESA measurements suggest that, during the pulse, the payload charged to collect current of the same sign as the net current being emitted. However, observations with a lower time resolution by the Plasma Wave Receiver (PWR) of the potential difference between the skin and a spherical probe show that, on a millisecond time scale, the payload potential may overshoot. Preliminary Langmuir probe observations confirm the overshoot phenomenon.

Langmuir probe and PWR data (Figure 49) show the enhanced charging effect from underneutralization. Most significantly, they suggest that low-voltage charging ($\sim$40 volts) occurred during the normal neutralization periods. Most features of the spacecraft charging observations can be explained by a simple capacitive relationship ($Q = CV$), with a payload effective capacitance of about 200 pF. The net charge, Q, includes both energetic particles leaving the payload and electrons flowing along $\mathbf{B}$ to compensate. Nevertheless, there is no evidence that the spacecraft charging that did occur interfered with the accelerator's operation or with NPB diagnostics.

Effects of Neutral Gas Effluents

There was some concern that neutral gases desorbed from spacecraft surfaces or emitted by discrete sources such as the ACS thrusters might affect NPB operation through high-voltage breakdown caused by trapped gases, beam stripping, or enhanced spacecraft charging (resulting from the depletion of the ambient neutralizing plasma). Neutral gas pressure and the ambient and disturbed plasma parameters were measured. In addition, the accelerator operation and beam propagation were monitored. To allow sufficient time for venting and outgassing to lower internal gas pressures in the BD Section, the beamline exit valve was not opened until T + 128 sec. Pulsing of the attitude control thrusters resulted in significant neutral effluent transients throughout the flight, as did varying the xenon flow to the neutralizer.

The CCIGs in the BD Section measured gas pressures very near but below the levels predicted before the launch (Figure 43). Neutral effluent transients, ACS firings, and neutralizer shutoff were not observed by the CCIGs. The more recessed CCIG, the one nearest the beamline gate valve,
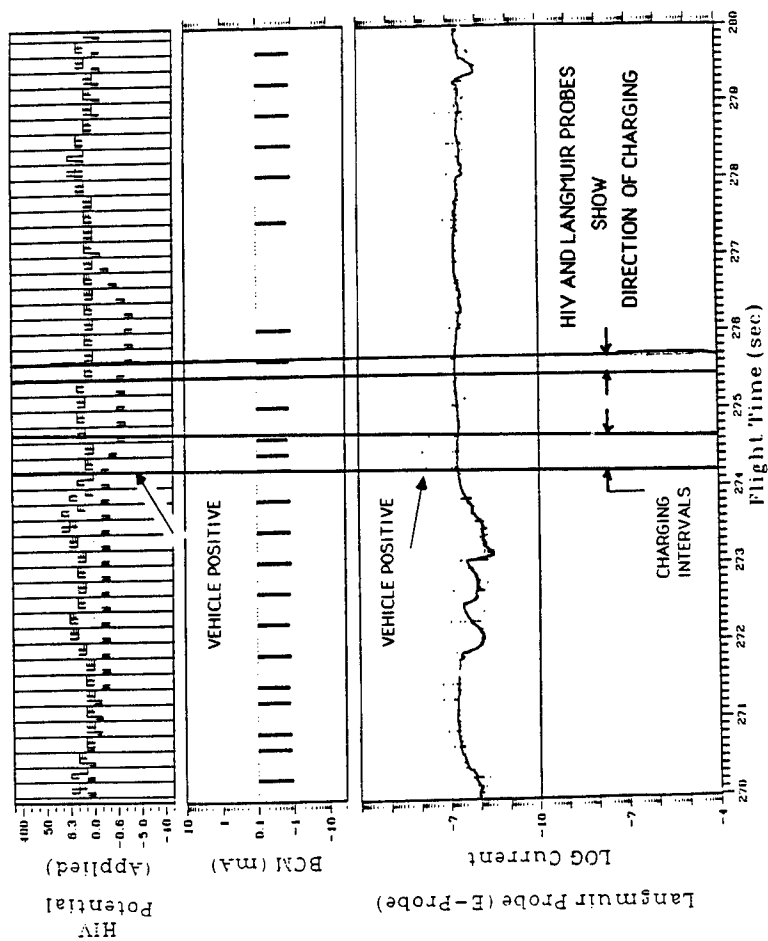
Figure 48. HIV and Langmuir probe data confirm spacecraft charging [NRL].
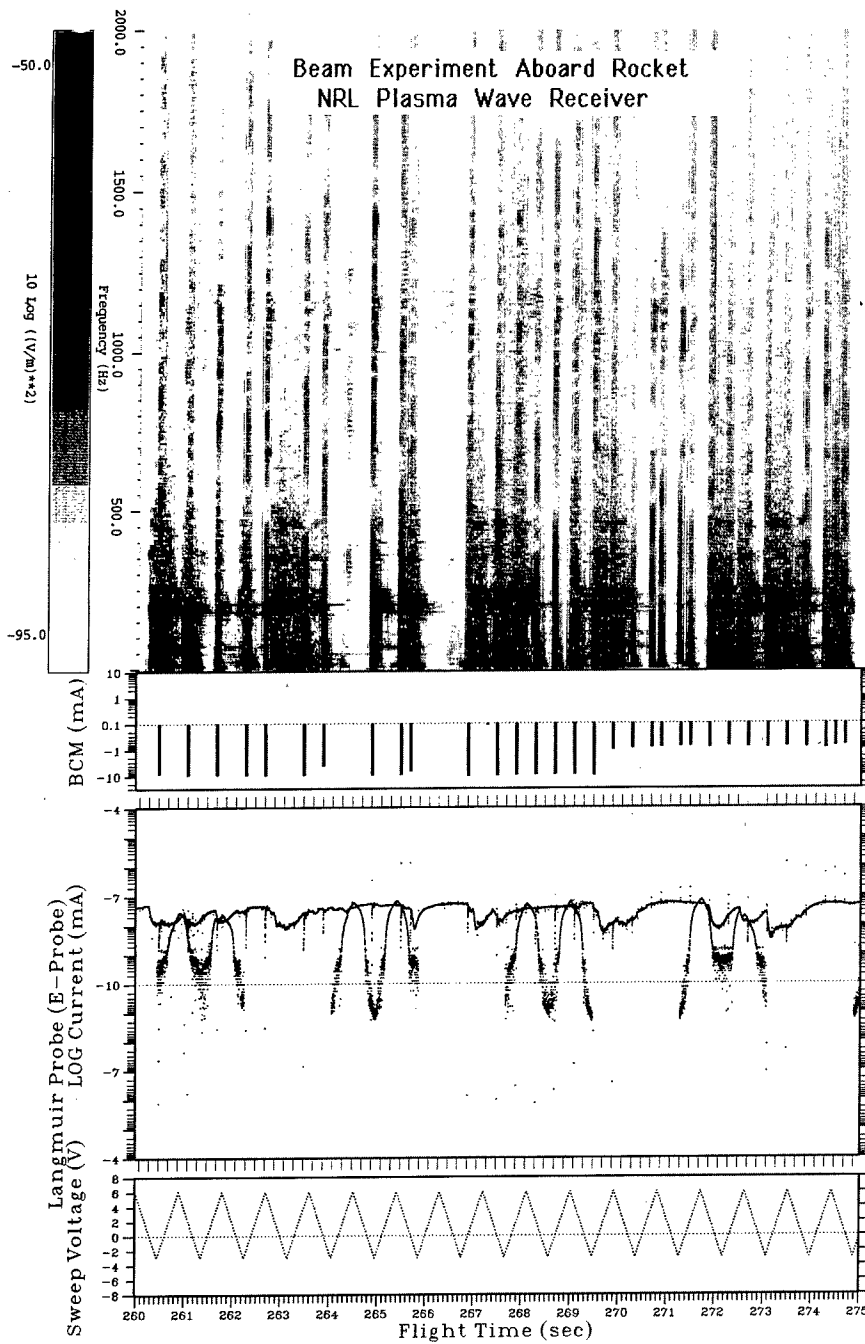
89

Figure 49. PWR and Langmuir probe data during first underneutraliza-
tion period [NRL].

90

showed a minimum pressure of 2×10^{-5} torr, while the CCIG more exposed to space indicated a minimum pressure of 9×10^{-6} torr. The difference is probably caused by outgassing and less efficient space pumping. Plasma depletion effects caused by thruster firings were observed by the Langmuir probes.

There is no indication that neutral effluent effects interfered with accelerator operation or with NPB diagnostics.

Beam Avoidance Considerations

The dynamics of the ions initially moving with the NPB were of concern for several reasons. Instabilities in the ion beams could produce strong electrostatic turbulence and perhaps cause anomalous stripping (Alfvén's critical ionization velocity phenomenon). A more mundane and likely possibility was the shoot-yourself-in-the-foot danger from ions gyrating within the geomagnetic field and returning to strike the accelerator payload. The predicted westward drift of positive ions should have provided adequate beam avoidance, but the actual effects of trapping energetic protons within the magnetosphere remained to be determined. The relevant information that the BEAR instrumentation provided concerned the return flux of magnetically trapped ions, divergence of the beam ions (rifle- or shotgunlike), plasma waves produced by instabilities, and ambient plasma density and temperature.

In flight, the beam injection pitch angle was varied to test for beam-produced instabilities as a function of the velocity of the ions perpendicular to the geomagnetic field while the SSD measured the conditions under which energetic protons returned to the payload and the PWR instrument searched for electrostatic waves. The trajectory provided the changing background of neutral and plasma parameters. Ideally, the NPB injection azimuth should also have been varied. This could not be done, however, as the injection azimuth was chosen primarily to use the SSD for the stripping cross-section measurement.

The TV cameras, the SSD, and PWR instruments provided excellent data for studying this issue. The uv TV observations near the end of the flight seem to rule out any shotgunlike increase in charged particle beam divergence at the neutral and plasma conditions characteristic of low altitudes. If the H^+ component of the beam had returned to the payload after only one gyration, the fluences measured by the SSD instrument would have been about 10,000 times greater than the observed values. The lower actual fluences suggest that single-particle dynamics adequately describes the ion motions to first order. However, the dramatic increase in electrostatic turbulence measured by the PWR when the accelerator pitched over and began injecting perpendicular to B does indicate that higher-order effects cannot be ignored. Hence, at this time it would be premature to rule out possible deleterious effects of stray charged particles resulting from improper beam neutralization in future space-based NPB experiments. Further data analysis and theoretical studies are necessary.

Unanticipated Phenomena

One gratifying result of the BEAR experiments was that no novel or unanticipated space physics phenomena—pernicious or benign—manifested themselves over the course of the flight. The absence of such phenomena lends great confidence to the engineer and physicist designing a future NPB space experiment.

5. CONCLUSIONS AND RECOMMENDATIONS

The major conclusions derived from conducting the BEAR Project and those related to operating NPB accelerator systems in space are presented in this section. The conclusions are predicated largely upon the flight data and observations, though they are sometimes augmented by prior or postflight ground test results. These conclusions are grouped in two categories: "firm" conclusions and "tentative" conclusions. The firm conclusions are those that represent unequivocal answers, as obtained from the data evaluated as of this writing, to the questions addressed by the BEAR mission. The tentative ones are those for which all of the critical data have not yet been reduced, correlated, and evaluated and/or those for which the issues were only partially addressed by the nature or range of measurements in the BEAR experiments.

Following the conclusions is a set of recommendations based upon the total BEAR Project experience. These should prove helpful in formulating future NPB space experiments.

FIRM CONCLUSIONS

1. Spaceworthy NPB Accelerator Demonstrated

With the BEAR mission a *fait accompli*, it is self-evident that an NPB accelerator can be designed for, and successfully operated in, the space environment. Factor-of-10 weight and size reductions and increased operational reliability relative to a typical ground-based system were achieved. Furthermore, the successful operation of the accelerator following the exposure of the beamline to high-pressure air during the aborted launch, and again following recovery, dramatically demonstrated the robustness of the NPB system.

2. Beam Jitter Unaffected by Flight

No anomalous or enhanced jitter was observed in either beam pointing or beam divergence during flight. The respective flight data are strictly comparable to the ground test results.

3. Support Subsystems Not Affected by Beam

Operation of the instrumentation, telemetry, and ancillary support subsystems was not adversely affected by either the operation of the accelerator or the beam's interaction with the ambient environment. Careful attention had to be given, however, to shielding and optical isolation requirements.

4. No Deleterious Zero Gravity Effects

Over the course of the flight, there were no observed effects that could be attributed to the zero-g environment. In particular, prelaunch concern about particulate matter drifting within the accelerator beamline appears to have been unfounded.

5. Beam Propagation as Predicted

The NPB does propagate over long distances in space. Its propagation is consistent with conventional single-particle collision theory.

6. Spacecraft Charging an Important Consideration

Spacecraft charging did indeed occur, as expected—in fact, the Experimentation Plan was designed to induce charging of the spacecraft. The charging cycle and peak potential reached are functions of the net charge emitted and, apparently, of the background plasma conditions. Charging, even to the level produced by deliberately turning off the neutralizer, caused no measurable deleterious effects.

7. Beam Particle Dynamics Predictable

The electrodynamics of the charged particles emitted in the beam are, at least to first order, predictable. Particle behavior is consistent with single-particle theory and is not dominated by collective effects.

8. Neutral Outgassing Not a Problem

Given adequate porting and reasonable materials selections in designing the spacecraft, neutral gas outgassing does not result in an effect large enough to significantly inhibit beam propagation.

9. No Unexplainable Phenomena Observed

In examining both the accelerator's performance and the plasma physics data, no evidence was encountered of any major unexplainable or novel phenomenon. While the limited range of conditions and instrument detection capabilities afforded by the BEAR experiments does not rule out the possibility that some such new phenomenon may still lie in wait, this null result provides increased confidence to the designer of a future NPB space system.

TENTATIVE CONCLUSIONS

1. Long-Term Orbital NPB System Feasible

The BEAR experiments did not uncover any physics or engineering restrictions (i.e., "show-stoppers") that would render an extended-orbital-mission NPB system, with multiple-start capability, infeasible. While appropriate engineering changes from the BEAR design would be required, e.g., in the ion source, vacuum pumping, and cooling subsystems, no "mandated breakthroughs" would be required.

2. Spacecraft Charging Analytically Predictable

The data on particle influx to the BEAR payload strongly suggest that in-space charging effects cannot be realistically simulated in ground tests within the dimensional constraints of even the largest existing plasma chamber. Fortunately, a relatively simple electrodynamic model quantitatively explains most of the features of spacecraft charging observed during the BEAR flight.

3. Enhanced Pumping Through Wake Effects

Aerodynamic wake effects can apparently enhance the rate of space pumping of the spacecraft's exposed regions. The cold-cathode ionization gage (CCIG) data suggest that the transient rate of evacuation of the Beam Diagnostics (BD) Section, which was open to the payload's wake, actually *exceeded* the rate at which ambient static pressure decreased as the vehicle climbed, down to the quasi-steady local pressure level established by outgassing.

4. Global Conclusion

All of the BEAR data and observations evaluated generally support and validate the methodology use in the prior assessment of the space physics issues and their impact (or lack thereof) on prospective future NPB space experiments.

RECOMMENDATIONS

Following are broad recommendations for the NPB space effort pursuant to the major conclusions drawn from the BEAR. Additional detailed recommendations are given in the appropriate sections of Volume II.

1. Go-Ahead for Next Phase

Proceed as planned with the next phase of NPB experimentation in space. To augment the BEAR results, the system orbited should address higher beam energy and current, more precise pointing and active steering, multiple accelerator restarts, beam/target interactions, possible far-field beam distortion effects, and a broader range of spacecraft chargeability

conditions. Techniques to mitigate charging effects must be implemented. Careful attention must be paid to shielding and optical isolation, where required.

2. Ion Source Characterization

Conduct a thorough characterization and parametric mapping of the ion source selected for the next NPB space mission, then provide "smart" (microprocessor-based) closed-loop control and/or an uplink for real-time interventive control of the ion source on orbit. Judicious prototyping is essential.

3. Conservative Environmental Testing

Obtain as much relevant empirical data as possible on the launch and payload deployment environments (shocks, vibration, aerodynamic heating, etc.) and develop conservative envelope specifications therefrom for component-level, subsystem-level, and system-level testing. Ensure that suspectedly sensitive items or assemblies are subjected to adequate environmental testing with respect to both quiescent and operating conditions—erring on the side of overtest if in doubt—with meticulous posttest evaluation.

4. Effective Project Team Organization

In addition to the scientific and technological conclusions and recommendations derived from the BEAR results, the BEAR Project itself may well serve as a positive model for multiple-government-agency and industrial team endeavors of this type. Its conduct required a large and dedicated—but not unwieldy—cadre (Figure 50). The performing government agencies involved—Air Force Geophysics Laboratory (AFGL), Naval Research Laboratory, Army Test and Evaluation Command, Research Rockets Division of Naval Ordnance Missile Test Station, and NASA's White Sands Test Facility Division all played their roles in an efficient and convivial manner—with patience and humor and without "territorial" issues—under the overall cognizance of LANL (a comparative neophyte in complex space vehicle integration). Likewise, the major industrial subcontractors—Northeastern University, SIE and Space Vector for the AFGL, and Grumman Space Systems, McDonnell Douglas Missile Systems Co., SAIC Northwest, and the Westinghouse Defense and Electronic Center for LANL—provided the required hardware and support often above and beyond contractual requirements. The sponsoring organization, too, did its part to facilitate the rapid and successful completion of the project. The Strategic Defense Initiative Organization's program managers were truly day-to-day members of the team. They participated in technical and programmatic decisions as temporary obstacles and minor setbacks arose and provided encouragement (as well as some additional funds, when critically needed) to overcome them, all with an amicable and evenhanded management style.
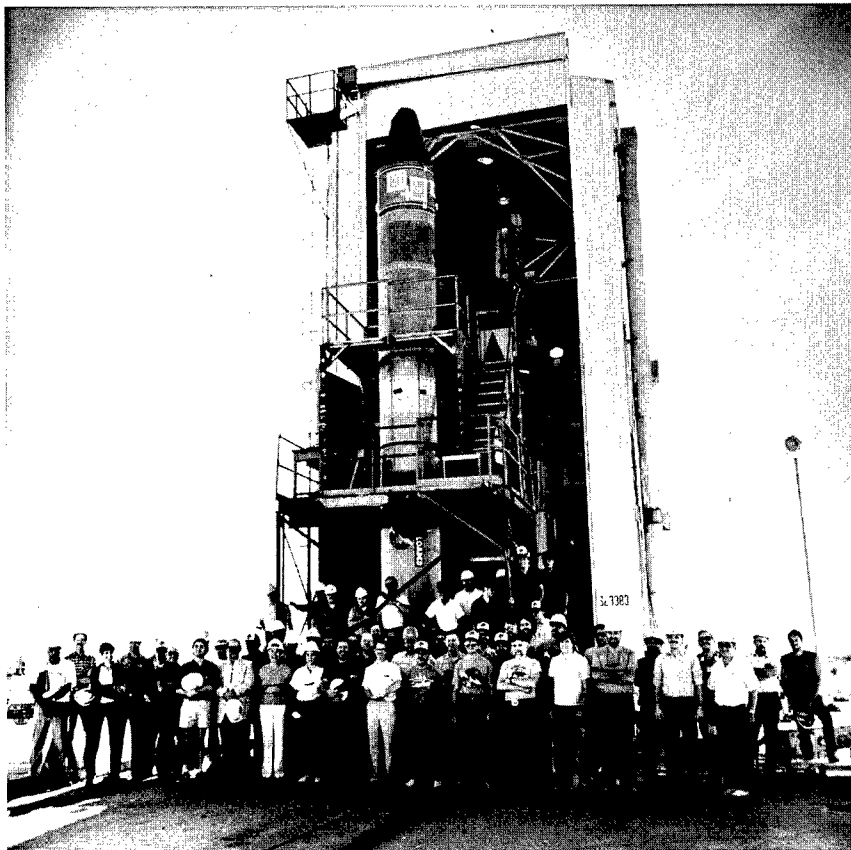
96

Figure 50. Multiorganizational BEAR Project team at launch site.

The teamwork manifested in executing this project resulted in an *esprit de corps* that persisted throughout the project. Although not quantitatively estimable, this team spirit was invaluable to the success of the project. Further, through those close interactions, not only was the *desired* technology transfer (accelerator technology, from LANL to its primary subcontractors) accomplished, but an even broader, mutual technology transfer took place among all the team participants. Thus, the experience base and versatility of these participants, governmental as well as industrial, is enhanced for their involvement in related future activities.

REFERENCES

1. G. J. Nunz, "BEAR Project Plan," BEAR-DM-3, prepared by the BEAR Project Staff, Los Alamos National Laboratory, Los Alamos, New Mexico, for the US Air Force Weapons Laboratory, Kirtland AFB, New Mexico (June 1986).

2. M. B. Pongratz, "Scientific Experimentation Plan," BEAR-DT-5, prepared by the BEAR Project Staff, Los Alamos National Laboratory, Los Alamos, New Mexico, for the US Air Force Weapons Laboratory, Kirtland AFB, New Mexico (June 1986).

3. "BEAR I Project: Accelerator Payload Segment Handbook," BEAR-I-DT-1, prepared by the BEAR Project Staff, G. Nunz, M. Duran, and A. McGuire, Eds., Los Alamos National Laboratory, Los Alamos, New Mexico, for the US Air Force Weapons Laboratory, Kirtland AFB, New Mexico (June 1986).

4. "Critical Design Review Summary," BEAR-DT-3, prepared by the BEAR Project Staff, G. Nunz and A. McGuire, Eds., Los Alamos National Laboratory, Los Alamos, New Mexico, for the US Air Force Weapons Laboratory, Kirtland AFB, New Mexico (June 1986).

5. "BEAR Interface Control Document, Part A—Flight," Baseline Issue, prepared by Systems Integration Engineering, Inc., for the Air Force Geophysics Laboratory, Hanscom AFB, Massachusetts, Los Alamos National Laboratory, Los Alamos, New Mexico (October 1986).

6. "BEAR Project: Accelerator Payload Segment (APS) Configuration," BEAR-DT-1.1-2, Revision 2, prepared by the BEAR Project Staff, G. Nunz and A. McGuire, Eds., Los Alamos National Laboratory, Los Alamos, New Mexico, for the Strategic Defense Initiative Organization, Directed Energy Office, Washington, DC (April 1989).

7. A. McGuire, "Beam Experiments Aboard a Rocket (BEAR), Postflight Mechanical Damage Assessment of the Accelerator Payload Segment," prepared by the BEAR Project Staff, Los Alamos National Laboratory, Los Alamos, New Mexico, for the Strategic Defense Initiative Organization, Directed Energy Office, Washington, DC (September 1989).

LIST OF ACRONYMS

ACS	Attitude Control Subsystem
AFB	Air Force Base
AFGL	Air Force Geophysics Laboratory
AFWL	Air Force Weapons Laboratory
AID	Accelerator internal diagnostic
APS	Accelerator Payload Segment
ARMTE	US Army Test and Evaluation (Command)
BCM	Beam Current Monitor
BD	Beam diagnostic
BEAR	Beam Experiments Aboard a Rocket
BLC	Beamline cryotrap
BPO	BEAR Project Office
CCIG	Cold-cathode ionization gage
CDR	Critical design review
CR	Control and recovery
DOE	Department of Energy
ESA	Electrostatic Analyzer
GTS	Ground Test Stand
HEBT	High-Energy Beam Transport
HIV	High-voltage detector
LANL	Los Alamos National Laboratory
LEBT	Low-Energy Beam Transport
LPS	Langmuir Probe Subsystem
LVS	Launch Vehicle Segment
MA	Motor Adapter
MDT	Mountain Daylight Time
NASA	National Aeronautics and Space Administration
NPB	Neutral particle beam
NRL	Naval Research Laboratory
PCM	Pulse code modulated
PDR	Preliminary design review
PPD	Plasma physics diagnostic
PWR	Plasma Wave Receiver
RFQ	rf quadrupole (cavity)
RM	Rocket Motor
SDIO	Strategic Defense Initiative Organization
SPS	Support Payload Segment
SSD	Solid-state (particle) detector
SWS	Shadow Wire Scanner
TP	Telemetry/Physics
WSMR	White Sands Missile Range

GLOSSARY

Airglow

Light emitted by atmospheric molecules excited by the beam (in this instance, specifically, ultraviolet light at 391.4 mm wavelength from excited nitrogen molecules was observed).

ARIES

Name given to a refurbished M56A-1 Minuteman I second-stage, solid-propellant rocket motor adapted for use as a single-stage booster.

Beam Blowup

Expansion of the beam orthogonal to its direction of propagation as a result of electrostatic repulsion among its like-charged constituent species.

Beam Loading

Fraction of rf power delivered (to the RFQ) that is transferred to the beam.

Bell Jar

A bell-shaped metal shell designed to fit and seal around the beam diagnostic instrument package and serving as its vacuum chamber in ground tests.

Bunching
(of H^- beam)

An effect produced by the time-varying electric fields within the RFQ that causes grouping of the beam particles around the synchronous phase angle of the rf field.

Coning

An induced precessional motion of the beam propagation axis in a small-angle cone about the direction of the vehicle's roll angular momentum vector.

Emittance

A measure of the dispersion of the beam in phase space (to be minimized as a design goal).

Fluence
(of particles)

The total number of particles incident per unit area within a specified time interval.

Getter Pump

A vacuum-maintaining pump whose pumping capability depends upon the accretion and holding ("getting") of specified gas(es) by adsorptive/

101

	reactive elements dispersed in a high surface-to-volume matrix.
Jitter	The statistical variation (one standard deviation) from the mean value—either within a given pulse or from one pulse to another—of beam pointing or beam divergence.
Matching (beam into the RFQ)	Adjustment of radial dimensions and angular divergences of the beam for maximum beam current acceptance by the RFQ.
Neutral Particle Beam	Theoretically, a directed stream of uncharged atomic particles; in practice, a mixed beam of charged and uncharged species with the maximum attainable fraction of neutrals and an approximate balance between positive and negative ions.
Overneutralize	To provide more than the optimum column density of neutralizer target material, resulting in a net positive beam current.
Powerdown	Automatic removal of electric power from the accelerator beamline and rf subsystem by the master controller upon completion of the flight sequence.
Radiance (of beam-excited air column)	Luminous energy emitted per unit time per steradian per unit projected area.
RF Conditioning	Final preparation of the internal surfaces of the RFQ by exposure to rf fields of increasing intensity, removing adsorbed gases and metallic microasperities through the resultant sporadic arcing.
RFQ (radio frequency quadrupole cavity)	A specially designed resonant rf cavity incorporating four axial modulated vanes, which focuses, bunches, and accelerates the traversing beam.
Stackup	A representation of the complete mission rocket assembly as it appears on the launch pad and showing its constituent sections.
Stripping Interaction	An interaction between a high-energy beam particles and an atmospheric gas atom wherein the former loses an electron to the latter.

Suborbital Trajectory   An approximately parabolic flight path that departs from, and returns directly to, the earth, i.e. does not become orbital.

Underneutralize   To provide less than the optimum column density of neutralizer target material, resulting in a net negative beam current.

Uplink   The capability to send a radio signal from a ground-based transmitter to a receiver in the payload, enabling the ground observer to activate, deactivate, and adjust payload subsystems in flight.